

AD-A034 829

UNITED TECHNOLOGIES CORP STRATFORD CONN SIKORSKY AIR--ETC F/G 13/8
FORGE-DIFFUSION BOND TITANIUM ROTOR HUB EVALUATION.(U)

JUL 75 M J BONASSAR, J J LUCAS

DAAG46-73-C-0126

UNCLASSIFIED

SER-50938

AMMRC-CTR-75-14

NL

1 of 2
ADA034829



ADA 034829

② FG

AD



AMMRC CTR 75-14

Production Engineering Measures Program
Manufacturing Methods and Technology

**FORGE-DIFFUSION BOND TITANIUM
ROTOR HUB EVALUATION**

July 1975

MARON J. BONASSAR and JOHN J. LUCAS

SIKORSKY AIRCRAFT  Division of
WESTINGHOUSE TECHNOLOGIES

Stratford, Connecticut 06602

Final Report - Contract Number DAAG-46-73-C-0126

Approved for public release; distribution unlimited.

Prepared for

ARMY MATERIALS AND MECHANICS RESEARCH CENTER
Watertown, Massachusetts 02172

U.S. ARMY AVIATION SYSTEMS COMMAND
St. Louis, Missouri 63166

Copy available to DDC does not
permit fully legible reproduction

DDC
RECEIVED
JAN 25 1977
RECEIVED
B

This project has been accomplished as part of the U.S. Army Materials Testing Technology Program, which has for its objective the timely establishment of manufacturing processes, techniques or equipment to insure the efficient production of current or future defense programs.

The findings in this report are not to be construed as an official Department of the Army position, unless so designated by other authorized documents.

Mention of any trade names or manufacturers in this report shall not be construed as advertising nor as an official indorsement or approval of such products or companies by the United States Government.

DISPOSITION INSTRUCTIONS

Destroy this report when it is no longer needed.
Do not return it to the originator.

↓

The purpose of this program was to establish the manufacturing methods and technology necessary to fabricate large Ti-6Al-4V components at low overall cost by means of the forge-diffusion bond process. The technical approach to achieve this concept consisted of three phases: the determination of an optimum process condition by evaluation of small test specimens cut from simple pancake forgings which had been fabricated with different processing conditions; the utilization of the optimum process condition in the fabrication and evaluation of a risk reduction component which was a single arm of the H-53 Helicopter Elastomeric Main Rotor Hub; and finally, the manufacture of the full-size main rotor hub. The first two phases of this concept have been successfully completed in this program. ← The forge-diffusion bond material of the risk reduction component was found to exhibit properties equivalent to parent material values. The process was shown not to be cost effective for the full-size H-53 Elastomeric rotor hub. Although technically feasible, fabrication of the full-size hub will not be demonstrated.

1.0 SUMMARY

Fabrication of complex titanium components by means of the forge-diffusion bond process has been successfully demonstrated and evaluated by mechanical properties testing. The process is technically feasible but, in its present approach, would not be cost effective for large components.

The purpose of this program was to establish the manufacturing methods and technology necessary to fabricate large Ti-6Al-4V components at low overall cost by means of the forge-diffusion bond process. The technical approach to achieve this concept consisted of three phases: the determination of an optimum process condition by evaluation of small test specimens from simple pancake forgings which have been fabricated with different processing conditions; the selection of an optimum process condition and subsequent fabrication and evaluation of a risk reduction component which was a single arm of the H-53 Helicopter Elastomeric Main Rotor Hub; and finally, the manufacture of the full-size main rotor hub. The first two phases of this concept have been completed in this program.

Determination of an optimum process condition was accomplished by evaluating different forging material conditions and processing temperatures using five trial pancake type forgings. After bonding, all five conditions were followed by a thermal treatment. Each pancake assembly, representing one of the five trial conditions, was ultrasonically inspected for joint quality, fabricated into small-scale specimens, and evaluated by testing in fatigue, fracture toughness, in-line shear, and tensile. Mechanical properties testing on the five diffusion bonded pancake forging assemblies revealed that the first four trial conditions were generally similar while the fifth condition exhibited a very limited bond area, insufficient for evaluation. By analysis of the test data and cost effectiveness, the optimum process condition was selected and incorporated into the fabrication of a risk reduction component, a single arm of the H-53 Helicopter Elastomeric Main Rotor Hub. The selected condition was an alpha-beta forging, forge-diffusion bonded at the alpha-beta temperature of 1750°F, diffusion treated at 1900°F, water-quenched, and then overaged at 1300°F for two hours.

Separately forged upper and lower halves of the H-53 Elastomeric Main Rotor Hub were produced using the existing forging dies. The use of the existing dies eliminated the expense of manufacturing a new set of dies to demonstrate the process. The half-forgings were machined to the

configuration to which they would have been forged, had new dies been fabricated. The upper and lower half-forgings provided six risk reduction single hub arm components available for diffusion bonding. It was necessary to forge-bond three arm segments before obtaining a satisfactorily bonded arm. The first two attempts to fabricate a satisfactorily bonded arm component were not successful because of contamination between the mating surfaces. The contamination was associated with the techniques employed during preparation for bonding. The third attempt modified the basic fabrication technique and successfully bonded the arm segments.

The procedure for bonding the third arm component included machining and chemically cleaning the surfaces to be joined. The machined and cleaned surfaces were mated and the component arms placed between a set of forge-bond dies which maintained the arms in position during the forge-bond process and transmitted pressure uniformly. The entire assembly was enclosed in a stainless steel retort, evacuated to 10^{-4} Torr, placed in a gas fired furnace, and the temperature gradually increased from room temperature to the forge-bond temperature of 1750°F. The rate of temperature increase was relatively slow because it was necessary to continually evacuate the retort through a small diameter tube during the heating cycle to prevent contamination. When the retort unit reached 1750°F, it was removed from the furnace and placed between the heads of the forging press and pressure was applied for bonding. Subsequent thermal treatment was completed and the bonded arm segment was machined top and bottom for ultrasonic inspection. Sonic C-scan recording indicated a satisfactorily bonded arm segment. Test specimens were fabricated from the risk reduction components. The specimens, consisting of nine fatigue and three each of fracture toughness, in-line shear, and tensile, were fabricated from material at the diffusion bonded joint and from material away from the diffusion bonded joint. Evaluation of the data indicated excellent properties with values from the forge diffusion bonded joint equivalent to values obtained in the parent material, away from the diffusion bonded joint.

Review of the program results showed that scaling-up the hardware and equipment necessary to accommodate a full-size H-53 Elastomeric Main Rotor Hub is technically feasible but would not be cost effective in its present approach. However, an intermediate size hub, such as a UTTAS Main Rotor Hub, is recommended as a candidate for a follow-on program to establish a manufacturing method which will be cost effective.

FOREWARD

This report was prepared by Sikorsky Aircraft, Division of United Technologies Corporation under the sponsorship of the U. S. Army Materials and Mechanics Research Center, under Contract DAAG46-73-C-0126. The Army technical supervisor is Mr. Paul J. Doyle, AMXMR-KB. This is the final report and covers work conducted from March 8, 1973 to May 15, 1975.

The authors wish to acknowledge the following Sikorsky individuals for their contributions and continuing efforts and assistance in the mechanical testing and material analysis portion of this program: G. Lattin, C. Matusovich, J. Rackiewicz, M. Saranich, Jr., and R. Scott.

Acknowledgement is also given to the following Wyman-Gordon personnel for their efforts on the forge-bonding approach and their constant support and cooperation freely given to make this program a success: R. Foley, J. Long, E. Strom, O. St. Thomas, and E. Weaver.

ACCESSION for	
NTIS	White Section <input checked="" type="checkbox"/>
DDC	Buff Section <input type="checkbox"/>
UNANNOUNCED	<input type="checkbox"/>
JUSTIFICATION	
BY	
DISTRIBUTION/AVAILABILITY CODES	
Dist. A, AIL, 200/30 SPECIAL	
A	

TABLE OF CONTENTS

	<u>PAGE</u>
1.0 SUMMARY	iii
FOREWARD	v
LIST OF ILLUSTRATIONS	ix
LIST OF TABLES	xv
2.0 INTRODUCTION	1
2.1 Aerospace Industry Needs	1
2.2 Forge-Diffusion Bonding	1
2.3 Program Scope	3
3.0 PROCESS OPTIMIZATION PANCAKE FORGINGS	6
3.1 Pancake Fabrication	6
3.2 Pancake Inspection	14
3.2.1 Procedure	14
3.2.2 Results	17
3.3 Pancake Mechanical Property Testing	26
3.3.1 Procedure	26
3.3.2 Results	30
3.4 Process Selection For Optimum Forge-Bonding Conditions	39
4.0 FORGE-DIFFUSION BONDED H-53 ELASTOMERIC MAIN ROTOR HUB, SELECTION OF BONDED PLANE LOCATION	44
4.1 Structural Analysis	44
4.2 Die Examination and Application Review	45
4.3 Final Selection	46
5.0 RISK REDUCTION FABRICATION AND EVALUATION OF H-53 ELASTOMERIC MAIN ROTOR HUB ARM	51
5.1 Hub Halves Fabrication	51
5.2 Bonding Operation Approach	59
5.3 Single Arm Fabrication	61
5.3.1 Fabrication Technique; 3rd and 4th Hub Arm Segment Two Satisfactory Diffusion Bonded Arms	61

	<u>PAGE</u>
5.3.2 Fabrication Procedure; 1st and 2nd Hub Arm Segment First Two Unsuccessful Attempts	76
5.4 Hub Arm Segment Inspection	87
5.4.1 Procedures	87
5.4.2 Inspection Results; 3rd and 4th Hub Arm Segment First Two Satisfactory Diffusion Bonded Arms.	91
5.4.3 Inspection Results; 1st and 2nd Hub Arm Segments First Two Unsuccessful Attempts	103
5.5 Hub Arm Segment (#3) Mechanical Property Testing of First "Good" Arm . . .	108
5.5.1 Procedure.	108
5.5.2 Results.	108
6.0 COST PROJECTION.	128
7.0 CONCLUSIONS.	129
8.0 RECOMMENDATIONS.	130
REFERENCES	131
LIST OF SYMBOLS.	132
DISTRIBUTION	133

LIST OF ILLUSTRATIONS

<u>FIGURE</u>		<u>PAGE</u>
1.	FORGE-DIFFUSION BOND CONCEPT.	2
2.	FINISHED MACHINED H-53 ELASTOMERIC MAIN ROTOR HUB	4
3.	FORGE-DIFFUSION BONDED HUB REDUCES INPUT FORGING WEIGHT BY 900 LBS	5
4.	PROGRAM CONCEPT	5
5.	MACROSTRUCTURE OF Ti-6Al-4V FORGING STOCK MATERIAL, FORGE-DIFFUSION BOND OF SAMPLE PANCAKE FORGINGS.	8
6.	MICROSTRUCTURE OF Ti-6Al-4V FORGING STOCK MATERIAL, FORGE-DIFFUSION BOND OF SAMPLE PANCAKE FORGINGS.	9
7.	TWO TYPICAL MACHINED AND CHEMICALLY CLEANED PANCAKES.	11
8.	PANCAKE ASSEMBLY POSITIONED ON STAINLESS STEEL PLATE	11
9.	STAINLESS STEEL RETORT PRIOR TO FINAL WELD SEALING.	11
10.	TEST RETORT WITH THERMOCOUPLE AND RECORDING INSTRUMENTATION	12
11.	REFERENCE BLOCK FOR ULTRASONIC INSPECTION STANDARD.	15
12.	FORGE-DIFFUSION BOND PANCAKE ASSEMBLY, ULTRASONIC INSPECTION CONFIGURATION	16
13.	SCHEMATIC OF ULTRASONIC SYSTEM.	19
14.	TYPICAL SCREEN PATTERN.	19
15.	DETAILS OF THE TRANSIGATE OPERATION	19
16.	C-SCAN RECORDINGS OF FIVE PANCAKE ASSEMBLIES, ALARM LEVEL 100% OF #2 fbh IN REFERENCE BLOCK	21

<u>FIGURE</u>		<u>PAGE</u>
17.	C-SCAN RECORDING OF FIVE PANCAKE ASSEMBLIES, ALARM LEVEL 100% OF #3 fbh IN REFERENCE BLOCK	23
18.	TYPICAL ABNORMALITIES OBSERVED AT BONDLINE. . .	25
19.	SKETCH OF PANCAKE HALF, ILLUSTRATING TYPE AND LOCATION OF TEST SPECIMENS.	26
20.	TENSILE SPECIMEN CONFORMS TO FEDERAL TEST METHOD STD. NO. 151a.	27
21.	COMPACT TENSION, FRACTURE TOUGHNESS SPECIMEN CONFORMS TO ASTM-E399-72.	28
22.	FRACTURE TOUGHNESS SPECIMEN, FATIGUE PRECRACKING SET-UP IN SONNTAG TESTING MACHINE	29
23.	FRACTURE TOUGHNESS SPECIMEN, SET-UP IN RIEHLE TESTING MACHINE.	29
24.	IN-LINE SHEAR TEST SPECIMEN	31
25.	IN-LINE SHEAR SPECIMEN IN GUILLOTINE FIXTURE, BETWEEN COMPRESSION HEADS OF TESTING MACHINE	31
26.	AXIAL CRACK INITIATION FATIGUE SPECIMEN UN-NOTCHED, ELLIPTICAL REDUCED SECTION.	32
27.	AXIAL FATIGUE TEST SET-UP IN SONNTAG TESTING MACHINE	32
28.	SUMMARY OF MECHANICAL TESTING, TRIAL PANCAKE ASSEMBLIES.	33
29.	TENSILE FRACTURE, TYPICAL DUCTILE BREAK, TRIAL PANCAKE ASSEMBLY.	34
30.	FRACTURE TOUGHNESS INTERFACE, TYPICAL FRACTURE INTERFACE, TRIAL PANCAKE ASSEMBLIES.	36
31.	FRACTURE TOUGHNESS INTERFACE CONDITION 4, NOTE COARSER STATIC FRACTURE SURFACE.	36
32.	IN-LINE SHEAR FRACTURE, TYPICAL STATIC OVERLOAD FRACTURE SURFACE, TRIAL PANCAKE ASSEMBLIES.	37

<u>FIGURE</u>		<u>PAGE</u>
33.	MEAN S/N CURVE FOR VARIOUS FORGE-DIFFUSION BOND PROCESS CONDITIONS	41
34.	FATIGUE FRACTURE, TYPICAL BRITTLE FRACTURE SURFACE WITH ORIGIN ON O.D., TRIAL PANCAKE ASSEMBLIES.	43
35.	PLAN VIEW OF ONE-SIXTH HUB ARM SEGMENT DEPICTING CROSS SECTION THROUGH CRITICAL AREAS	47
36.	STRESS DISTRIBUTION ACROSS SECTION B-B FOR VARIOUS FLIGHT LOAD CONDITIONS.	49
37.	MACROSTRUCTURE OF Ti-6Al-4V FORGING STOCK MATERIAL, FORGE-DIFFUSION BOND OF RISK REDUCTION SEGMENT	53
38.	MICROSTRUCTURE OF Ti-6Al-4V FORGING STOCK MATERIAL, FORGE-DIFFUSION BOND OF RISK REDUCTION SEGMENT	54
39.	HALF-FORGING SHOWING CUT-OUT AREAS.	58
40.	HALF-FORGING SHOWING PARTIALLY MACHINED CONFIGURATION	58
41.	SKETCH OF BONDING DIES WITH HUB ARM SEGMENT IN POSITION	59
42.	TOP AND BOTTOM BONDING DIES, ROUGH MACHINED.	60
43.	HUB ARM SEGMENTS PRIOR TO BONDING	62
44.	BONDING DIE, GUSSET PLATE, AND HUB SEGMENT ASSEMBLY FOR THIRD HUB ARM.	63
45.	RETORT AFTER ASSEMBLY	64
46.	DIAGRAM OF RETORT IN FURNACE.	65
47.	PLOT OF HEATING-OUTGASSING IN VACUUM OF THIRD ARM SEGMENT, TEMPERATURE AND PRESSURE VERSUS TIME	67
48.	FORGE-BOND OPERATION OF THIRD ARM SEGMENT, FORCE AND DISPLACEMENT VERSUS TIME.	69

<u>FIGURE</u>		<u>PAGE</u>
49.	RETORT UNIT AFTER POST-BOND ANNEAL, THIRD ARM SEGMENT	70
50.	RETORT, DIE AND ARM SEGMENT AFTER THE FORGE-BOND AND POST BOND ANNEAL, THIRD ARM SEGMENT	71
51.	PLOT OF HEATING-OUTGASSING IN VACUUM OF FOURTH ARM SEGMENT, TEMPERATURE AND PRESSURE VERSUS TIME	73
52.	FORGE-BOND OPERATION PLOT OF FOURTH ARM SEGMENT, FORCE AND DISPLACEMENT VERSUS TIME.	75
53.	FIRST ARM SEGMENT TACK WELDED AND SEATED BETWEEN BONDING DIES.	77
54.	FIRST ARM SEGMENT, RETORT UNIT BEFORE SEALING WITH FINAL WELD	77
55.	FORGE-BOND OPERATION OF FIRST HUB ARM SEGMENT, FORCE AND DISPLACEMENT VERSUS TIME.	78
56.	RETORT UNIT AFTER FORGE-BOND AND THERMAL TREATMENT, FIRST HUB ARM SEGMENT.	80
57.	FIRST HUB ARM SEGMENT AFTER BONDING	80
58.	SKETCH OF CROSS SECTION THROUGH HUB ARM, BEFORE AND AFTER FORGE-BONDING.	81
59.	SKETCH OF OUTGASSING FURNACE, SECOND HUB ARM SEGMENT	82
60.	PLOT OF HEATING-OUTGASSING IN VACUUM OF SECOND ARM SEGMENT, TEMPERATURT AND PRESSURE VERSUS TIME	84
61.	RETORT UNIT AFTER FORGE-BOND AND POST-BOND ANNEAL, SECOND HUB ARM SEGMENT.	85
62.	FORGE-BOND OPERATION OF SECOND HUB ARM SEGMENT, FORCE AND DISPLACEMENT VERSUS TIME.	86
63.	CRACKING CONDITION OBSERVED IN PARENT MATERIAL OF RETORT UNIT, SECOND HUB ARM SEGMENT	86

<u>FIGURE</u>	<u>PAGE</u>
64. FORGE-DIFFUSION BOND HUB ARM SEGMENT, ULTRASONIC INSPECTION CONFIGURATION	88
65. PULSE-ECHO IMMERSION ULTRASONIC EQUIPMENT USED IN INSPECTION OF HUB ARM SEGMENTS.	89
66. CLOSE-UP OF SONIC SEARCH UNIT AND ARM SEGMENT IN TANK	90
67. THIRD HUB ARM SEGMENT AS REMOVED FROM RETORT.	91
68. SKETCH OF THIRD ARM SEGMENT ILLUSTRATING PRELIMINARY ULTRASONIC INSPECTION INDICATIONS BEFORE FINAL BETA HEAT TREAT.	92
69. MACROSTRUCTURE ACROSS BONDLINE OF THIRD HUB ARM SEGMENT, BEFORE FINAL BETA HEAT TREAT DISCLOSES NO GROSS LACK OF BOND	94
70. MICROSTRUCTURE ACROSS BONDLINE OF THIRD HUB ARM SEGMENT, AFTER FINAL BETA HEAT TREAT AGAIN DISCLOSES NO GROSS LACK OF BOND.	94
71. BEND SPECIMEN ACROSS BONDLINE, THIRD HUB ARM SEGMENT	95
72. BEND SPECIMEN FROM PARENT MATERIALS, THIRD HUB ARM SEGMENT	95
73. C-SCAN RECORDING OF MACHINED TEST BLOCK "A" FROM THIRD HUB ARM SEGMENT WITH PRELIMINARY SONIC INDICATION.	97
74. C-SCAN RECORDING OF MACHINED TEST BLOCK "B" FROM THIRD HUB ARM SEGMENT WITH PRELIMINARY SONIC INDICATION.	99
75. C-SCAN RECORDING OF THIRD HUB ARM SEGMENT, ALARM LEVEL 80% OF #4 fbh IN REFERENCE BLOCK	101
76. C-SCAN RECORDING OF FOURTH HUB ARM SEGMENT, ALARM LEVEL 80% OF #4 fbh IN REFERENCE BLOCK	105
77. C-SCAN RECORDING OF FIRST HUB ARM SEGMENT, ALARM LEVEL 80% OF #4 fbh IN REFERENCE BLOCK	109

<u>FIGURE</u>	<u>PAGE</u>
78.	CROSS SECTION OF FIRST ARM SEGMENT THROUGH TYPICAL AREA OF SONIC INDICATION ILLUSTRATES GROSS NONBONDED CONDITION 111
79.	CONTAMINATION ON OUTSIDE SURFACE EXTENDS ONTO FAYING SURFACE FIRST ARM SEGMENT 111
80.	SUBSURFACE REGIONS OF NONFONDING ENVELOPED IN A LAYER OF CONTAMINATION, FIRST ARM SEGMENT 111
81.	MACROSTRUCTURE ACROSS BONDLINE OF SECOND ARM SEGMENT FROM AN AREA OF SOUND BOND INDICATION DISCLOSE NO GROSS LACK OF BOND 113
82.	MACROSTRUCTURE ACROSS BONDLINE OF SECOND ARM SEGMENT FROM AN AREA OF SONIC INDICATION DISCLOSES GROSS LACK OF BOND 113
83.	MICROSTRUCTURE ACROSS BONDLINE OF SECOND ARM SEGMENT FROM AN AREA OF SOUND BOND DEPICTING ALPHA CONTAMINATION ALONG BONDLINE. 113
84.	SKETCH OF THIRD HUB ARM SEGMENT ILLUSTRATING TYPE AND LOCATION OF TEST SPECIMENS 115
85.	SUMMARY OF MECHANICAL TESTING, HUB ARM RISK REDUCTION SEGMENT. 116
86.	TYPICAL CROSS SECTION OF BONDLINE, NO EVIDENCE OF ANY ANOMALIES, BOND JOINT IS NOT DISTINGUISHABLE FROM PARENT MATERIAL. 117
87.	TENSILE FRACTURE, TYPICAL DUCTILE BREAK, HUB ARM SEGMENT 118
88.	FRACTURE TOUGHNESS TYPICAL FRACTURE INTERFACE, HUB ARM SEGMENT. 120
89.	IN-LINE SHEAR FRACTURE, TYPICAL STATIC OVERLOAD FRACTURE SURFACE, HUB ARM SEGMENT 120
90.	MEAN S/N CURVE FOR HUB ARM SEGMENT, BONDLINE MATERIAL AND PARENT MATERIAL 125
91.	FATIGUE FRACTURE, TYPICAL FRACTURE SURFACE WITH ORIGIN ON O.D., HUB ARM SEGMENT. 127

LIST OF TABLES

<u>TABLE</u>		<u>PAGE</u>
I	PROCESS GUIDE DIFFUSION BOND CONDITIONS.	6
II	CHEMICAL ANALYSIS OF FORGING STOCK MATERIAL PANCAKE ASSEMBLY	7
III	DETAILED PROCESS PARAMETERS PANCAKE FORGING ASSEMBLIES	13
IV	TENSILE TEST RESULTS TRIAL PANCAKES.	35
V	PLAIN-STRAIN FRACTURE-TOUGHNESS TEST DATA TRIAL PANCAKES	37
VI	IN-LINE SHEAR TEST RESULTS TRIAL PANCAKES.	38
VII	FATIGUE TEST RESULTS TRIAL PANCAKES.	40
VIII	CHEMICAL ANALYSIS OF FORGING STOCK MATERIAL MAIN ROTOR HUB HALVES.	52
IX	TENSILE TEST RESULTS FORGING STOCK MATERIAL MAIN ROTOR HUB HALVES.	55
X	UPSET FORGING OPERATIONS MAIN ROTOR HUB.	56
XI	FIRST FINISH FORGING OPERATION MAIN ROTOR HUB.	57
XII	SECOND FINISH FORGING OPERATION MAIN ROTOR HUB.	57
XIII	ROOM TEMPERATURE "V"-NOTCH IMPACT RESISTANCE TEST THIRD HUB ARM SEGMENT	103
XIV	TENSILE TEST RESULTS HUB ARM SEGMENT	118
XV	PLANE-STRAIN FRACTURE-TOUGHNESS TEST DATA HUB ARM SEGMENT.	119
XVI	IN-LINE SHEAR TEST RESULTS HUB ARM SEGMENT	121
XVII	FATIGUE TEST RESULTS HUB ARM SEGMENT	123

2.0 INTRODUCTION

Large titanium forgings have been used extensively in helicopter applications for fatigue loaded dynamic components; however, the ratio of forged weight to finish machined part must be reduced by the application of concepts such as forge-diffusion bonding.

2.1 Aerospace Industry Needs

The continuing demand of the helicopter industry in the area of increased performance, payload, speed, and reliability has led to the extensive use of titanium forgings for fatigue loaded dynamic components. These forgings are often very large with intricate shapes, angles, recesses, and depressions. Typically, these components are machined from an integral forging which weighs five times more than the finished machined part. Because of the high cost involved in machining, the ever increasing price in titanium, and the diminishing availability of raw material, there exists a real and distinct need for manufacturing technology which produces less costly large, complex components from a minimum of raw material.

A prime candidate for alleviating this problem is the utilization of solid-state diffusion bonding. This concept allows the fabrication of large complex parts by joining separately forged details into a large component with intricate configurations, such as hollow bores and recesses. Solid-state diffusion bonding involves heating the material significantly below its melting temperature and applying sufficient pressure to achieve intimate contact. Over a period of time, a metallurgical bond is produced and under an optimum combination of time, temperature, and pressure, offers parent material mechanical properties. This process produces assemblies which are inherently stronger than components joined by welding where fusion creates a cast microstructure and where voids and impurities due to gaseous entrapment, filler wire, and electrodes are commonly experienced.

2.2 Forge-Diffusion Bonding

Titanium is a highly reactive metal and has a natural affinity for itself, therefore, making it very eligible for solid-state bonding. Several successful techniques have been developed to exploit solid-state bonding, each having their particular advantages and disadvantages. Forge-diffusion bonding as discussed in this report, appears very promising for use with large parts. In this process, the items to be

diffusion bonded are cleaned, mated, and encased in a steel container. The container is evacuated, heated to the bonding temperature, and the assembly placed in a forging press. While the items are kept at elevated temperature, and adequate vacuum is maintained, standard forging pressures are applied across the interface to produce intimate contact and local upsetting of metal, at the bondline. The bonding time is short, approximately equal to a standard forging sequence. Section size is not a problem since the bonding occurs between a special set of forging dies which can be machined to accommodate changes in section. Therefore, a complex part, such as a helicopter rotor hub, can be readily adapted. An illustration of the concept is provided in Figure 1. The inherent cost savings of fabricating small forging details and the sound bond achieved during diffusion makes this an ideal method for fabrication of large titanium forgings.

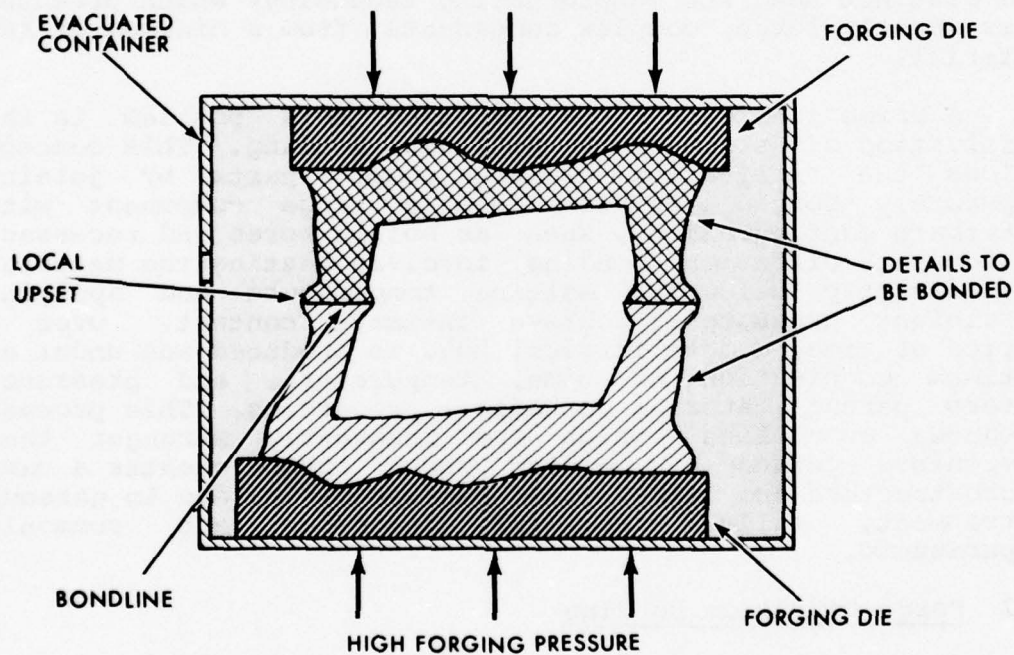


FIGURE 1. FORGE-DIFFUSION BOND CONCEPT.

Wyman-Gordon Company, North Grafton, Massachusetts, forging manufacturer, has extensive titanium forging capabilities and experience with forge-diffusion bonding. In 1968, Wyman-Gordon developed a forge-diffusion bonding technique which was directly applied to practice on a forty-inch diameter by twelve-inch thickness, eleven hundred pound gas turbine compressor disk. A rib and web structure was fabricated by Wyman-Gordon as an internal research effort. Bondlines in this component were both parallel and at right angles to forging force vectors. Mechanical properties tests across bondlines verified that the structural strength was in accordance with all specification requirements. The information gained from these efforts significantly advanced the state of forge-bond in design. Additional research was performed on a series of trial blocks. Smooth and notched crack initiation, fracture toughness, room and elevated temperature tensile, creep stress rupture, and notch-time-fracture tests all showed that forge-diffusion bonded material was equivalent to parent material. In researching advanced means of producing pressure vessels, Wyman-Gordon has developed a forge-diffusion bond process which would demonstrate both parent material strength and low-cost fabrication methods. Combining Sikorsky's requirements for large low-cost titanium forgings and Wyman-Gordon's forge-diffusion bond process, the U. S. Army, AMMRC funded a program to establish preliminary forge-diffusion bond manufacturing technology. The component selected as the prototype was the Sikorsky H-53 Elastomeric Main Rotor Hub.

2.3 Program Scope

The Sikorsky H-53 Helicopter Elastomeric Main Rotor Hub was selected as the component to demonstrate the Forge-Diffusion Bond Process because of its unique adaptability. Details of the rotor hub construction are provided in Reference (1). The main rotor hub is a spoked wheel-shaped component having a five foot diameter and a 12-inch thickness. An overall view of a machined hub is depicted in Figure 2. The hub material is Titanium alloy, 6% Aluminum -4% Vanadium, (Ti-6Al-4V) beta forged or beta heat treated. This hub has been built and flown for several years. The original hubs were fabricated from integral Ti-6Al-4V beta forgings which weighed approximately 3,000 pounds and required considerable machining to obtain the finished configuration weight of 560 pounds. The cost in material and machining was extremely high and a method of manufacture to reduce overall cost was greatly desired. The configuration of the hub, with the forging die parting plane perpendicular to the rotor axis, precluded forging the I-beam shape into the spokes of the "wheel" to reduce input weight. Forge-diffusion bonding of the hub was selected as one means

of significantly reducing forging input weight and subsequent machining cost. The hub would be fabricated from two T-shape half-forgings which would be subsequently diffusion bonded at approximately the location of the existing die parting plane. The resultant I-beam forging would require considerable less machining and input weight than the conventional forgings as illustrated in Figure 3. For demonstration of the concept, the existing forging dies were to be used in conjunction with flat plates to fabricate the two T-shape half-forgings. This technique would provide a baseline for comparing the cost of the conventionally forged hub and the forge-diffusion bonded hub. A manufacturing technology program was therefore established which was based on forge-diffusion bonding two separately forged halves to reduce input weight and subsequent machining cost.

The program concept involved three phases. The first phase consisted in the selection of an optimum, cost-effective, forge bonding condition by comparing the processing costs and bond strengths of five simple pancake forgings bonded at different combinations of process conditions. A single hub arm was to be fabricated in the second phase as a risk reduction segment. The risk reduction segment was machined from two half-forgings of the main rotor hub and forge bonded at the optimum condition selected in Phase I and tested. Finally, the fabrication of a full-size H-53 Elastomeric Main Rotor Hub was to be fabricated. The program concept is illustrated diagrammatically in Figure 4. The first two phases of the concept have been successfully completed in this contract.

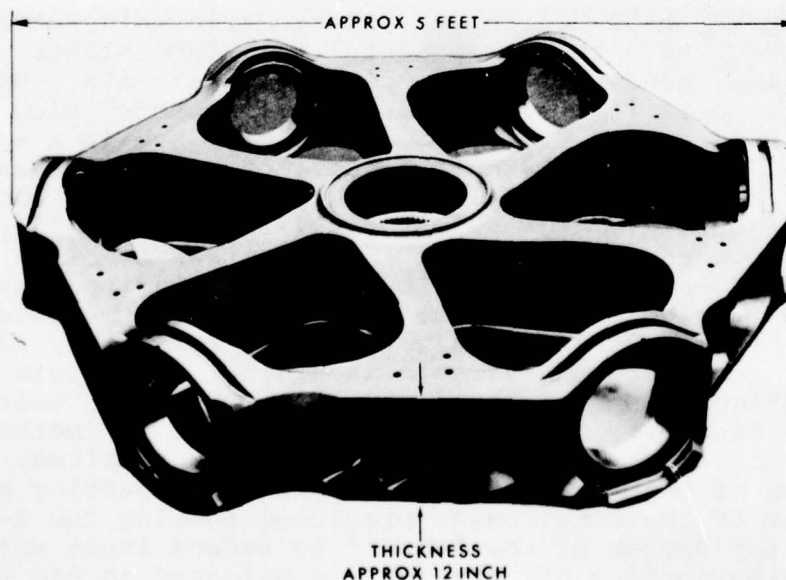


FIGURE 2. FINISH MACHINED H-53 ELASTOMERIC MAIN ROTOR HUB.

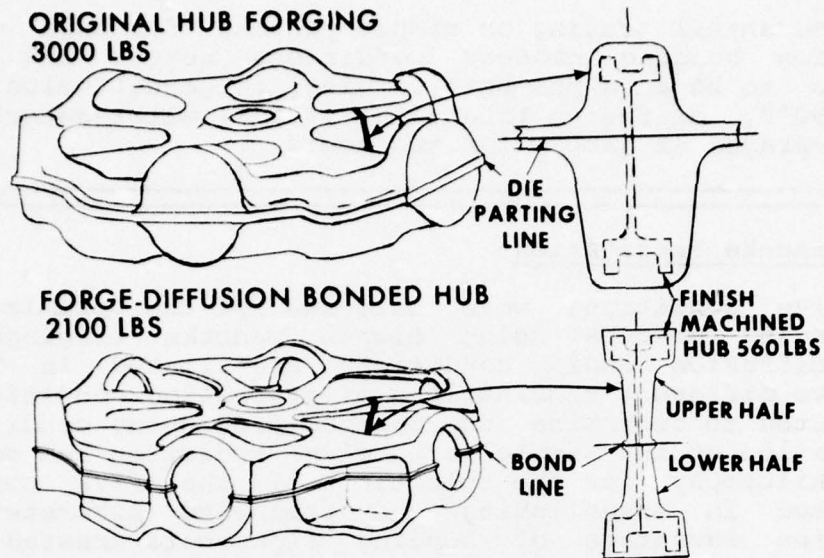


FIGURE 3. FORGE-DIFFUSION BONDED HUB REDUCES INPUT FORGING WEIGHT BY 900 LBS.

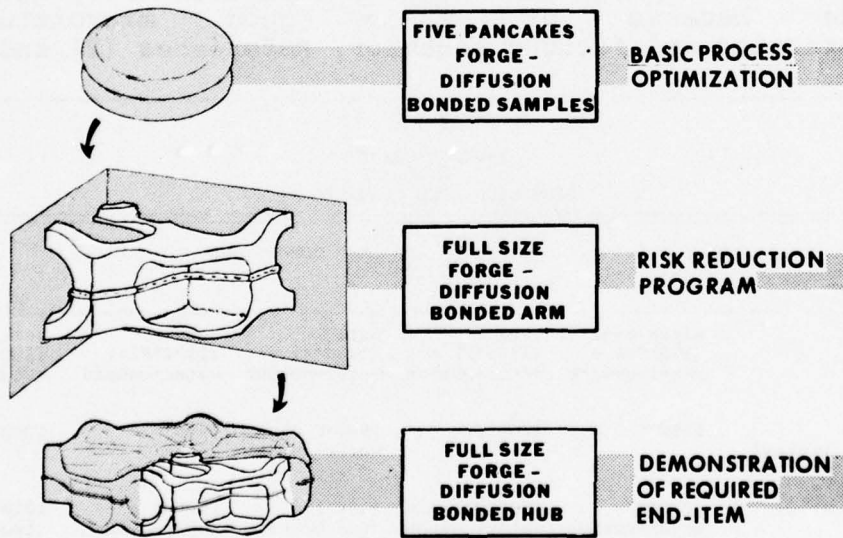


FIGURE 4. PROGRAM CONCEPT.

3.0 PROCESS OPTIMIZATION PANCAKE FORGINGS

Mechanical testing on simple pancake forgings of five diffusion bonding process conditions reveal the optimum process to be an alpha-beta forging, forge-diffusion bonded at 1750°F, diffusion treated at 1900°F, water-quenched, and then overaged at 1300°F for two hours.

3.1 Pancake Fabrication

Five conditions were selected for the optimization of the forging process using simple pancake forgings. The forge-diffusion bonding conditions are listed in Table I. The five different combinations of processing conditions were fabricated to determine the optimum processing condition for fabrication of the single arm risk reduction hub segments. The philosophy for the selection of the five conditions consisted in establishing the following parameters: to determine advantage of bonding alpha-beta treated forging stock material; to verify the most desirable forge-bond treatment among beta, alpha-beta, or annealing temperatures; and to substantiate the benefits of subsequent diffusion treatment or overaged thermal treatments after forge-bonding. The operations of the five evaluated conditions were performed in such a manner that all the pancake assemblies were finalized as beta processed material. Previous experience has shown that beta heat treated forgings are desirable because of their good microstructure characteristics and fatigue behavior, References (2) and (3).

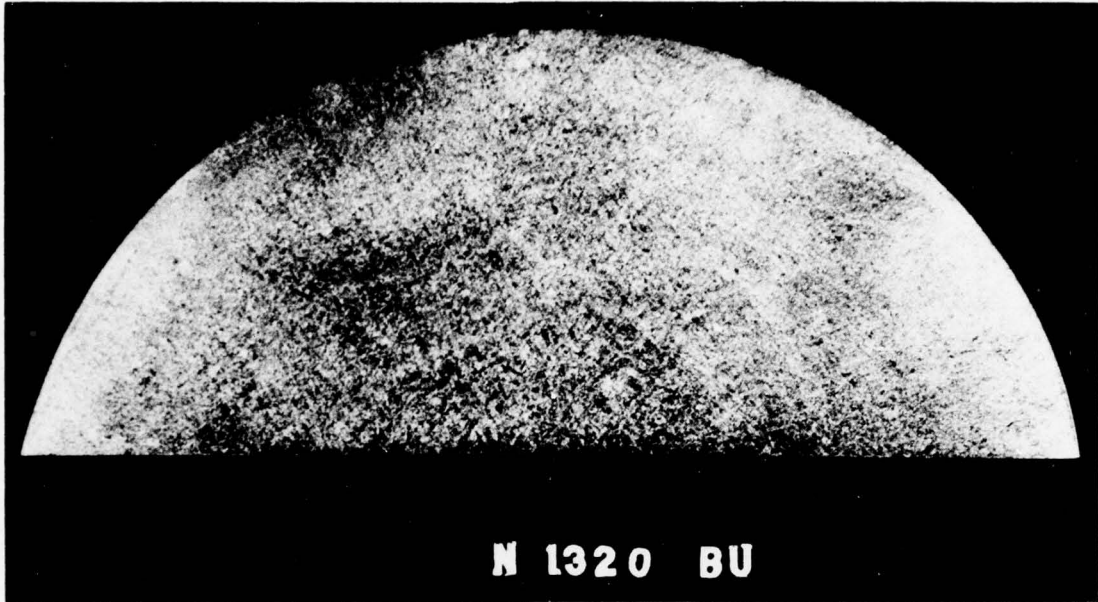
TABLE I PROCESS GUIDE DIFFUSION BOND CONDITIONS					
OPERATIONS	PROCESS CONDITIONS				
	1	2	3	4	5
Forge	alpha-beta (1750°F) + water-quench	beta (1900°F) + water-quench	beta (1900°F) + water-quench	beta (1900°F) + water-quench	beta (1900°F) + water-quench
Forge-Bond (one to two minutes)	1750°F	1750°F	1900°F + water-quench	1900°F	1300°F
Diffusion Treat or Over-Age as applicable	1900°F + water-quench	1900°F + water-quench	1300°F (two hours)	1900°F + water-quench	1300°F (two hours)
Overage	1300°F (two hours)	1300°F (two hours)	----	1300°F (two hours)	----

Nine-inch round Ti-6Al-4V alloy forging stock material conforming to the requirements of Sikorsky Standard 8445 Reference (4) was procured from Titanium Metals Corporation of America (TMCA). Chemical analysis of the material is provided in Table II and indicates its acceptability. Metallographic examination of the top and bottom of the forging stock material indicated a material of good quality. The macrostructure was uniform with recrystallized fine beta grains, as shown in Figure 5. The microstructure exhibited a very acceptable alpha particle size for forging stock material, as shown in Figure 6.

TABLE II
CHEMICAL ANALYSIS OF FORGING STOCK MATERIAL
PANCAKE ASSEMBLIES

ELEMENTS PERCENTAGE BY WEIGHT	ANALYSIS SOURCE		
	TMCA HEAT #N-1320	WYMAN-GORDON D-3476	REQUIREMENT OF SIKORSKY STANDARD SS8445, Ref. 4
Al	6.4	6.4	5.50 - 6.75
V	4.2	4.2	3.50 - 4.50
Fe	0.19	0.19	0.30 Max.
C	0.026	0.026	0.08 Max.
N	0.019	0.019	0.025
O	0.20	0.185	0.2 Max.
H	0.007	0.0047	0.0125 Max.
B	---	---	0.0125 Max.
Ti	---	---	Balance
Other	---	---	0.40 Max.

TOP SIDE



BOTTOM SIDE



FIGURE 5. MACROSTRUCTURE OF Ti-6Al-4V FORGING STOCK MATERIAL, FORGE-DIFFUSION BOND OF SIMPLE PANCAKE FORGINGS. .75X

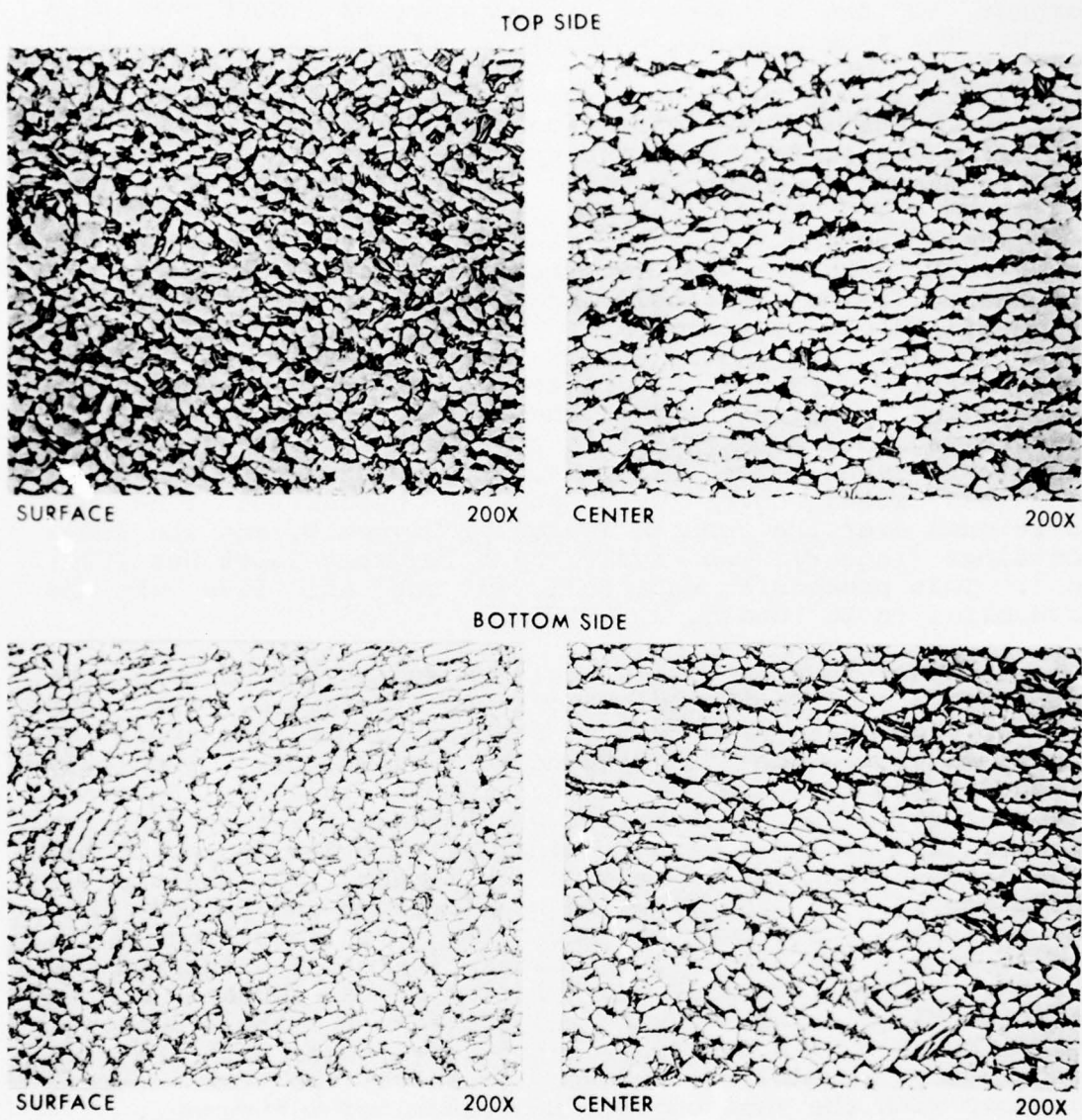


FIGURE 6. MICROSTRUCTURE OF Ti-6Al-4V FORGING STOCK MATERIAL,
FORGE-DIFFUSION BOND OF SIMPLE PANCAKE FORGINGS.

Ten segments, 9-inches round by 9-inches long, each weighing approximately one hundred pounds, were cut from the forging stock material. Two of the segments were heated in a furnace to the alpha-beta temperature of 1750°F for five hours. The remaining eight segments were heated to the beta temperature of 1900°F for five hours. All the segments were upset forged from 9-inches to 3.75-inches thickness on a 1500-ton press in one operation resulting in a diameter of approximately 14-inches. Each upset segment was subsequently water-quenched immediately after the forge operation.

The pancakes were sandblasted and one forged surface from each pancake was machined to a final thickness of 3.5-inches. The machined pancakes were chemically milled (chem-milled) in a standard hydrofluoric-nitric acid aqueous solution (3% HF, 30% HNO₃) for removal of surface contaminants. Figure 7 depicts two typical machined and chem-milled pancakes. The chem-milled surfaces of two pancake segments were mated and the assembly was placed on a stainless steel plate, Figure 8. A prefabricated expendable stainless steel cover with an air evacuation tube was positioned over the pancake assembly, Figure 9, and the steel container (retort) was sealed by a Tungsten Inert Gas (TIG) weld. This procedure was followed for all five of the assemblies to be bonded.

In order to establish a heating cycle for an evacuated retort, an additional test retort was fabricated. The same general procedures were used in fabrication of this unit as described for the five pancake assemblies. The only exception was the use of a 6.5-inches thick by 16-inches diameter solid Ti-6Al-4V billet which had a 1/2-inch diameter hole drilled along its longitudinal axis to the center of the 6.5-inches thickness dimension in order to position a thermocouple. A thermocouple was inserted and packed into the stainless steel tube and connected to a recording unit. The assembly was helium leak tested, thermally outgassed and sealed. The assembly was placed in a furnace and a relationship of time versus temperature for the billet was established. This data was subsequently used with the five test retort assemblies. Figure 10 shows the test retort assembly with the thermocouple and recording instrument.

A preheat cycle was used to outgas the pancake forgings prior to bonding. Each retort was evacuated to 10⁻⁴ Torr, heated to 1350°F for one hour and cooled to room temperature. The evacuation tube was sealed with a minimum of 10⁻⁴ Torr inside the retort. The sealed retort units were subsequently heated to their respective bonding temperature and approximately 10% linear deformation was attempted. Conditions 1 through 4 were forge-diffusion bonded on a 1500-ton press. Because of the low bonding temperature,

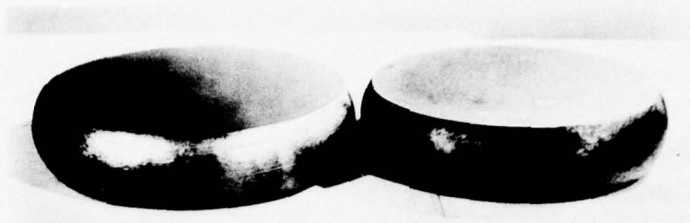


FIGURE 7. TWO TYPICAL MACHINED AND CHEMICALLY CLEANED PANCAKES.



FIGURE 8. PANCAKE ASSEMBLY POSITIONED ON STAINLESS STEEL PLATE.

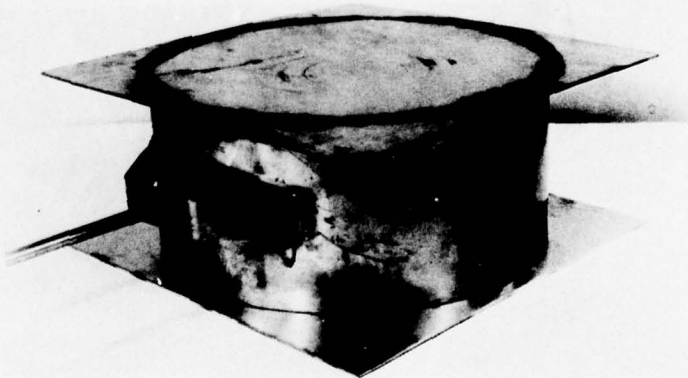


FIGURE 9. STAINLESS STEEL RETORT PRIOR TO FINAL WELD SEALING.



FIGURE 10. TEST RETORT WITH THERMOCOUPLE AND RECORDING INSTRUMENTATION.

1300°F, of pancake assembly Condition 5, it was upset on a 6000-ton press. The entire capacity of the press was used and only an 8% reduction could be achieved. Details of the forge-diffusion bond process parameters are provided in Table III.

TABLE III						
DETAILED PROCESS PARAMETERS						
PANCAKE FORGING ASSEMBLIES						
PROCESS PARAMETERS		PROCESS CONDITION				
		1	2	3	4	5
FORGE	Pre Heat Temp. (°F)	1750	1900	1900	1900	1900
	Pre Heat Time (Hrs.)	5	5	5	5	5
	Forge Temp. (°F)	1750	1900	1900	1900	1900
	Cool	Water-Quench	Water-Quench	Water-Quench	Water-Quench	Water-Quench
FORGE-BOND	Pre Heat Temp. (°F)	1350	1350	1350	1350	---
	Pre Heat Time (Hrs.)	1	1	1	1	---
	Bond Temp. (°F)	1750	1750	1900	1900	1300
	Total Furnace Time (Hrs.)	8	8	10	10	8
	Bond Pressure (Tons)	550	550	250	300	6000
	Bond Time (Min.)	1.5	3.25	1.2	1.4	1.83
	Component Thickness Start (inches)	7	7	7	7	7
	Component Thickness Finish (inches)	6.27	6.38	6.24	6.30	6.45
DIFFUSION TREATMENT	Post Heat Temp. (°F)	1900	1900	---	1900	1300
	Post Heat Furnace (Hrs.)	4	4	---	4	4
	Cool	Water-Quench	Water-Quench	Water-Quench	Water-Quench	Air Cool
	1300°F Anneal	2 Hrs.	2 Hrs.	2 Hrs.	2 Hrs.	---
	Air Cool	At Heat	At Heat	At Heat	At Heat	

3.2 Pancake Inspection

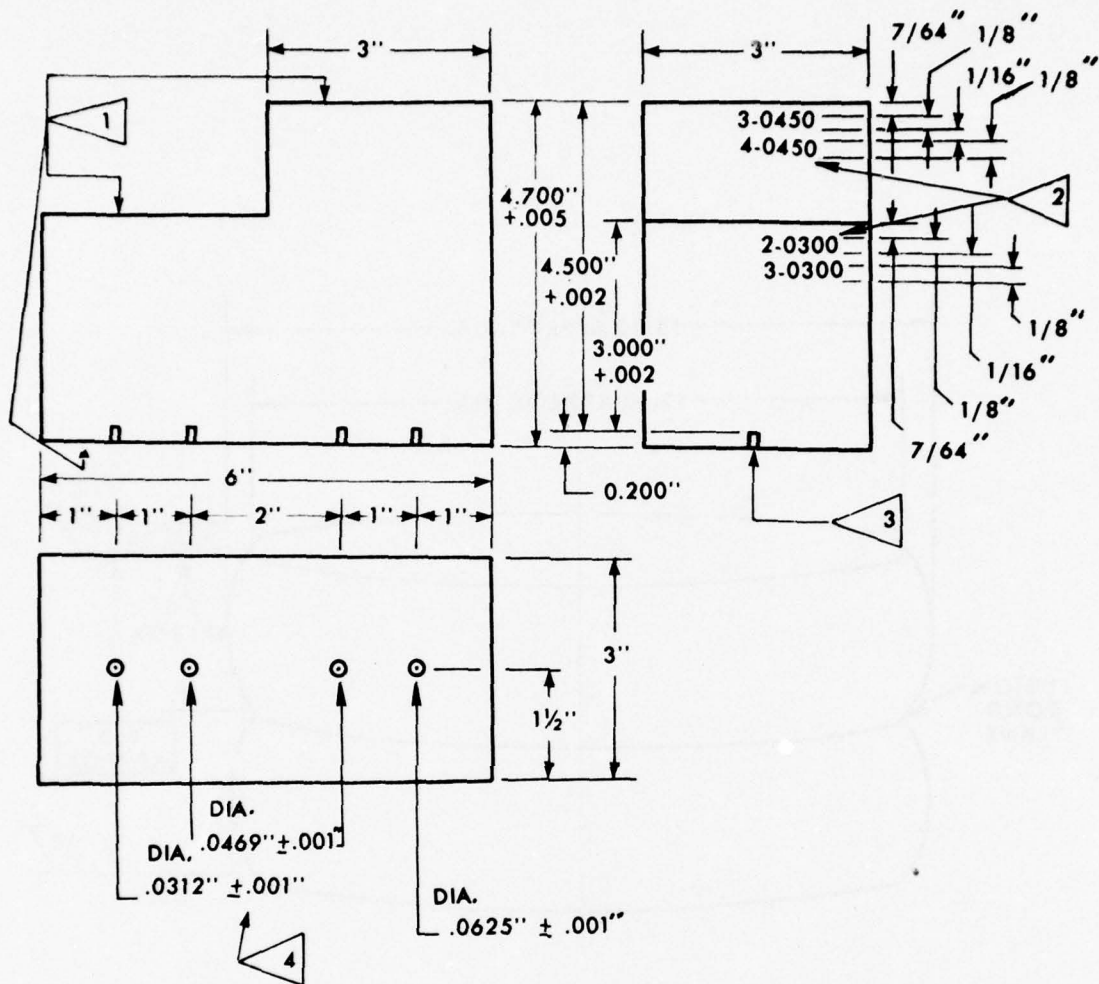
3.2.1 Procedure

Visual inspection was performed for any obvious defects or abnormalities. Ultrasonic evaluation was performed to detect areas of nonbonding at the bondline. Metallographic examination was conducted on those areas at the bondline that manifested ultrasonic indications.

Prior to detailed ultrasonic inspection of the bonded pancake assemblies, a reference block was fabricated. The block was of a required configuration and dimension. The design incorporated the distances from the bondline to the external surface of both the pancake assemblies and the hub arm segment. Flat bottom holes (fbh) of specific diameters and depths were drilled into the block. The dimension from the base of the holes to the opposite surfaces of the reference block corresponded to the dimensions from the bondline to the outer surface of the pancake assemblies and the hub arm segment. The reference block was machined from Ti-6Al-4V beta solution treated and overaged (β -STOA) forging material in accordance with the drawing requirements specified in Figure 11.

The five bonded pancake assemblies, approximately sixteen-inches in diameter, six-inches thick, and weighing two-hundred pounds each, were machined on the top and bottom surfaces to an ultrasonic inspection configuration as shown in Figure 12. Ultrasonic inspection was performed by Automation Industries, Inc., Danbury, Connecticut. The inspection technique used was a pulse-echo immersion method equipped with a direct read-out C-scan which manifested signals from the bond area above the sensitivity setting of a known anomaly as calibrated by the reference block.

An ultrasonic application study successfully demonstrated the feasibility of detecting lack of bond in diffusion bonded pancake assemblies. The search unit directed a pulse beam through water, normal to the flat face of the upper pancake. A schematic of the system is illustrated in Figure 13. Three principle echo signals appeared: an echo from the water-to-pancake interface (IF); an echo from the bond area (BA) between the two pancakes; a back reflection (BR) from the bottom of the lower pancake. For convenience in viewing the three principal signals in detail, the start of the sweep was delayed in order that the transmitted initial pulse was not displayed. Figure 14 illustrates a typical screen pattern observed from the test. A transgate was adjusted in gate Start and gate Width to select the echo from the bond. Its alarm level was adjusted to select the minimum amplitude signal to be recorded.



NOTES:

1. Faces must be flat within 0.0002" and parallel within 0.001".
2. Vibroetch these numbers on indicated faces at locations shown.
3. Holes must be straight and perpendicular to entry surface within 0° - 30' and located within 0.010" of longitudinal axis.
4. Hole bottoms must be flat within 0.001" and finished size must be the required diameter +0.001".
5. All surfaces to have a surface roughness not to exceed 63AA.

FIGURE 11. REFERENCE BLOCK FOR ULTRASONIC INSPECTION STANDARD.

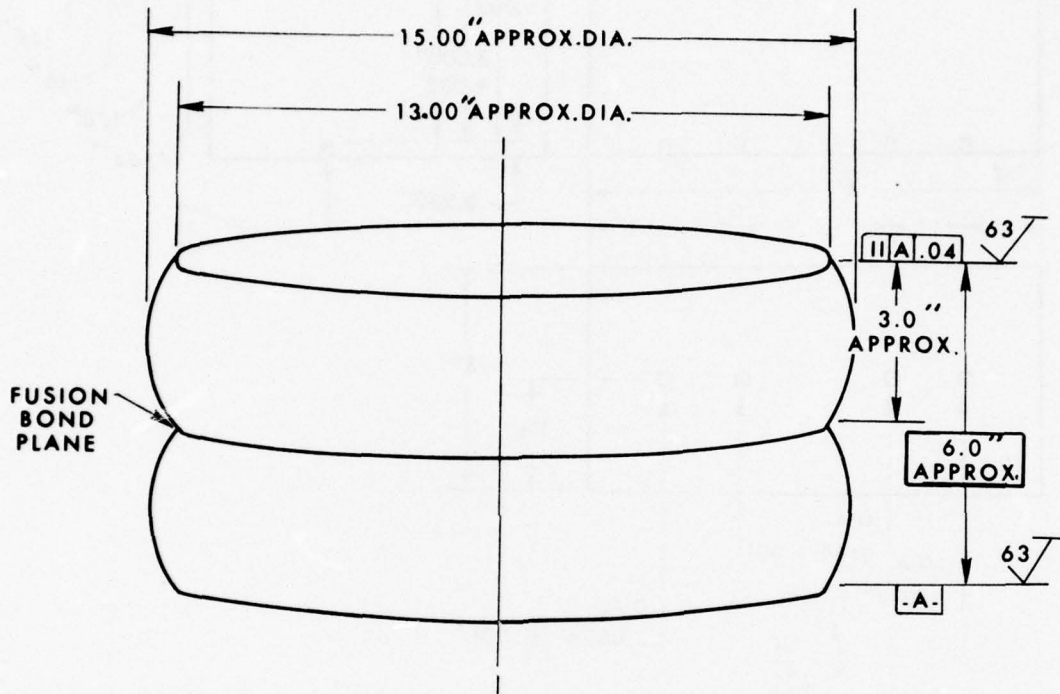


FIGURE 12. FORGE-DIFFUSION BOND PANCAKE ASSEMBLY,
ULTRASONIC INSPECTION CONFIGURATION.

Details of the Transigate operation are provided in Figure 15. A bond echo signal occurring within the gate and above the selected alarm level, was transmitted to a C-scan recorder. The search unit, carried by a bridge above the tank, scanned in the lateral dimension of the tank. At the end of each scan, the bridge indexed a small increment, 1/64-inch in the longitudinal dimension of the tank, such that, a complete XY-scan of the assembly was obtained. A paper recorder followed the motion of the search unit in a one-to-one ratio. Signals from the bond area above the alarm level record negatively-blank, void, no indication; signals below the alarm level record positively - visually observed on the paper. Best results were obtained through the use of Search Unit SIL 5MHz/ 3/4" --- 57A8375 at a water distance of 2 1/2".

Metallographic examination was conducted on longitudinal cross sections of the pancake assemblies that manifested ultrasonic indications at the bondline. Metallurgical samples cut from the bondline of the longitudinal cross sections were mounted in Bakelite resin, polished to a mirror finish, etched with Krolls etchant for 30 to 45 seconds and examined metallographically up to 1000 magnification. This inspection was conducted in an attempt to correlate the ultrasonic indications as related to their qualitative and dimensional characteristics.

3.2.2 Results

After the bonded pancake assemblies were removed from the retort, visual examination showed no gross discoloration due to elevated temperature contamination. Four of the pancake assemblies, Conditions 1 through 4 indicated bonded assemblies, while the fifth, Condition 5, displayed considerable lack of bond. The low bonding temperature, 1300°F is the significant variable for Condition 5 and is attributed as the cause for the lack of bonding.

Ultrasonic inspection of the five pancake assemblies, Conditions 1 through 5, to 100% of the signal from a #2 fbh in the reference standard block revealed that each of the assemblies manifested indications of nonbonded area. The nonbonded areas were located predominately along the circumference, in a ring, around the periphery of the mating surfaces. The indications of nonbonded areas located away from the peripheral faying surface ranged less than 5% in pancake assembly Condition 1, 15% - 25% in assemblies Conditions 2, 3, and 4; and greater than 90% in assembly Condition 5. Figure 16 depicts C-scan recordings of each of the five pancake assemblies at this sensitivity level. When the sensitivity level was decreased to 100% of the signal from the #3 fbh in the reference standard block, the

indications of nonbonded areas were significantly decreased. The indication of nonbonded areas were less than 1% for assemblies Condition 1, and less than 5 to 15% for assemblies Conditions 2, 3, and 4. The most severe condition was Condition 5, the low temperature bonded assembly which exhibited 89% nonbonded area. C-scan recordings of each of the five pancake assemblies at this sensitivity level are provided in Figure 17.

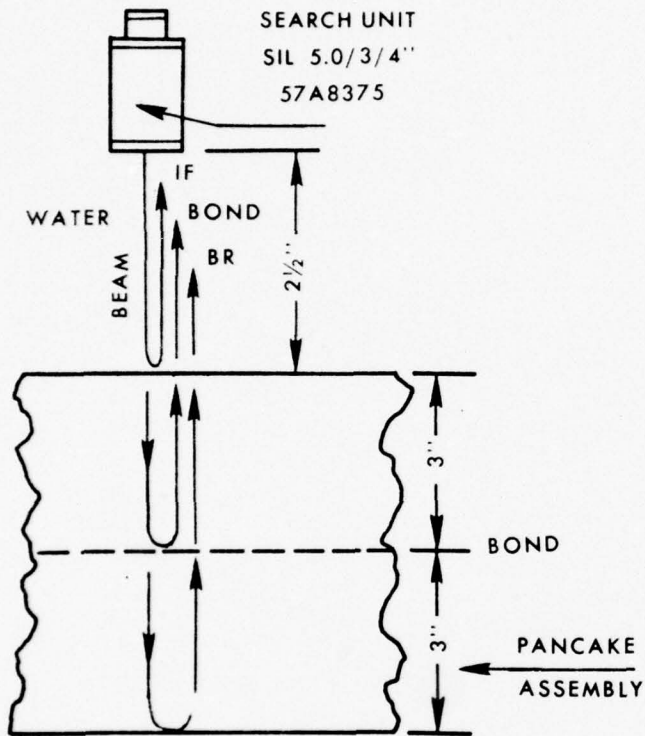


FIGURE 13. SCHEMATIC OF ULTRASONIC SYSTEM.

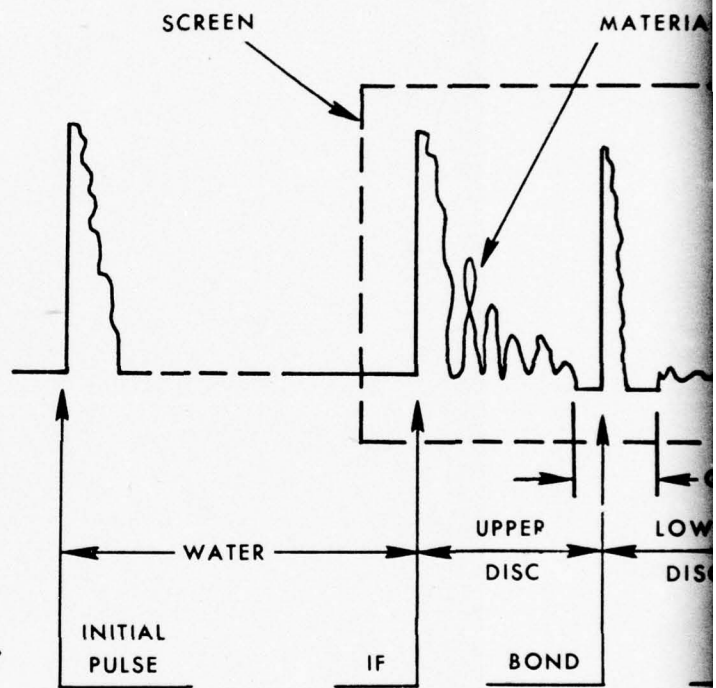


FIGURE 14. TYPICAL SCREEN PATTERN.

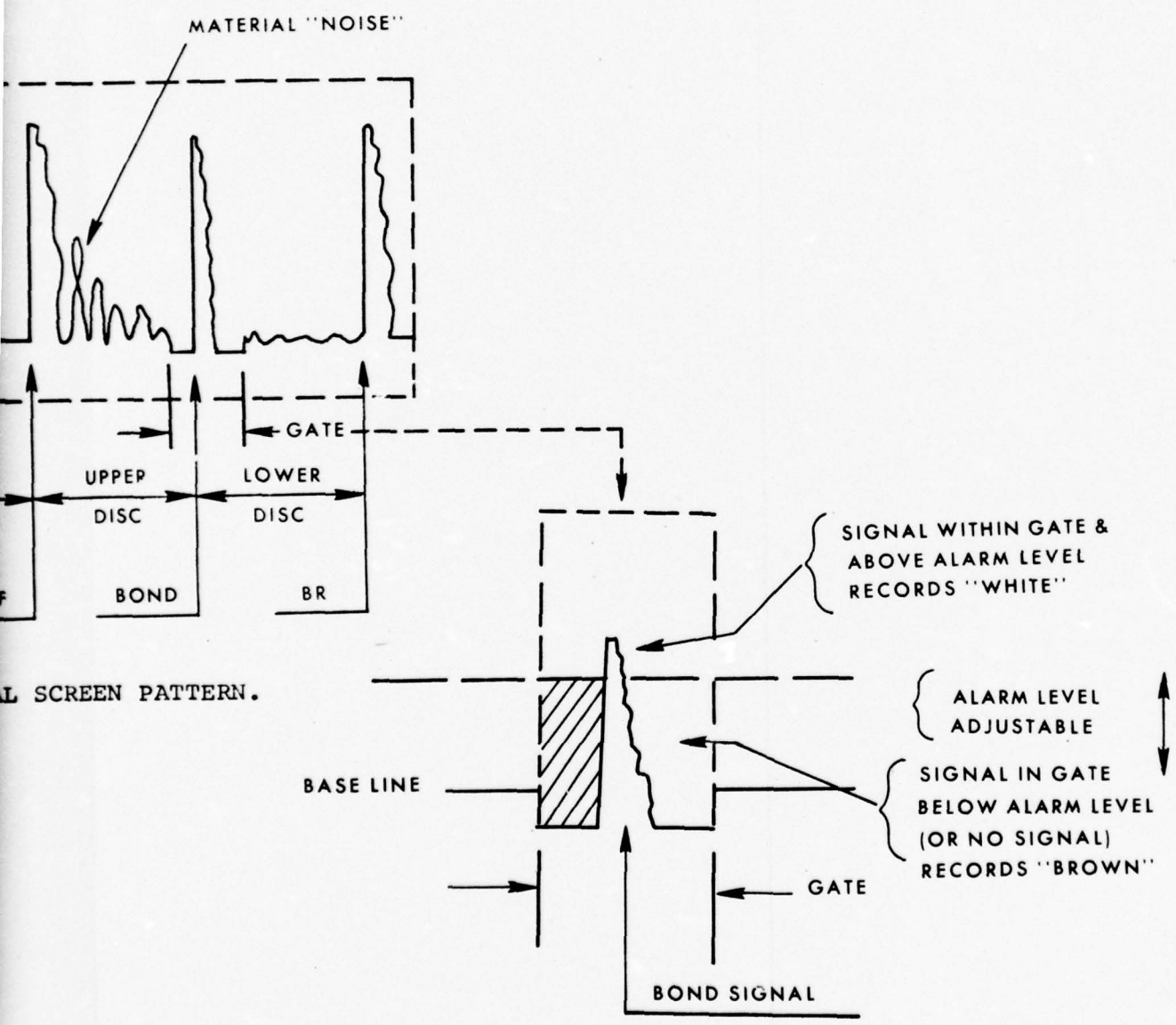


FIGURE 15. DETAILS OF THE TRANSIGATE OPERATION.

2

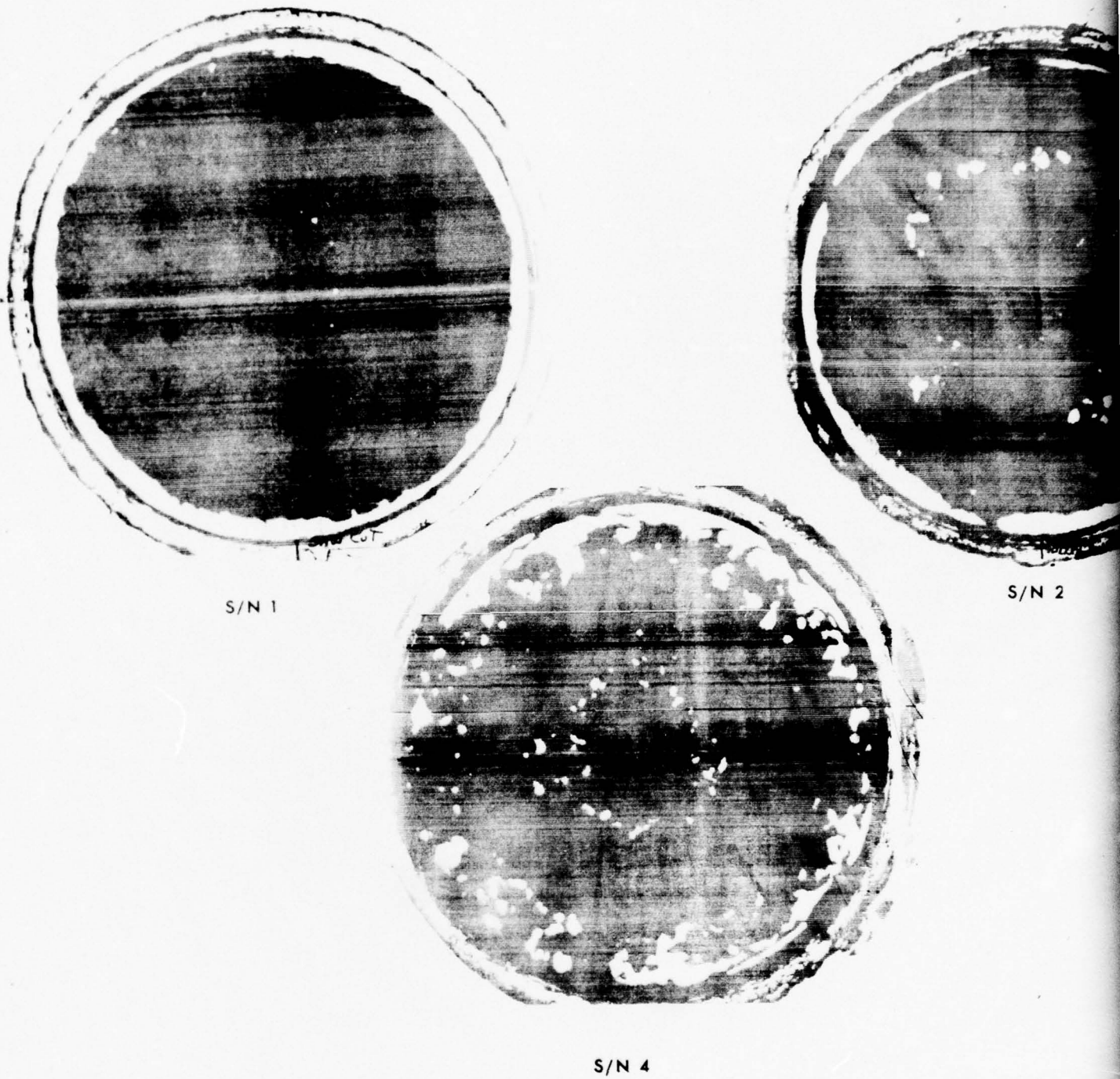
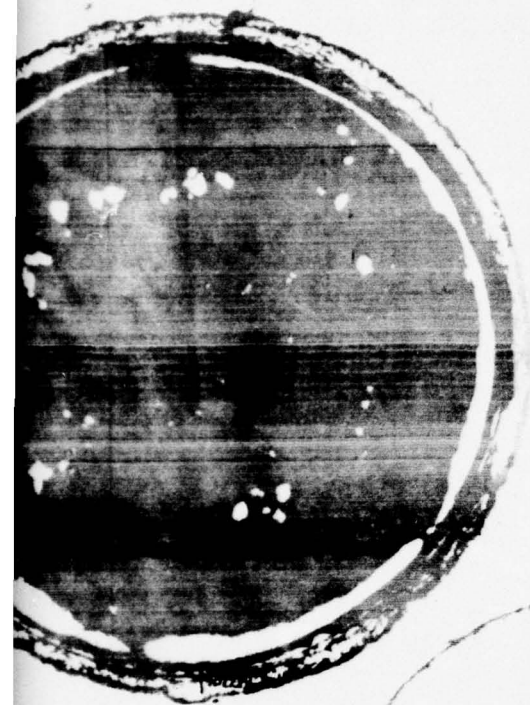


FIGURE 16. C-SCAN RECORDINGS OF FIVE PANCAKE ASSEMBLIES,
ALARM LEVEL 100% OF #2 fbh IN REFERENCE BLOCK.



S/N 2



S/N 3

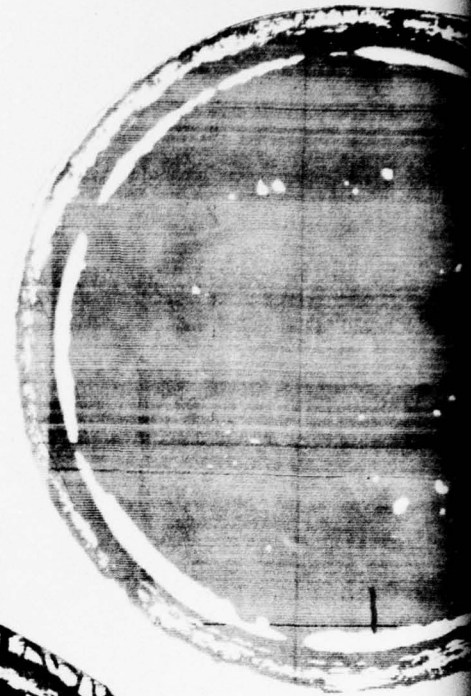


S/N 5

2



S/N 1

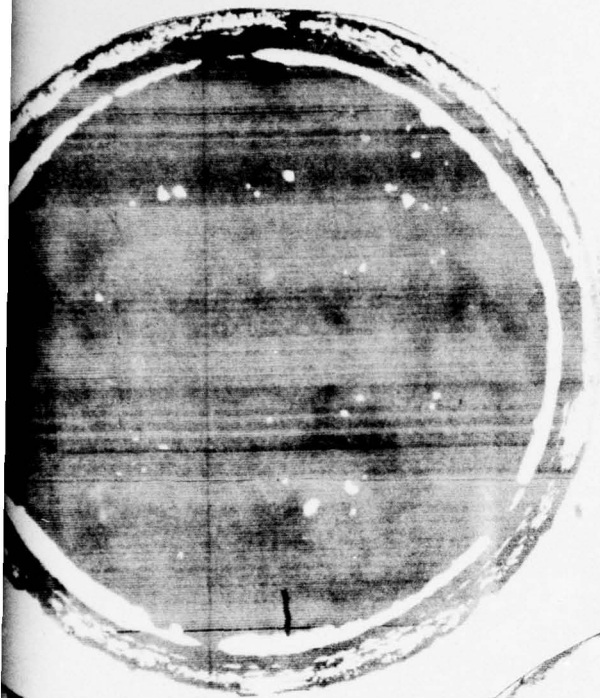


S/N 2



S/N 4

FIGURE 17. C-SCAN RECORDINGS OF FIVE PANCAKE ASSEMBLIES,
ALARM LEVEL 100% OF #3 fbh IN REFERENCE BLOCK.



S/N 2



S/N 3



S/N 5

2

Metallographic examination of longitudinal cross sections of pancake assemblies at areas manifesting ultrasonic indications confirmed the evidence of contamination or possible lack of bond along the bondline at the outer periphery of all of the pancakes. Other abnormalities were detected at some of the other sonic indications within the center areas of the pancakes but they could not be directly correlated to the indications observed on the C-scan recordings as related to size and shape. Figure 18 shows typical abnormalities at the bondline within the center area of one of the pancakes. The ultrasonic inspection would detect an abnormality above the alarm level established on the standard reference block. However, the actual size and shape of the abnormality was not directly represented on the C-scan recording. Later in the program, during inspection of the risk reduction segment, it was demonstrated, that the lack of correlation between sonic and metallographic examination was associated with the difference in material acoustic behavior and configuration between the reference standard block and pancake assemblies. The consistent lack of bond in the periphery of the pancakes is attributed to contamination caused by outgassing of the retort assemblies when heated from 1350°F up to the bonding temperature. As discussed previously in Section 3.1, the assemblies had been preheated to 1350°F, evacuated and sealed. This procedure was subsequently changed during the risk reduction single arm fabrication.

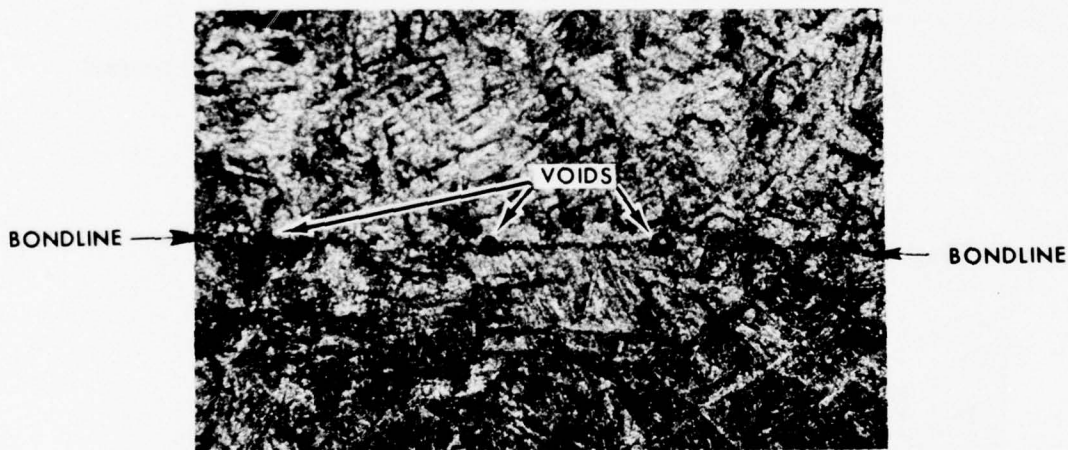


FIGURE 18. TYPICAL ABNORMALITIES
OBSERVED AT BONDLINE. 50X

3.3 Pancake Mechanical Property Testing

3.3.1 Procedure

General - The five diffusion bonded pancake assemblies were used to provide a mechanical property data base to aid in the selection of the processing of the single hub arm risk reduction segment. Mechanical properties tests consisting of tensile, fracture toughness, in-line shear, and fatigue initiation were conducted on all pancake assemblies except Condition 5. This pancake assembly Condition 5 exhibited a very limited bond area, insufficient for adequate testing. Condition 5 was, therefore, eliminated as a possible candidate for the risk reduction component. The remaining bonded pancake assemblies, Conditions 1, 2, 3, and 4, were sectioned in half, along the sixteen-inch diameter. Nine fatigue initiation specimens and three each: tensile, fracture toughness, and in-line shear specimens were fabricated and tested from each of the four pancake assemblies. Figure 19 illustrates the type of specimen tested and the general location of the specimens within the assembly. All test specimens, tensile, fracture toughness, in-line shear, and fatigue initiation, were fabricated in a manner to insure testing along the bondline.

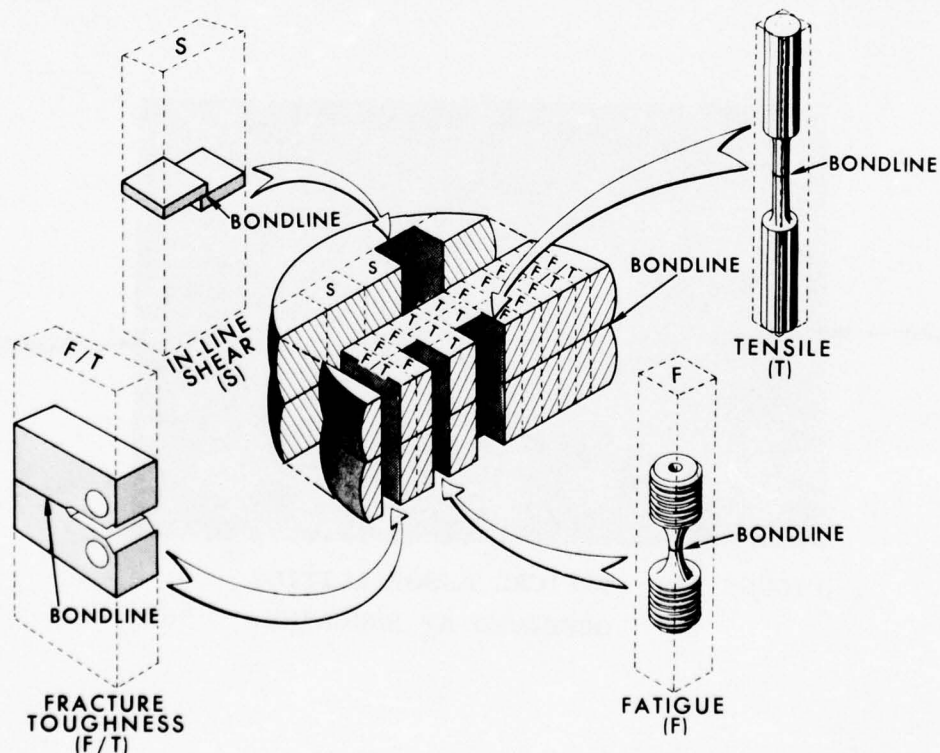


FIGURE 19. SKETCH OF PANCAKE HALF ILLUSTRATING TYPE AND LOCATION OF TEST SPECIMENS.

Tensile - Tensile tests were performed on a Riehle PS-60 Universal Testing Machine in general accordance with ASTM Method E8-68 (Reference 5) and Federal Test Method STD 151a (Reference (6)) on standard round two-inch gage length specimens as shown in Figure 20. Yield strength at 0.2% offset, ultimate tensile strength, elongation in two-inch and reduction of area were determined.

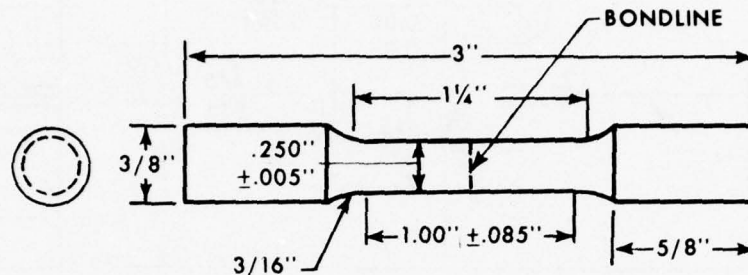


FIGURE 20. TENSILE SPECIMEN CONFORMS TO FEDERAL TEST METHOD STD NO. 151a.

Fracture Toughness - Fracture toughness, K_{IC} testing was performed on Compact Tension Specimens in accordance with ASTM Method E399-72, Reference (7). The specimen design selected is shown in Figure 21. Fatigue precracking was accomplished on a Sonntag SF-1-U Universal Fatigue Testing Machine by loading through spherical bearings. Microwire was bonded to the sides of the specimens in order to shut-off the machine at the desired crack length. Figure 22 provides a view of a typical fatigue precracking set-up. Fracture testing was performed on a Riehle PS-60 testing machine as shown in Figure 23. Loads were determined from a calibrated load cell with a 20,000 pound capacity. Deflection at the notch was recorded from a MTS Model-632.01 deflection gage which was attached to the specimen by means of integral knife edges machined into the specimen. Load deflection graphs were automatically plotted using an Electro-Instrument General Purpose Amplifier Model 420 and Moseley X-Y Recorder. A physical calibration of the deflection gage and R_{cal} values for load and deflection were obtained prior to testing each group of specimens. Testing was performed in the normal laboratory environment at a loading rate of 6,000 pounds per minute, equivalent to a stress intensity loading rate of about 40,000 psi $\sqrt{\text{in.}}$ per minute.

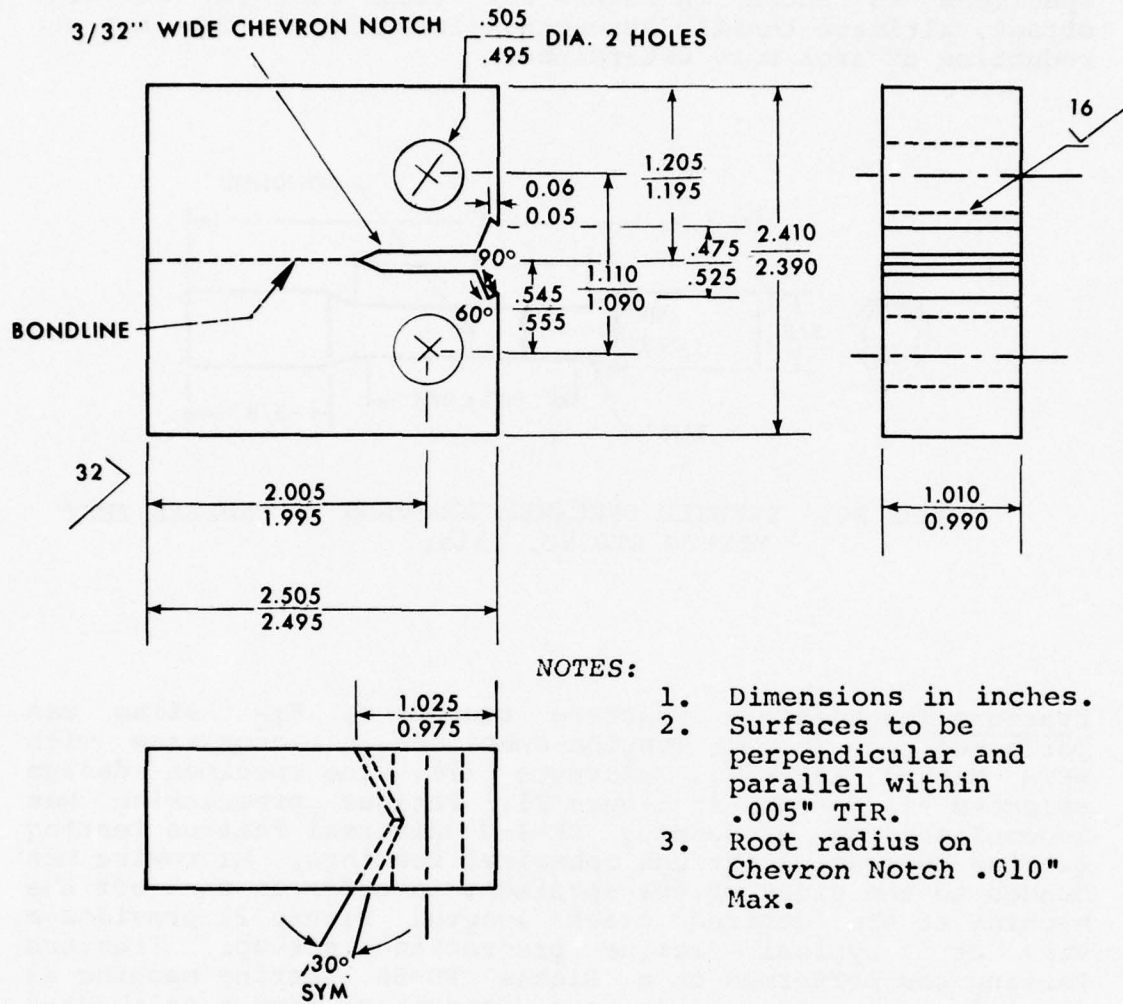


FIGURE 21. COMPACT TENSION, FRACTURE TOUGHNESS SPECIMEN CONFORMS TO ASTM-E399-72.

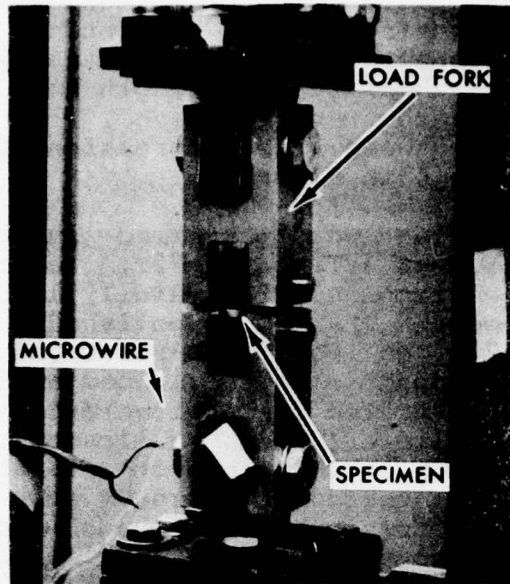


FIGURE 22. FRACTURE TOUGHNESS SPECIMEN, FATIGUE PRECRACKING SET-UP IN SONNTAG TESTING MACHINE.

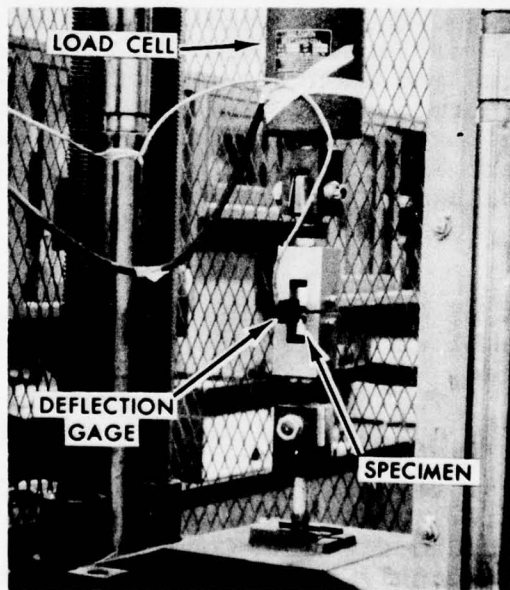


FIGURE 23. FRACTURE TOUGHNESS SPECIMENS, SET-UP IN RIEHLE TESTING MACHINE.

Shear - In-line shear tests were performed on a Riehle PS-20 Universal Testing Machine in a guillotine fixture with specially designed square stepped specimens, as illustrated in Figure 24. Single shear yield strength at 0.2% offset and ultimate shear strength were obtained. A view of the guillotine fixture between the compression heads of the testing machine is shown in Figure 25.

Fatigue - Fatigue testing was performed in accordance with the general procedures of ASTM-E-466-72T, Reference (8) in a room temperature environment with axially loaded elliptical reduced section smooth ($K_t = 1.0$) polished specimens, as shown in Figure 26, on Sonntag SF-1-U-Universal Fatigue Testing Machine equipped with a 5:1 load amplifier. Loads were measured by a calibrated full bridge axial load cell and Ellis BA-12 Bridge Amplifier and Oscilloscope Console. An overall view of the fatigue testing system is shown in Figure 27. All specimens were tested at a steady mean stress of +20 KSI. At least two specimens from each bonded pancake assembly, were tested at each of the following three test levels: Maximum stresses of 90,000 psi (20,000 + 70,000 psi), 80,000 psi (20,000 + 60,000 psi) and 70,000 psi (20,000 + 50,000 psi).

Failure Analysis - Fractographic analysis and metallographic examination was performed on failed test specimens to confirm the mode of failure, establish the location of failure initiation, determine the presence of any abnormality that could have caused or contributed to the failure and to attempt to correlate and identify the ultrasonic indications with the mechanical properties. All fracture interfaces and cross sections were examined utilizing low power (up to 25X magnification) stereomicroscope and high power (up to 1000X magnification) metallographic equipment.

3.3.2 Results

General - Analysis of the mechanical properties testing data on the bonded assemblies revealed that all four of the assemblies evaluated, Conditions 1, 2, 3, and 4 were generally similar. The remaining Condition 5 had been eliminated previously as a candidate for the risk reduction component because of insufficient bond area. Although the data from mechanical testing of Conditions 1, 2, 3, and 4 were generally similar, the results from pancake assemblies processed in accordance with Conditions 3 and 4 were statistically significantly lower, in three of the four modes tested, than those values of Conditions 1 and 2. Mechanical properties testing on the bonded pancake assemblies are summarized in Figure 28. Visual examination of the tensile, fracture toughness, in-line shear, and fatigue initiation specimens of each of the trial process conditions showed that

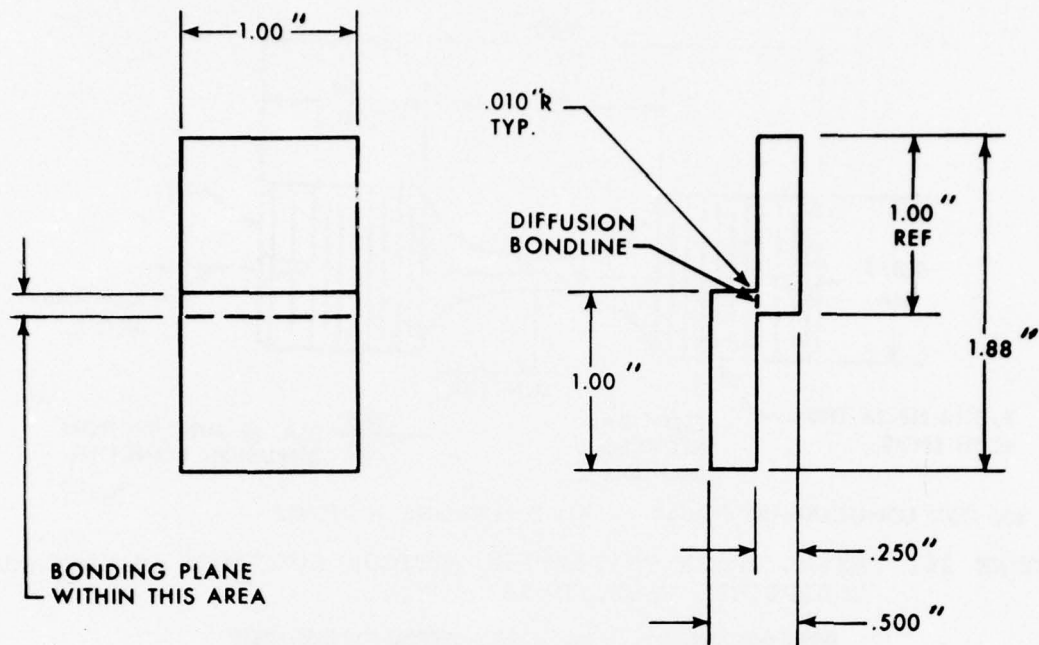


FIGURE 24. IN-LINE SHEAR TEST SPECIMEN.

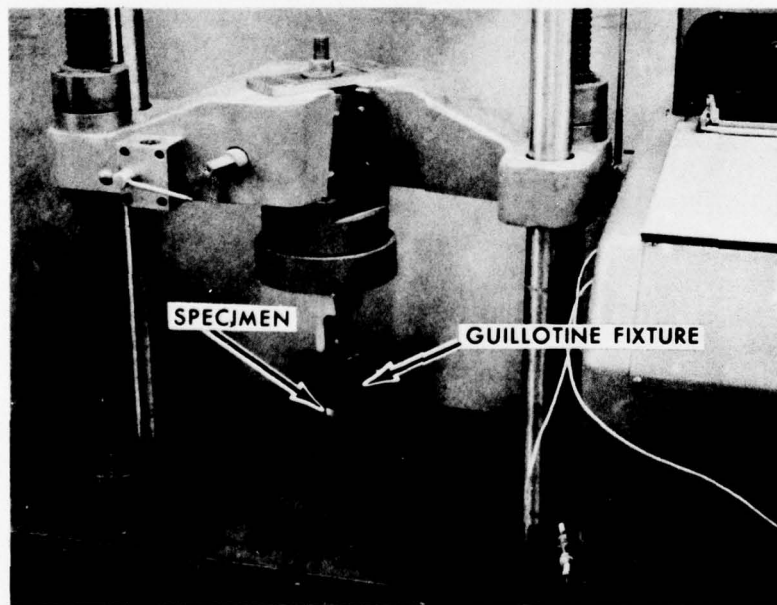


FIGURE 25. IN-LINE SHEAR SPECIMEN IN GUILLOTINE FIXTURE,
BETWEEN COMPRESSION HEADS OF TESTING MACHINE.

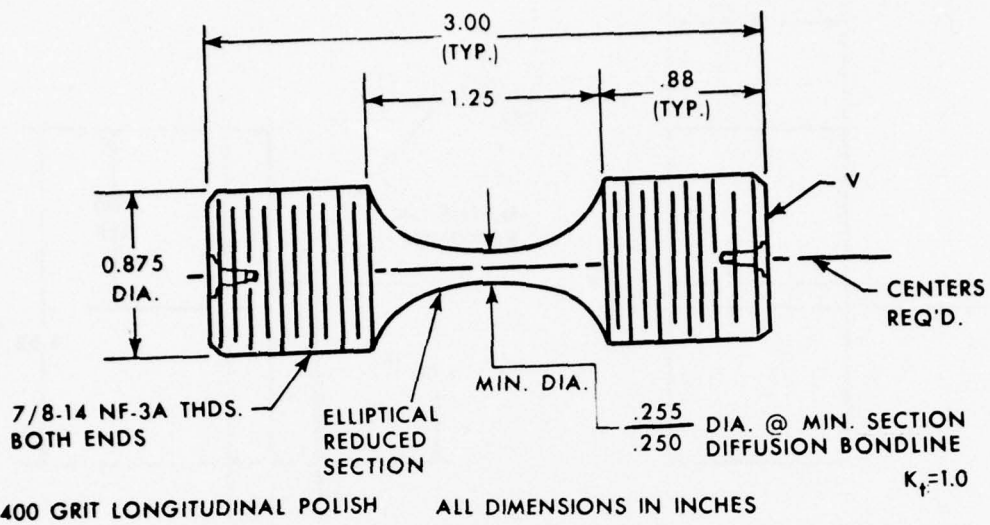


FIGURE 26. AXIAL CRACK INITIATION FATIGUE SPECIMEN UN-NOTCHED, ELLIPTICAL REDUCED SECTION.

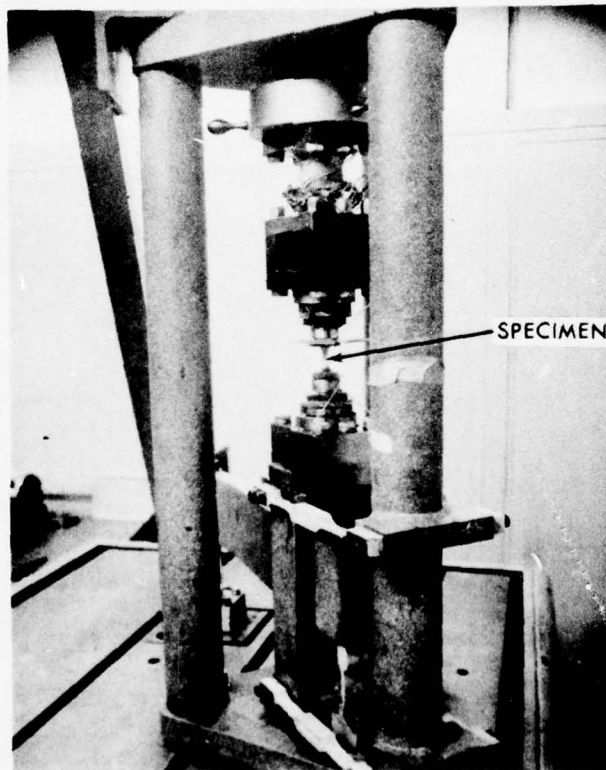


FIGURE 27. AXIAL FATIGUE TEST SET-UP IN SONNTAG TESTING MACHINE.

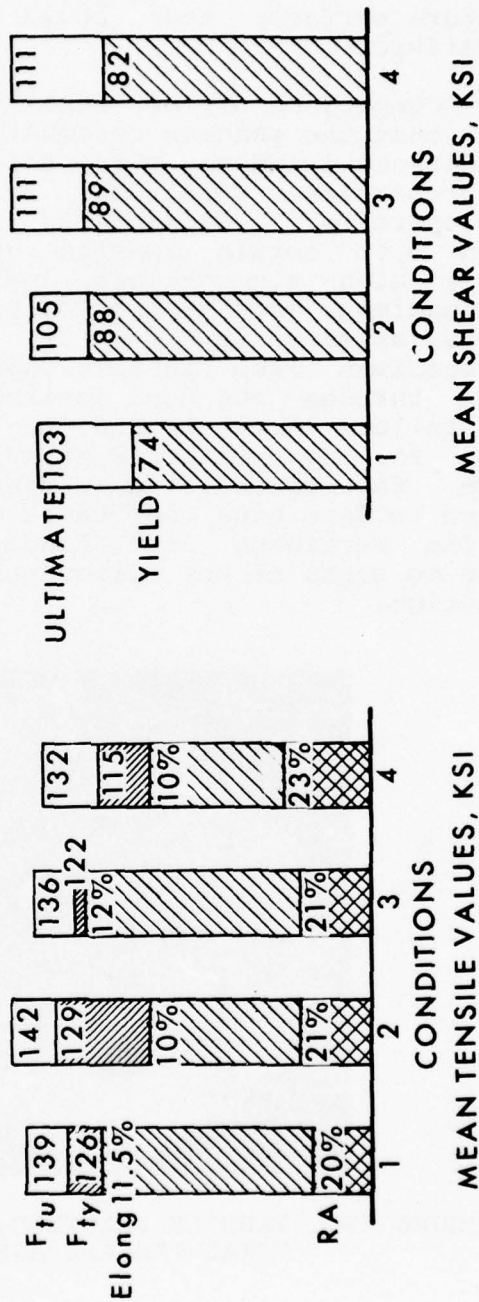
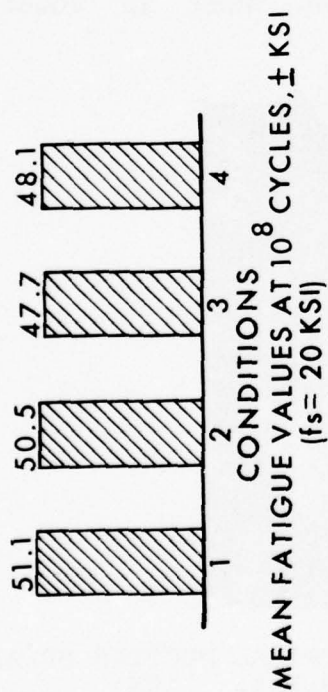
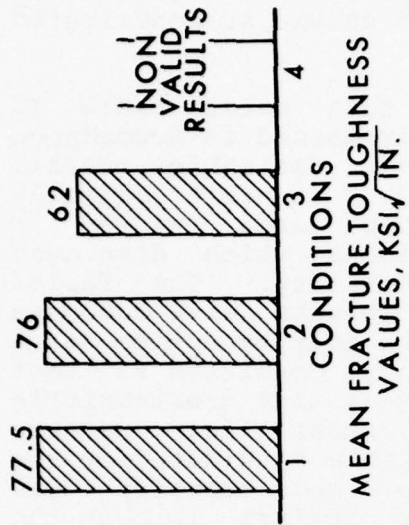


FIGURE 28. SUMMARY OF MECHANICAL TESTING, TRIAL PANCAKE ASSEMBLIES.

all the specimens separated at the test section with no apparent abnormalities present. Fracture examination of each of the specimens tested revealed the mode and mechanism of failure to be typical as related to the particular test performed. No evidence of any abnormalities were detected on the fracture surfaces that could have caused or contributed to the failure.

Tensile - Comparison of the tensile test data, Table IV revealed that the pancake assemblies processed in accordance with Conditions 1 and 2 portray the most desirable overall tensile properties. Conditions 3 and 4 exhibit generally lower properties. Sufficient bonded area existed in Condition 5 to obtain tensile specimens which displayed relatively high strength but low ductility. The failed tensile specimens were typical ductile breaks with cup-cone interfaces, as shown in Figure 29. The only exception was a single specimen from pancake assembly Condition #5 that separated through the bond manifesting a flat quasi-brittle static failure with little or no shear lip. Because Condition #5 was eliminated as a possible candidate for the hub arm fabrication, no extensive investigation was undertaken to determine the cause for failure through the bond. The remaining four Conditions, 1, 2, 3, and 4 disclosed no signs of any discrepancies such as voids or contamination.

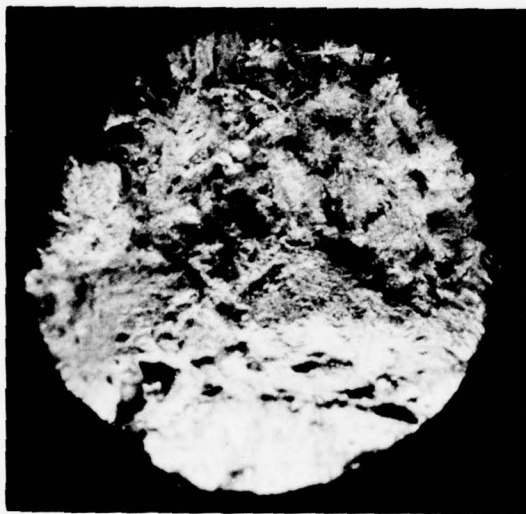


FIGURE 29. TENSILE FRACTURE, TYPICAL DUCTILE BREAK TRIAL PANCAKE ASSEMBLIES. 10X

TABLE IV
TENSILE TEST RESULTS
TRIAL PANCAKES

PROCESS CONDITION (Ref. Table III)	SPECIMEN NUMBER	YIELD STRENGTH F _{ty} (KSI)	TENSILE STRENGTH F _{tu} (KSI)	ELONGATION (%)	REDUCTION OF AREA (%)
1	T-1	128.3	141.0	11	22.0
	T-2	127.7	140.0	12	18.5
	T-3	123.5	136.7	12	21.0
	T-4	126.5	138.2	11	19.0
	AVERAGE	126.5	139.0	11.5	20.1
2	T-1	128.4	142.5	9	21.0
	T-2	129.5	142.0	9	22.0
	T-3	128.3	141.5	10	23.0
	T-4	128.8	141.5	12	19.5
	AVERAGE	128.8	141.9	10	21.4
3	T-1	118.3	134.6	13	22.5
	T-2	121.8	137.1	10	15.5
	T-3	120.9	137.0	13	22.5
	T-4	126.0	135.2	12	22.5
	AVERAGE	121.8	136.0	12	20.8
4	T-1	114.0	131.2	10	26.0
	T-2	113.7	130.5	11	21.0
	T-3	116.9	134.5	10	22.5
	AVERAGE	114.9	132.1	10.3	23.2
5	T-1	139.5	153.9	9	18.5
	T-2	138.4	152.0	10	20.5
	T-3	138.0	152.5	9	23.0
	T-4*	139.7	152.0	6	8.5
	T-5	140.1	152.0	10	19.5
	AVERAGE	139.1	152.5	8.8	13.4
Specification Requirement		SS8445 120Min.	130Min.	10Min.	25Min.

*Fractured Through Bond

Fracture Toughness - Fracture toughness results are presented in Table V. Review of the test data discloses valid and nonvalid values, as defined by the requirements in ASTM-E399-72, Reference (7). K_{IC} values which do not meet the requirements of Reference (7) cannot be reported as valid K_{IC} values and are reported as K_Q values. Condition 1 exhibits slightly higher fracture toughness characteristics than Condition 2 and 20% higher than Condition 3. All of the Condition 4 results are invalid. The fracture toughness specimens displayed fracture surfaces with normal flat brittle fatigue precracking followed by overload plane strain cracking. Crack propagation was transgranular in nature exhibiting a fine grain fracture interface for both the precrack and plane strain cracking regions as shown in Figure 30. The only variation was Condition #4 which manifested a relative coarser static fracture surface, as shown in Figure 31. No evidence of voids or contamination was observed on these fracture interfaces that could have generated the different fracture surface texture.



FIGURE 30. FRACTURE TOUGHNESS INTERFACE,
TYPICAL FRACTURE INTERFACE
TRIAL PANCAKE ASSEMBLIES. 1.5X

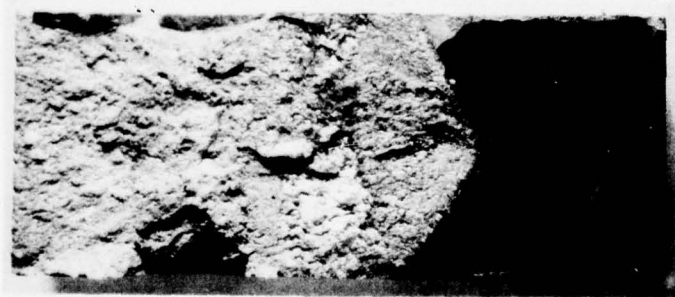


FIGURE 31. FRACTURE TOUGHNESS INTERFACE
CONDITION 4, NOTE COARSER
STATIC FRACTURE SURFACE. 1.5X

TABLE V				
PLANE-STRAIN FRACTURE-TOUGHNESS TEST DATA				
TRIAL PANCAKES				
PROCESS CONDITION (Ref. Table III)	SPECIMEN NUMBER	YIELD STRENGTH F_{ty} (KSI) (Ave. Ref. Table IV)	K_{Ic} (KSI \sqrt{in}) (K_Q)	VALID TEST Per Ref. 7
1	FT-1	127	77.7	Yes
	FT-2	127	77.3	Yes
	FT-3	127	80.0	Yes
2	FT-1	129	75.9	Yes
	FT-2	129	81.5	Yes
	FT-3	129	71.0	Yes
3	FT-1	122	52.7	Yes
	FT-2	122	70.9	Yes
	FT-3	122	(86.7)	No
4	FT-1	115	(87.9)	No
	FT-2	115	(82.6)	No
	FT-3	115	(97.0)	No
	FT-4	115	(108.4)	No

Shear - In-line shear test results are provided in Table VI. Comparison of the test data disclosed no significant differences among bonded assemblies 1, 2, 3, and 4. Slightly lower values were manifested by Condition 1, but, it does not appear to be meaningful since this amount of variation could occur within the normal scatter of testing and is typical of that found away from the bondline. In-line shear specimens manifested standard overload fractures as shown in Figure 32. The morphology of these specimens were very similar among the conditions tested with no outstanding deviations or differences. No voids or contamination were detected on the fracture surfaces.



FIGURE 32. IN-LINE SHEAR FRACTURE, TYPICAL STATIC OVERLOAD FRACTURE SURFACE, TRIAL PANCAKE ASSEMBLIES. 4X

TABLE VI
IN-LINE SHEAR TEST RESULTS
TRIAL PANCAKE

PROCESS CONDITION (Ref. Table III)	SPECIMEN NUMBER	SHEAR STRENGTH	
		ULTIMATE F _{Su} (KSI)	YIELD F _{Sy} (KSI)
1	S-1	102.0	66.0
	S-2	105.0	79.0
	<u>S-3</u>	<u>102.8</u>	<u>78.0</u>
	AVERAGE	103.3	74.3
2	S-1	106.0	96.0
	S-2	101.0	87.0
	<u>S-3</u>	<u>117.4</u>	<u>82.0</u>
	AVERAGE	108.1	88.3
3	S-1	113.8	91.0
	S-2	110.0	80.0
	<u>S-3</u>	<u>108.0</u>	<u>80.6</u>
	AVERAGE	110.6	83.9
4	S-1	108.7	85.7
	S-2	112.0	81.5
	S-3	116.0	83.2
	<u>S-4</u>	<u>106.0</u>	<u>78.0</u>
	AVERAGE	110.7	82.1
Parent Material		106.0	68.0

Fatigue - Results of the fatigue test data are summarized in Table VII. This data is also presented with mean S/N curves in Figure 33. Statistical analysis of the mean fatigue strength at 10^8 cycles for each of the four conditions plus base metal revealed no significant differences among Conditions 1, 2, and base metal. The remaining two Conditions, 3 and 4, indicated slightly lower strength. The fatigue initiation specimens exhibited surface fatigue origins. Cracking propagated in cyclic loading before complete separation of the specimens due to overload. The relationship of cyclic propagation and overload was contingent on the load level of testing. That is, the specimen tested at the higher load level manifested the smaller cyclic region and a larger static overload zone, as is expected. The fracture interfaces were generally similar with no evidence of any stress risers such as voids at the origin sight that could have initiated cracking. A typical fatigue interface is provided in Figure 34.

3.4 Process Selection For Optimum Forge-Bonding Conditions

Based on the mechanical property test data inspection of the bonded areas, and projected manufacturing costs of the five conditions evaluated, one condition was selected for fabrication of the one-sixth hub arm risk reduction segments. The selected condition was Condition #1, an alpha-beta forging which would be forge-diffusion bonded at the alpha-beta temperature of 1750°F, subsequently diffusion treated at the beta temperature of 1900°F for two hours, water-quenched, and finally, overaged at 1300°F for two hours. This condition provides the best general overall mechanical property characteristics, the highest degree of bonding of the conditions evaluated, and the most cost effective approach. The expense required to adequately control forging and bonding in the beta range (1900°F) would add considerable cost to the processing with no increase in mechanical property characteristics.

TABLE VII
FATIGUE TEST RESULTS
TRIAL PANCAKES

PROCESS CONDITION (Ref. Table III)	SPECIMEN NUMBER	VIBRATORY LOAD (+KSI)	CYCLES x1000	PROCESS CONDITION (Ref. Table III)	SPECIMEN NUMBER	VIBRATORY LOAD (+KSI)	CYCLES x1000
1	F-10	70	239	4	F-1	70	55
	F-1	70	346		F-2	70	43
	F-2	70	39		F-3	60	297
	F-12	60	1,452		F-6	60	432
	F-11	60	918		F-11	60	780
	F-3	60	482		F-4	50	4,619
	F-5	60	499		F-8	50	10,004+
	F-9	50	5,837		F-5	50	10,087+
	F-4	50	4,906		F-7	50	247
	F-8	50	10,115+				
2	F-9	70	27	Parent Material	2-3	70	265
	F-10	70	405		3-5	70	35
	F-6	70	442		3-6	70	47
	F-7	60	1,009		2-4	60	1,215
	F-8	60	38		2-1	60	1,304
	F-1	60	518		3-1	60	1,605
	F-4	50	12,663+		2-2	50	1,536
	F-5	50	2,829		3-3	50	10,000+
	F-2	50	10,000+		3-4	50	10,011+
	3	F-7	70		19		
F-2		70	84				
F-9		70	19				
F-5		60	702				
F-4		60	2,073				
F-3		60	557				
F-15		60	28				
F-6		50	4,384				
F-1		50	3,454				
F-8		50	1,174				

Steady Stress = +20KSI For All Specimens

+ Runout

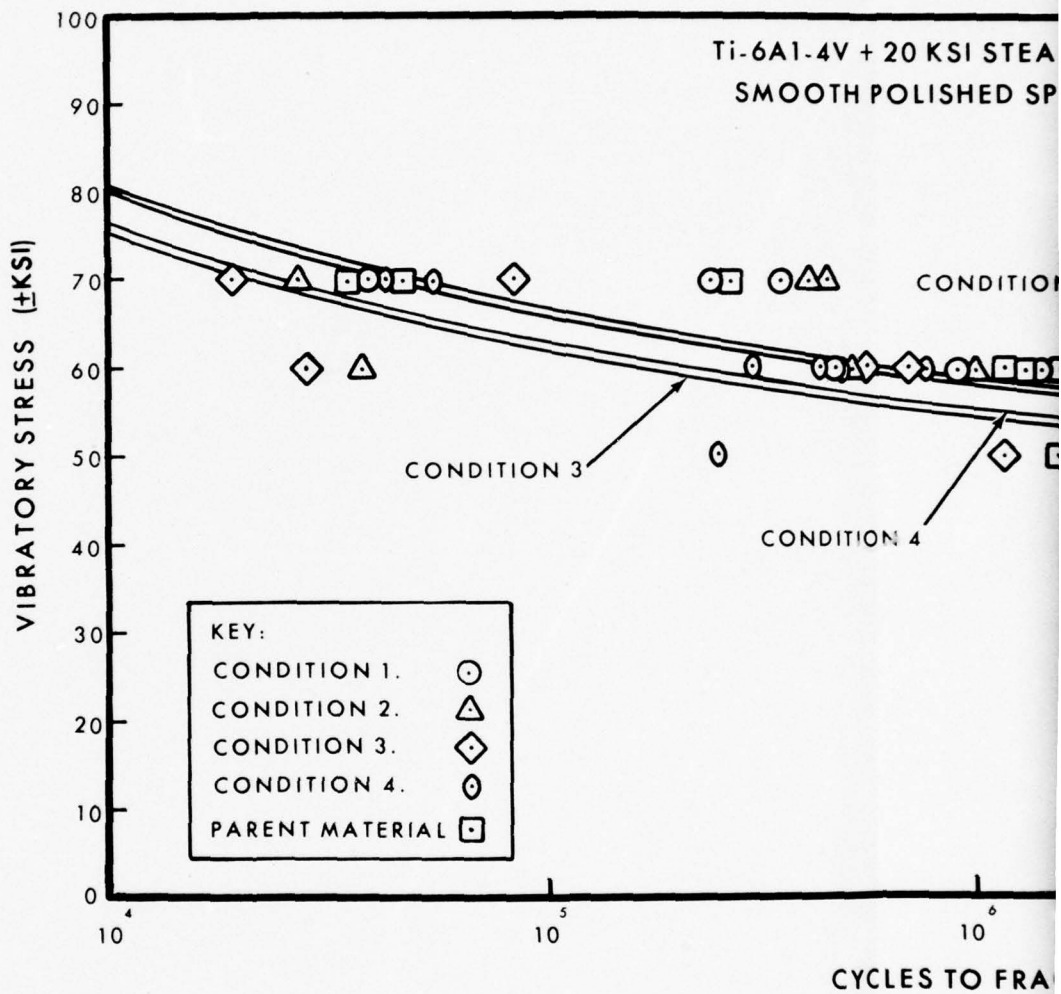
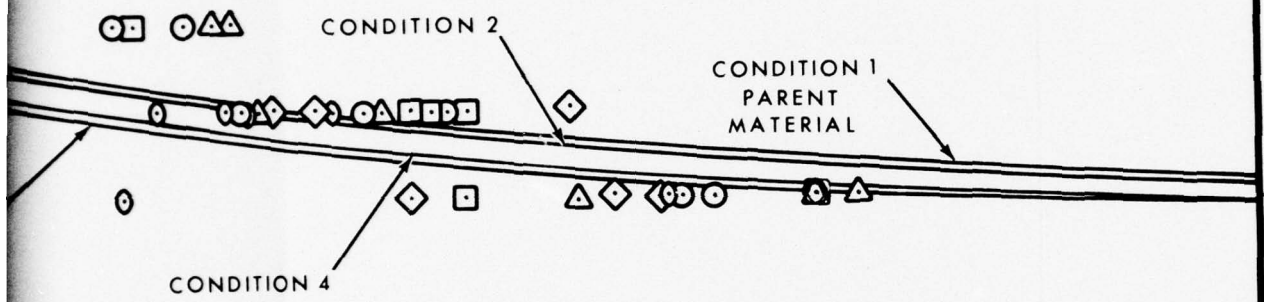


FIGURE 33. MEAN S/N CURVES FOR VARIOUS FORGE-DIFFUSION BOND PROCESS CONDITIONS.

Ti-6Al-4V + 20 KSI STEADY STRESS
SMOOTH POLISHED SPECIMENS
 $K_t=1.0$



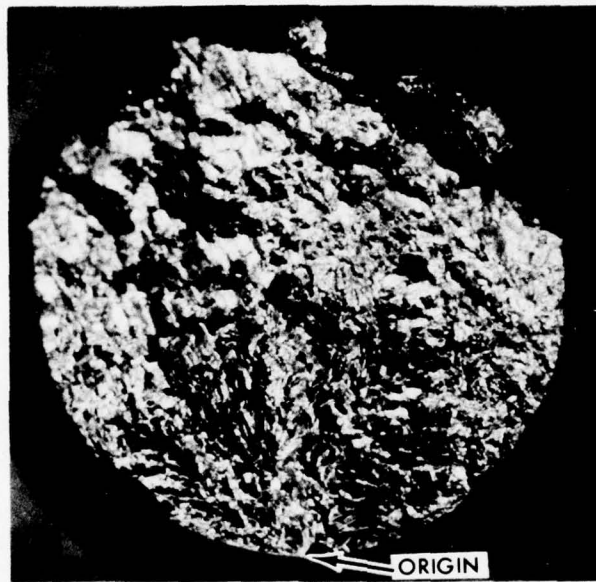


FIGURE 34. FATIGUE FRACTURE, TYPICAL BRITTLE FRACTURE SURFACE WITH ORIGIN ON O.D., TRIAL PANCAKE ASSEMBLIES. 12X

4.0 FORGE-DIFFUSION BONDED H-53 ELASTOMERIC MAIN ROTOR HUB, SELECTION OF BOND PLANE LOCATION

Structural analysis of the H-53 Elastomeric Main Rotor Hub, visual and dimensional examination of the upper and lower half of the existing forging dies and application review of the diffusion-bond process disclosed the most advantageous location for the bond plane is approximately 4.8 inches from the bottom surface of the hub.

4.1 Structural Analysis

The diffusion bond plane was selected because it was perpendicular to the rotor shaft and parallel to the former die parting plane of the integral forging. The selection of the exact location involved structural analysis of the H-53 Elastomeric Main Rotor Hub in three high stresses areas: the outer ring section, the radial spoke cross section and the central spline surfaces. The recommendation for the diffusion bonding plane was based upon the stress distribution at each of these sections. A sketch of the one-sixth arm segment and cross sections through the critical areas is depicted in Figure 35.

The outer ring section presents no real problem because the large 8-inch diameter bore is located on the outer ring between the radial spokes. Section D-D of the figure precludes the diffusion bonded surfaces from intersecting the more highly stressed vertical plane which passes through the centerline of the outer ring member, Section C-C. The total vibratory stresses, in the lower vertical section, at areas adjacent to the ring member where diffusion bonded planes might be placed, are approximately 70% lower than vibratory stresses in the upper vertical section of the ring. Therefore, it may be more advantageous for the bonding plane to be located in the lower vertical section.

The radial spoke cross section is shown in Section B-B in Figure 35. The stress distribution across this section varies from a minimum at the neutral axis plane to a maximum at the extreme top and bottom surfaces. Although the neutral axis plane is the best choice for this particular critical section, alternate horizontal planes up to 3-inches above the neutral axis still exhibit approximately 1/3 the stress levels experienced at the cross sections extreme fibers. The diagrams in Figure 36 illustrate the stress distribution across section B-B for various flight conditions.

The final hub section investigated, the central spline surface, is considered to be the highest stressed as related to the location of the diffusion bond plane. The spline tooth geometry in the central bore of the Elastomeric Hub is the same as on the current CH-53 conventional Main Rotor Hubs. The primary failure mode for the conventional CH-53 Hub has been determined from laboratory fatigue tests to be the hub splines. The origin sites of these cracked splines exhibited fretting of their contacting surfaces. Because of the high localized Hertzian stresses and relative motions developed at spline contact surfaces, an accurate comparison between analysis and service stresses is not feasible. However, since fretting is known to significantly reduce the fatigue characteristics of conventional titanium alloys and no fretting data is currently available for diffusion bonded titanium material, a diffusion bonded plane which is located just above the spline contact region is desirable.

4.2 Die Examination and Application Review

An a priori decision was made to use the existing forging dies to demonstrate the forge bond process without committing to the expense of new dies. Visual and dimensional examination of the existing dies and application review of the diffusion bond process disclosed a limitation on the vertical dimension of the upper half-forging die of the integrally forged hub and no restrictions on the bonding process providing adequate tooling is available.

Examination of the upper and lower half of the existing integral forging dies revealed that a maximum of 1-1/2 to 1-3/4 inches of material build-up in the vertical dimension of the upper die could be readily added. This limitation therefore establishes the maximum displacement of the bonding place from the parting line of the conventional hub for the fabrication of the demonstration diffusion bonded hub. The lower die presented no problem since material can be easily machined from the vertical dimension of the half-forging in order to obtain the desired bond plane location.

Review of the diffusion bond process presents no significant limitation to the bond plane location providing adequate tooling can be designed and built to maintain noncontaminated intimate surface contact during the forge-bond process.

4.3 Final Selection

The final diffusion bond plane was selected by establishing the lowest stress area within the limitation of material build-up of the existing upper die.

The final diffusion bond plane selection was approximately 1-7/16 inches above the neutral axis plane of the radial spoke cross section and approximately 1-7/16 inches below the parting line of the original integral H-53 Elastomeric Main Rotor Hub forging. That is, the bond plane is located approximately 4.8 inches from the bottom surface of the bonded hub with a vertical bond affected region of one inch. The selected diffusion bond plane is depicted in Figures 35 and 36. Selection of this location as the diffusion bond plane keeps bondline stresses to approximately 1/3 of material stresses in adjacent zones not containing a diffusion bond plane, avoids any potential surface fretting problems in the spline area, and is close enough to the hub's original forging parting plane to eliminate the need for extensive tooling being required to prepare the top and bottom halves for the demonstration of the diffusion bond process.

NOTE: DOTTED LINES INDICATE
MACHINED PART CONFIGURATION

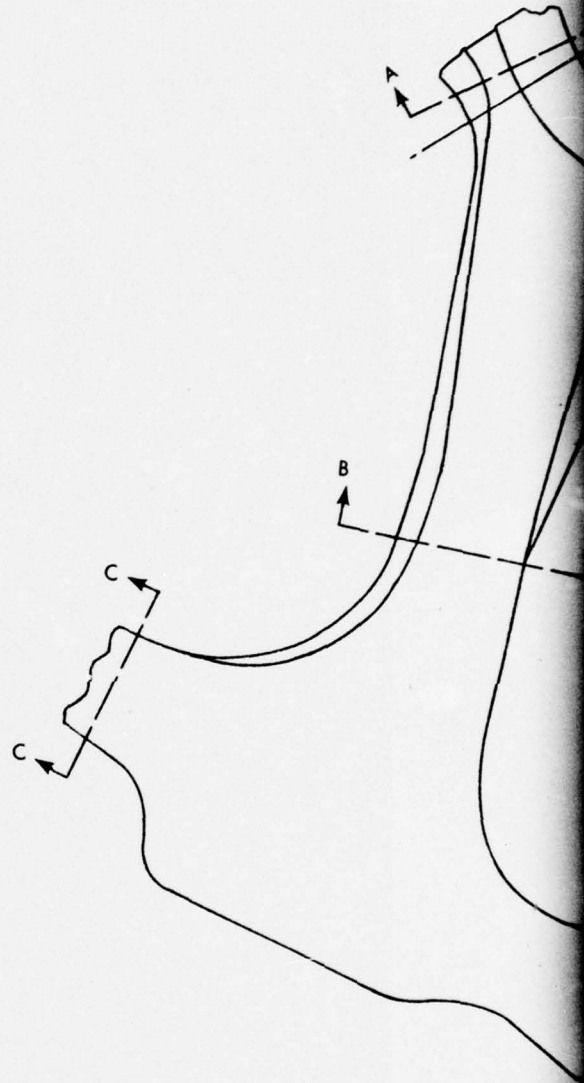
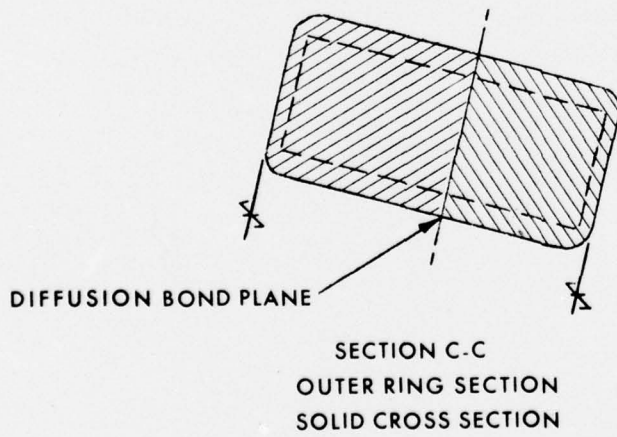
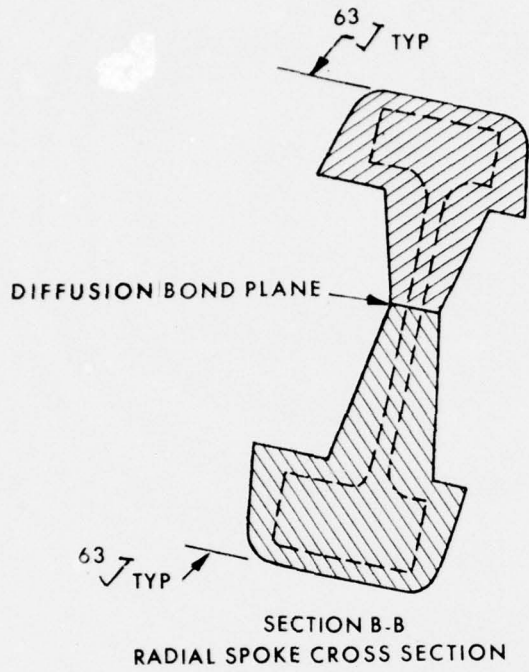
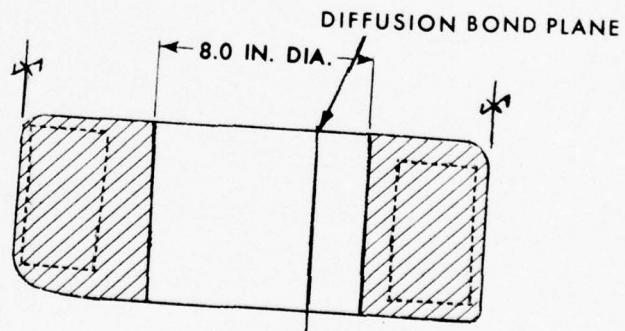
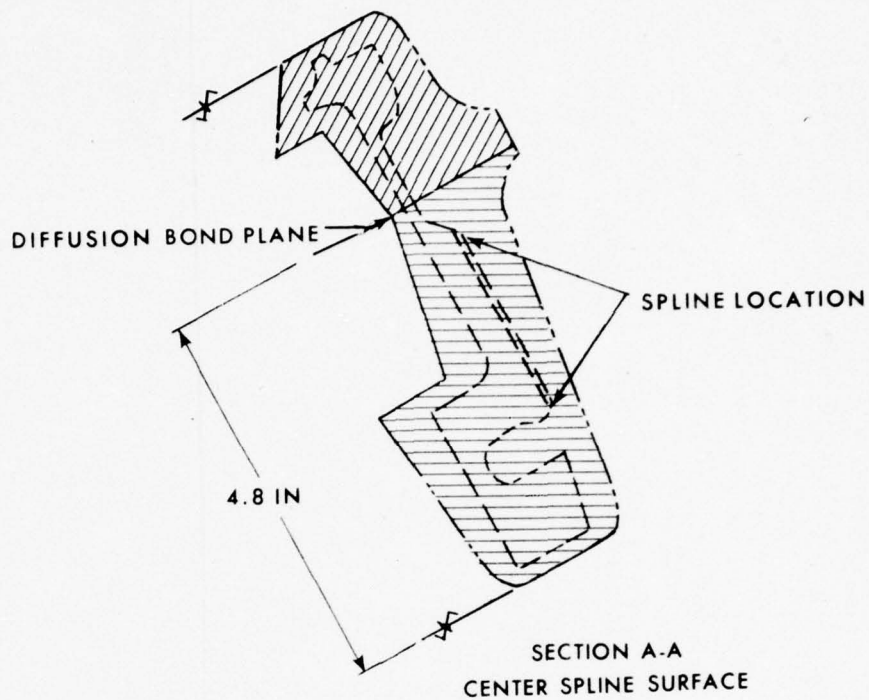
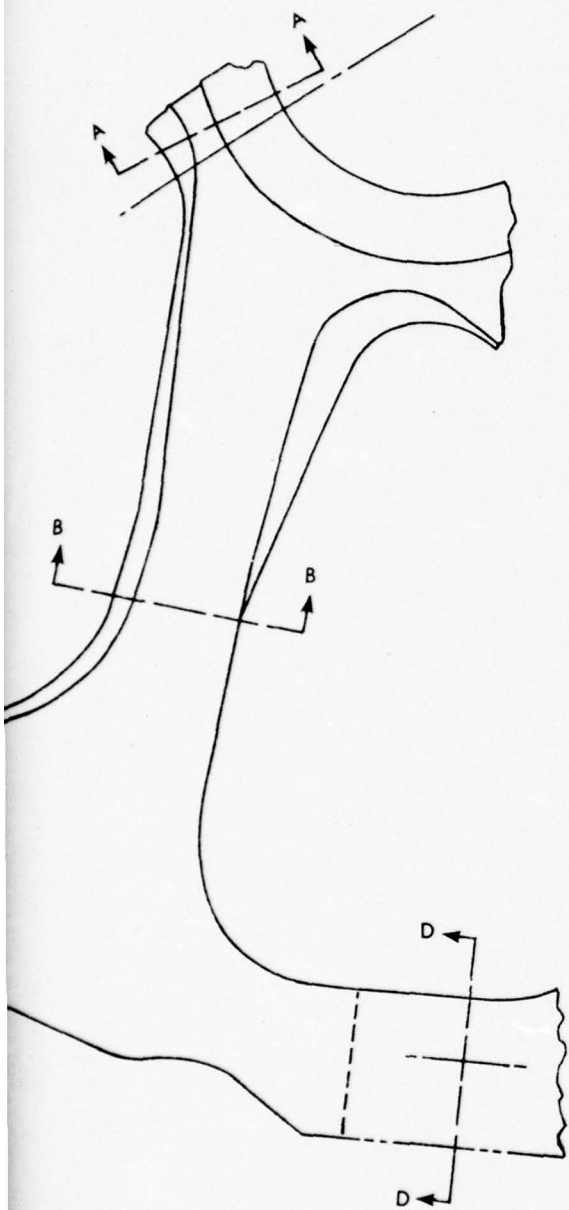


FIGURE 35. PLAN VIEW OF ONE-SIXTH HUB ARM SEGMENT
DEPICTING CROSS SECTION THROUGH CRITICAL
AREAS.



J

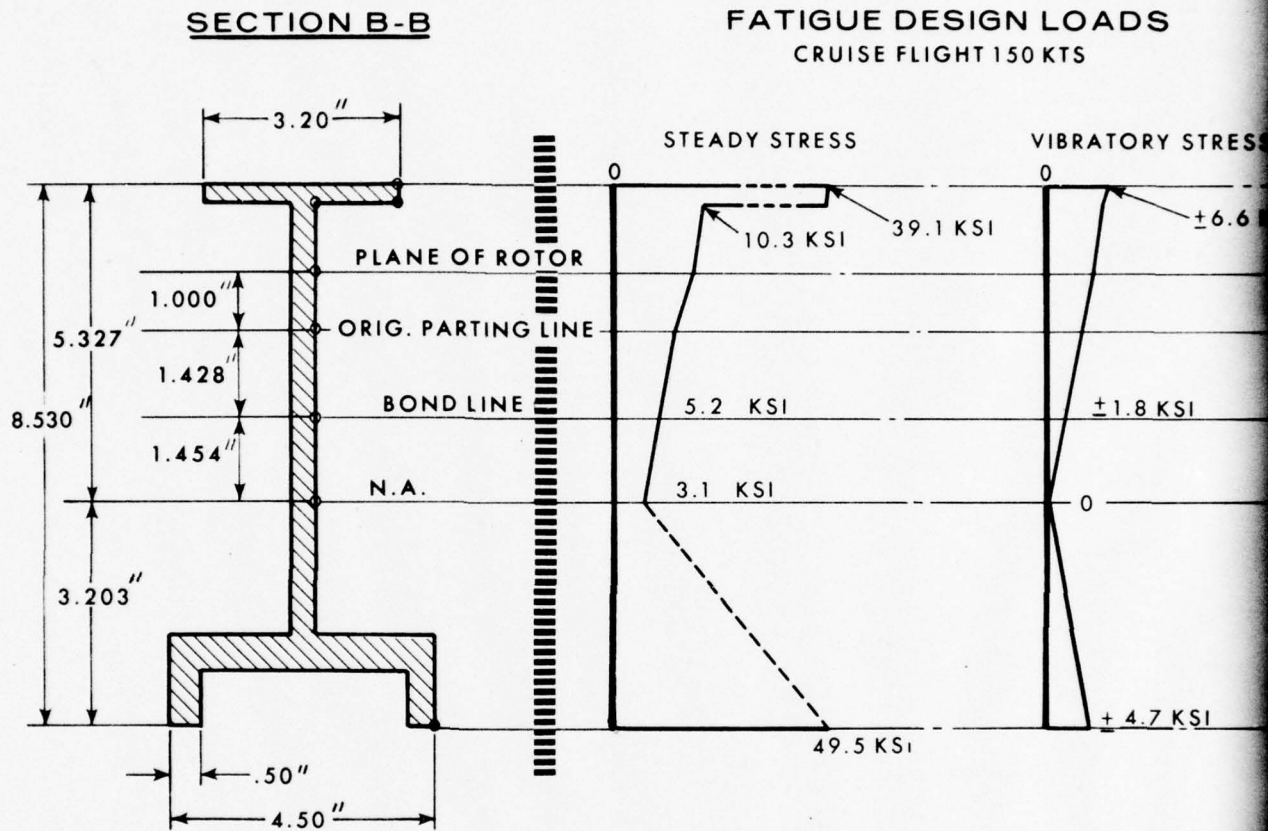


FIGURE 36. STRESS DISTRIBUTION ACROSS SECTION B-B FOR VARIOUS FLIGHT LOAD CONDITIONS.

LOADS
KTS

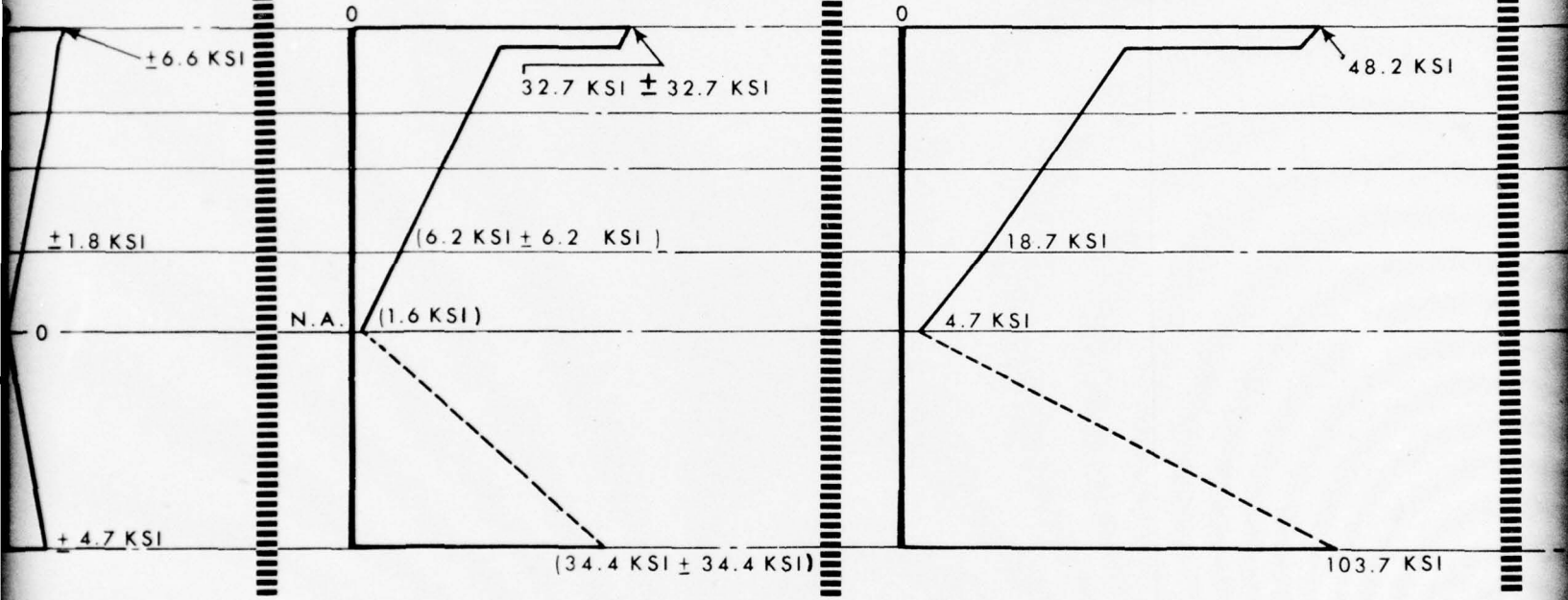
GROUND-AIR-GROUND (G.A.G) FATIGUE
AUTOROTATIVE CONDITION

ULTIMATE LOAD KSI
AUTOROTATIVE OVERSPEED
CONDITION

VIBRATORY STRESS

STEADY \pm VIBRATORY

MAX STRESS

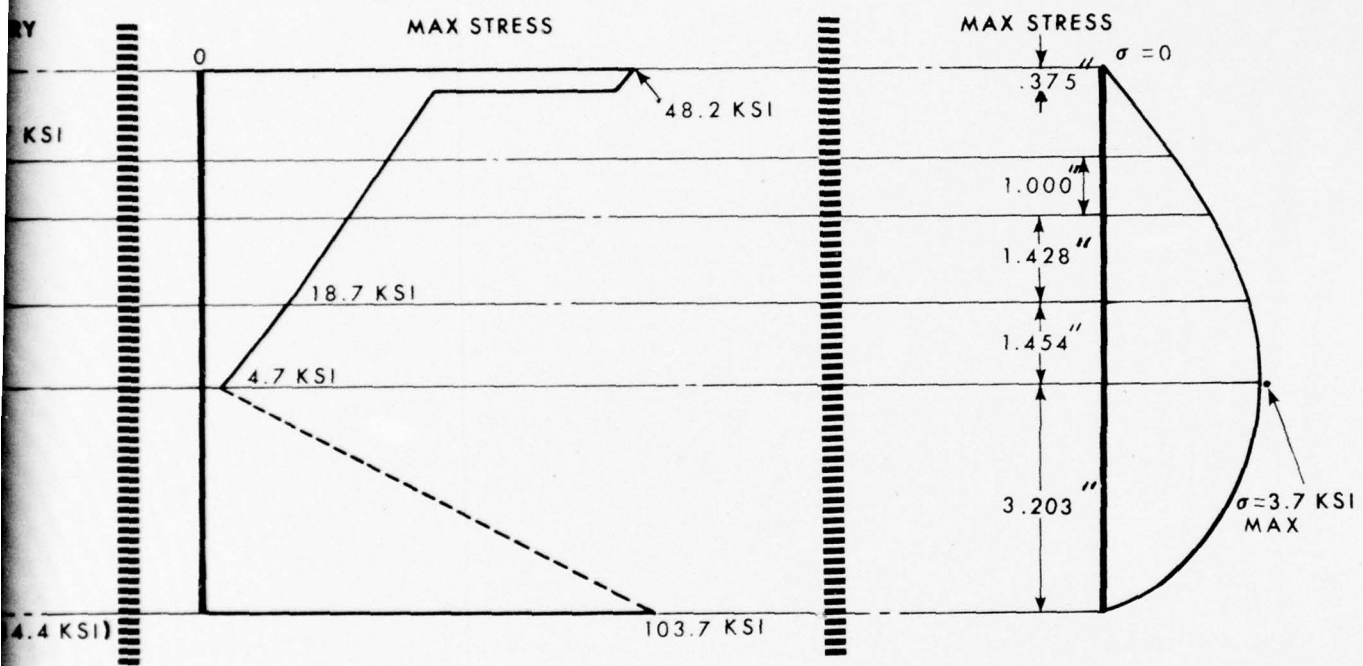


2

G) FATIGUE
ON

ULTIMATE LOAD KSI
AUTOROTATIVE OVERSPEED
CONDITION

SHEAR STRESS
IN FLIGHT STEADY



3

5.0 RISK REDUCTION FABRICATION AND EVALUATION OF H-53 ELASTOMERIC MAIN ROTOR HUB ARM

Two fully bonded single hub arm segments were successfully fabricated; one was destructively tested and the mechanical properties of the bondline material were found to be equivalent to values obtained from the parent material.

5.1 Hub Halves Fabrication

Based on the test results generated from Phase I, process optimization, and the structural analysis of the H-53 Elastomeric Main Rotor Hub, fabrication of the risk reduction single hub arm segment was initiated.

Forging stock material consisting of one billet of 21.5 inch diameter Ti-6Al-4V alloy weighing 3,500 pounds and conforming to the general requirements of SS8445, Reference 4, was procured from TMCA. Chemical analysis of the material is provided in Table VIII. Metallographic examination of the top and bottom of the billet indicated a material of good structure for forging stock material of this large size. The macrostructure was uniform with recrystallized fine grains as shown in Figure 37. The microstructure exhibited an acceptable alpha particle size for large forging stock material as depicted in Figure 38. Specimens from the billet, as received, were annealed for two hours at 1300°F, air cooled and tensile tested as a measure of billet capability. Results of the tensile tests were typical of that obtained for this size forging stock. The tensile values are presented in Table IX.

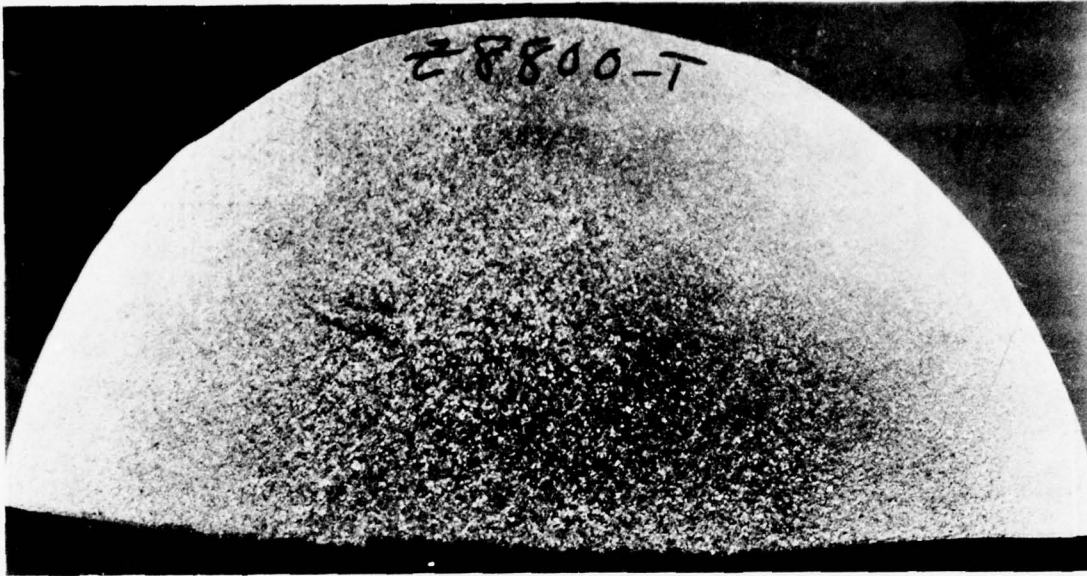
The weight of titanium procured, 3,500 pounds, was predicated on providing a minimum of .25-inch material available for machining the mating surface of the upper and lower half-forgings and producing a forging with a die opening of 1.5-inch between the lower half-forging parting line and the mating surface. This additional material permits machining of the mating surfaces and provides adequate material thickness required for deformation during the bonding operation.

The billet was cut into two pieces, 1,630 pounds for the upper half-forging and 1,865 pounds for the lower half-forging. The upper half-forging was identified with "NBI 7-12" and the lower half-forging with "NBI 1-6". Both ends of each billet were chamfered with a 5/8-inch x 45°. The billets were shotblast cleaned and coated with a proprietary coating used for forging titanium. The billets were heated in a gas-fired rotary hearth furnace at 1750°F and upset forged on an 18,000 ton press with flat dies at a pressing speed of 35-inch per min. Details of the heating and upset forging are provided in Table X.

TABLE VIII
 CHEMICAL ANALYSIS OF FORGING STOCK MATERIAL
 MAIN ROTOR HUB HALVES

ELEMENTS PERCENT BY WEIGHT	ANALYSIS SOURCE						REQUIREMENTS OF SIKORSKY STANDARD SS8445 Ref. (4).
	TMCA HEAT N-2758		WYMAN-GORDON Z-8300		BOTTOM		
	TOP	BOTTOM	TOP	BOTTOM	TOP	BOTTOM	
Al	6.4	6.6	6.30	6.29	5.50 - 6.75		
V	4.4	4.2	4.07	4.06	3.50 - 4.50		
Fe	0.21	0.17	0.18	0.17	0.3 max.		
C	0.022	0.022	0.018	0.016	0.08 max.		
O ₂	0.19	0.20	0.191	0.188	0.20 max.		
N	0.012	0.016	0.016	0.016	0.025 max.		
H ₂	0.007	0.008	0.0066	0.0081	0.0125 max.		
B	---	---	<0.003	<0.003	0.003 max.		
Ti	---	---	---	---	Balance		
Mo	---	---	0.02	0.02	} Other .4 Max.		
Mn	---	---	<0.01	<0.01			
Cu	---	---	<0.01	<0.01			
Zr	---	---	<0.05	<0.05			

TOP SIDE



BOTTOM SIDE

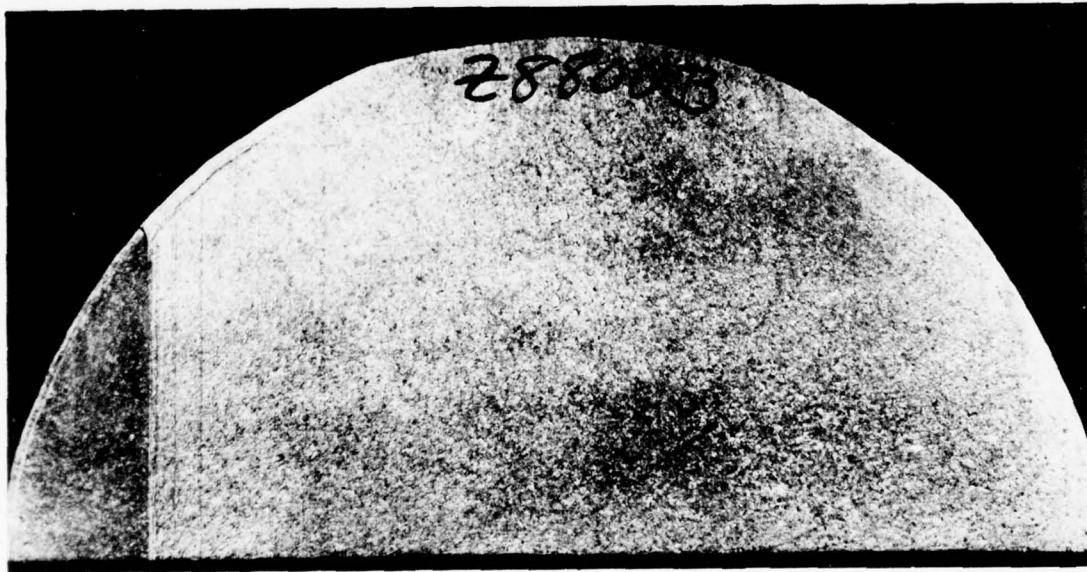


FIGURE 37. MACROSTRUCTURE OF Ti-6Al-4V FORGING STOCK MATERIAL, FORGE-DIFFUSION BOND OF RISK REDUCTION SEGMENT.

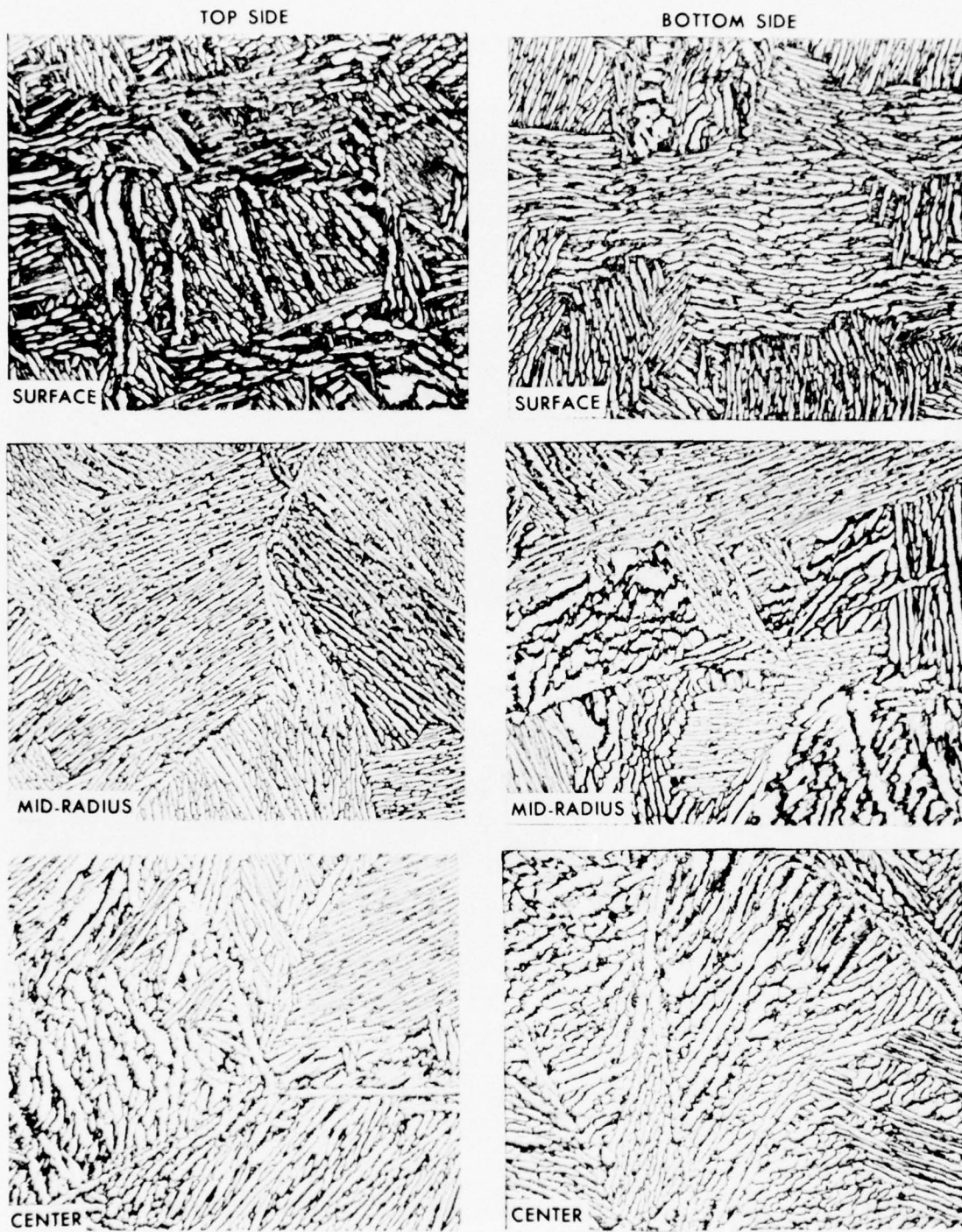


FIGURE 38. MICROSTRUCTURE OF Ti-6Al-4V FORGING STOCK MATERIAL,
 FORGE-DIFFUSION BOND OF RISK REDUCTION SEGMENT.
 (200X)

TABLE IX						
TENSILE TEST RESULTS						
FORGING STOCK MATERIAL - MAIN ROTOR HUB						
BILLET END	LOCATION	YIELD STRENGTH F _{ty} (KSI)	TENSILE STRENGTH F _{tu} (KSI)	ELONGATION (%)	REDUCTION OF AREA (%)	
Top	Center	114.2	125.8	8.0	21.7	
Top	Mid-radius	118.2	130.8	7.0	20.3	
Top	Surface	124.2	137.2	8.0	18.8	
Bottom	Center	122.6	135.2	10.0	19.7	
Bottom	Mid-radius	123.2	135.8	8.0	18.2	
Bottom	Surface	131.7	143.8	7.0	13.1*	
*Outer-Quarter Specimen Failure						
Heat Treatment:						
As-Received Billet, Anneal At 1300°F Two Hours, Air Cool						

TABLE X
UPSET FORGING OPERATIONS
MAIN ROTOR HUB

HUB HALF	SERIAL NUMBER	START BILLET DIMENSIONS		WEIGHT (Pounds)	TOTAL TIME IN FURNACE (Hours)	FINISH DIMENSIONS		
		DIAMETER (Inches)	LENGTH (Inches)			BULGE DIAMETER (Inches)	THICKNESS (Inches)	FORCE (Tons)
Lower	NBI-1	21.5	31.9	1,865	10.5	46	7.5	9,700
Upper	NBI-7	21.5	27.8	1,630	10.5	47	6.3	10,800

Furnace Temperature - 1750°F
Unit - 18,000 Ton Press

The upset upper and lower half-forgings were steel shotblast cleaned and ground with hand tools to remove minor abnormalities. The upset forgings were again blast cleaned and ceramic coated prior to heating for the first finish impression forging operation. After heating at 1750°F for six hours, the two half-forgings were pressed using a 50,000 ton press with a force intended to produce a thickness approximately 0.50-inch in excess of the requirement. The forgings were then water-quenched, cleaned and ceramic coated prior to the final pressing at full press tonnage. Tables XI and XII outline the first and second finish forge operation parameters.

As previously discussed, the separately forged upper and lower halves of the H-53 Elastomeric Main Rotor Hub were produced using the existing dies for the integrally forged hub. Flat steel plates were used in conjunction with the existing upper and lower dies to produce the upper and lower half-forgings. The use of the existing dies in this manner eliminated the expense of manufacturing a new set of dies to demonstrate the process. The upper and lower half-forgings were dimensionally inspected after cleaning to determine the amount of material to be removed in order to achieve the configuration to which they would have been forged, had new dies been fabricated. An overall view of one of the half-forgings showing the initially cut-out areas between the hub arms and the center is provided in Figure 39. After material removal from the web and center areas, both half-forgings were prepared for the Kellering operation, three axis contour machining. Four, one-sixth arm segments, from each half-forging were Kellered machined as partially shown in Figure 40. The eight arm segments, four from each half-forging, were removed from the total forgings in a Tysaman abrasive cutoff saw.

TABLE XI				
FIRST FINISH FORGING OPERATION				
MAIN ROTOR HUB				
SERIAL NUMBER	IMPRESSION DIE	TOTAL TIME IN FURNACE (Hours)	THICKNESS OVER AIM DIMENSIONS (Inches)	FORCE (Tons)
NBI-7	Upper	6.1	+0.75	30,000
NBI-1	Lower	6.3	+0.36	36,000
Furnace Temperature - 1750°F				
Unit - 50,000 Ton Press				
Water Quenched After Forging				

TABLE XII				
SECOND FINISH FORGING OPERATION				
MAIN ROTOR HUB				
SERIAL NUMBER	IMPRESSION DIE	TOTAL TIME IN FURNACE (Hours)	THICKNESS OVER AIM DIMENSIONS (Inches)	FORCE (Tons)
NBI-7	Upper	5.0	+0.37	50,000
NBI-1	Lower	5.7	+0.22	50,000
Furnace Temperature - 1750°F				
Unit - 50,000 Ton Press				
Water Quenched After Forging				

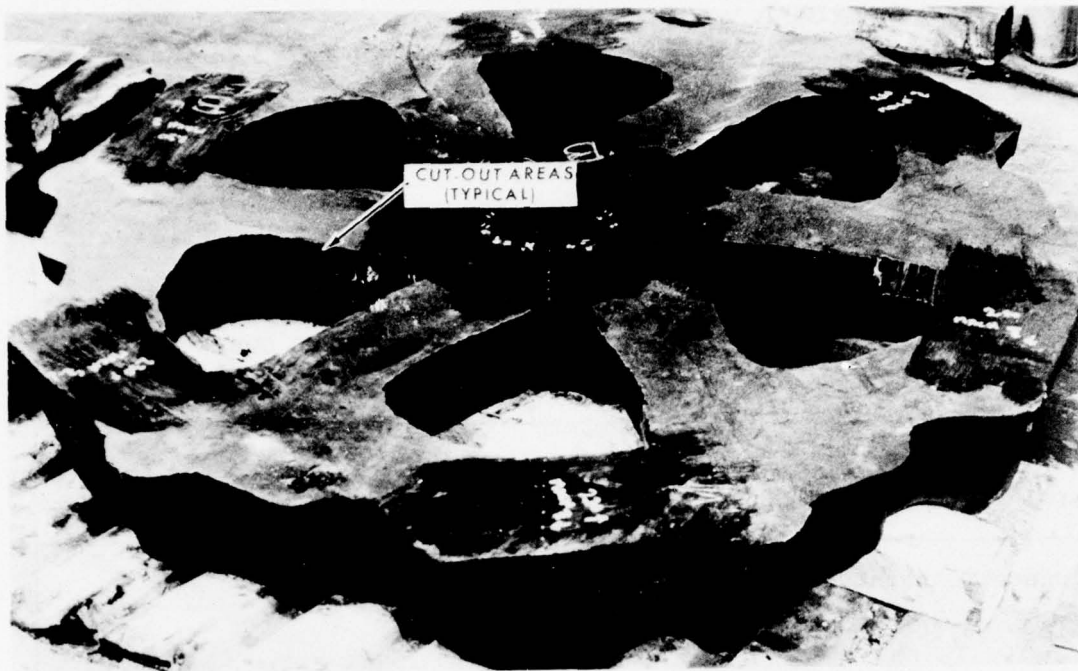


FIGURE 39. HALF-FORGING SHOWING CUT-OUT AREAS.



FIGURE 40. HALF-FORGING SHOWING PARTIALLY MACHINED CONFIGURATION.

5.2 Bonding Operation Approach

The bonding deformation stroke was to be the same 10% as established in Phase I. The hub forging thickness varies from 13-inches at the center to 9.4-inches at the periphery. An average thickness of the arm segment appeared to be approximately 10-inches. A 10% reduction would require a 1-inch bonding press stroke. Because of the size and shape of the upper and lower arm segments, it was necessary to fabricate forge bonding dies to transmit pressure uniformly, maintain alignment and to utilize a container or retort of a relatively simple geometry. This would increase the reliability of obtaining an adequate vacuum. Bonding dies were machined from forge flattened billets of type 304 stainless steel. The dies were designed with sufficient impression depth to assure the upper and lower arm segments would be held securely during the bond stroke. Adequate clearance was provided in the impression to allow for variation in thermal expansion of stainless steel and titanium. Two 2-inch diameter type 304 stainless steel leader pins were installed vertically between the top and bottom bonding dies to minimize shifting of the dies during the bond stroke. Figure 41 illustrates the general arrangements of the arm segments in bonding die. Figure 42 shows the top and bottom bonding dies with the machined impression before grinding and leader pin installation.

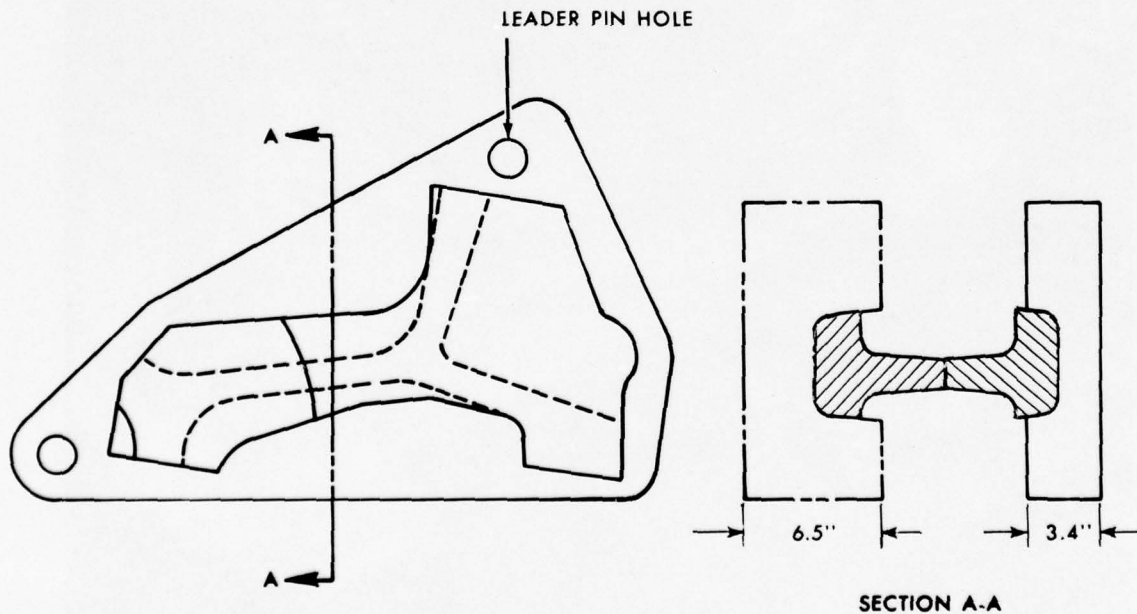


FIGURE 41. SKETCH OF BONDING DIES WITH HUB ARM SEGMENT IN POSITION.

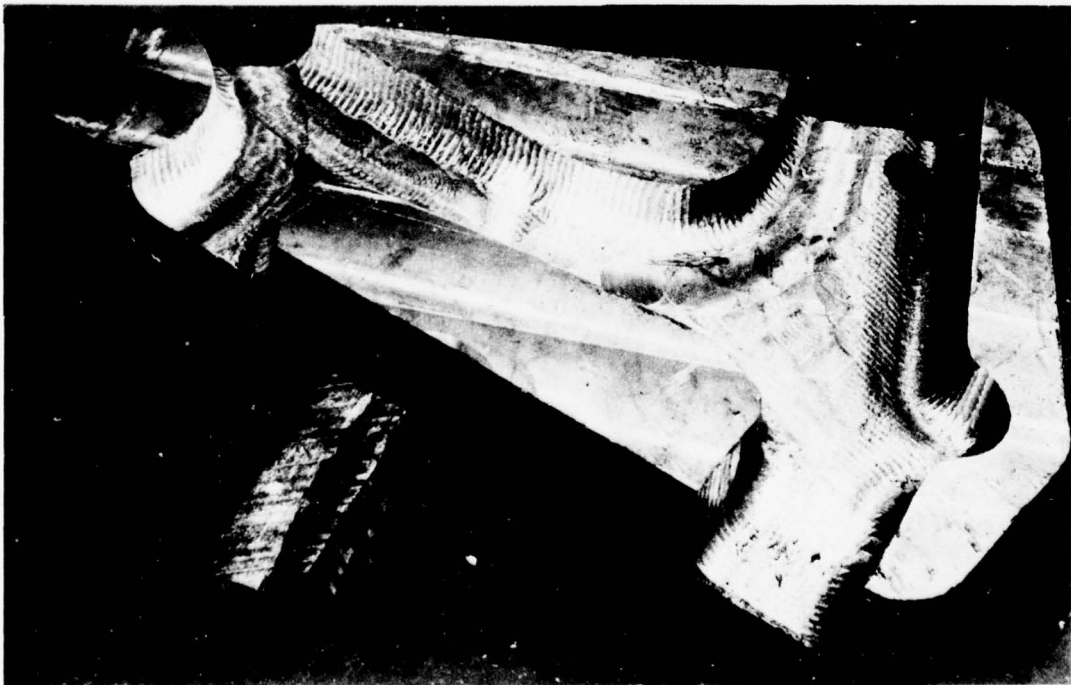
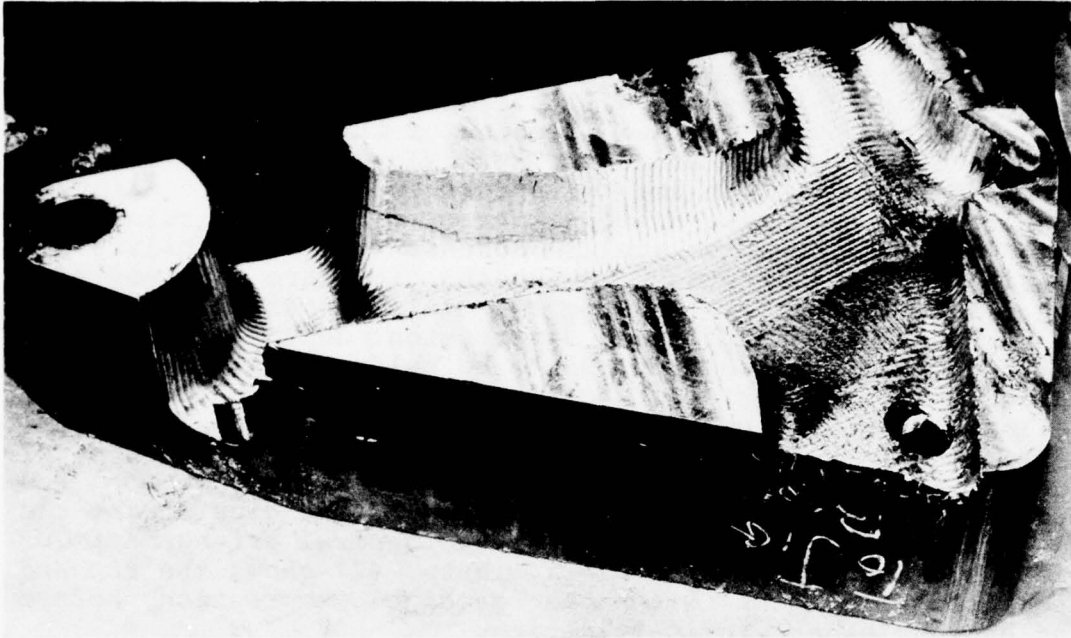


FIGURE 42. TOP AND BOTTOM BONDING DIES, ROUGH MACHINED.

5.3 Single Arm Fabrication

General - The first approach to diffusion-bond component arms employed the same general technique used in the fabricating and bonding of the pancake assemblies. This attempt was unsuccessful because of the formation of contamination between the mating surfaces of the component arms. The contamination was associated with the technique employed during welding of the retort and during the heating-outgassing cycle to prevent contamination of the mating surfaces. The contamination condition existed in the fabrication of the pancake assemblies as discussed in Section 3.2.2, but became more apparent in the arm segment because of differences in the arm configuration and bond surface areas. The second attempt to diffusion-bond an arm segment corrected only a portion of the problem. The contaminated condition still existed. The third attempt modified the basic fabrication technique and successfully bonded the arm segment to the established criteria. The modified methods included the use of an inert atmosphere during welding and the continuous removal of the evolved gasses during the heating-outgassing cycle. The fourth arm segment was processed in the same general manner as the third arm segment and was also successful.

5.3.1 Fabrication Technique; 3rd and 4th Hub Arm Segment Two Satisfactory Diffusion Bonded Arms

3rd Hub Arm - The detailed fabrication procedure for the bonding of the third arm segment was initiated by preparing the surfaces of the component arms to be joined by machining and cleaning. The surfaces to be bonded were machined flat to a surface finish of 100AA or better. The machined surface was cleaned by chemically milling in a standard HF-HNO₃ solution, similar to the technique used on the pancake assemblies. The machined and chemically cleaned surfaces were mated as shown in Figure 43. The component arms were placed between a set of bonding dies and the entire assembly was placed on a 1/8-inch thick stainless steel plate. The die impressions had been coated with magnesium hydroxide (Mg(OH)₂) used as a parting agent. A stainless steel container was fabricated from 1/8-inch material by vertical seam welding the sides; drilling holes for the evacuation tube, vacuum tube, and the thermocouple tube; and welding the side unit to the top plate. Three, 1/4-inch thick stainless steel gusset plates were welded to the bottom bonding die, providing a scabbard for the top die. The bonding dies, gusset plates, and the stainless steel container interior were cleaned by abrasive grit blasting and rinsed with acetone prior to assembly. A view of the arm segments, bonding die, and container prior to assembly is provided in Figure 44. Figure 45 depicts the exterior of the stainless steel container or retort after assembly. The retort was filled with argon and a positive pressure environment was

maintained as the retort was TIG weld sealed with the exception of the 1/4-inch diameter thermocouple tube; the 1/2-inch diameter vacuum gage tube; and the 3/4-inch diameter air evacuation tube. A thermocouple was inserted and packed into the retort through the 1/4-inch tube and connected to the recording instrumentation. A Pirani vacuum gage was attached to the dead end of the 1/2-inch tube and monitored the minimum vacuum inside the retort unit. The air evacuation tube was connected to the vacuum system and the retort unit was evacuated to a vacuum level below 10^{-4} Torr at room temperature. The evacuation system consisted of a mechanical and diffusion pump system with an Ion vacuum gage at the pump's intake port. The retort unit was tested for leaks by the use of a mass spectrometer leak detector before committing it to the furnace for the heating-outgassing operation. Leak testing at room temperature disclosed the retort unit to be free from leaks greater than 2×10^{-9} cubic centimeter per second (cc/sec).

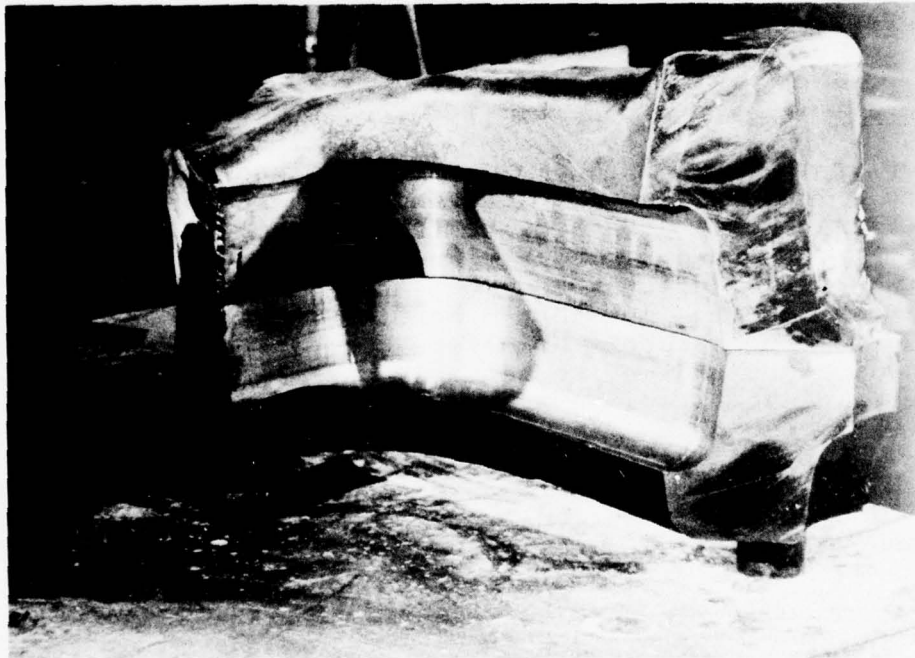


FIGURE 43. HUB ARM SEGMENTS PRIOR TO BONDING.

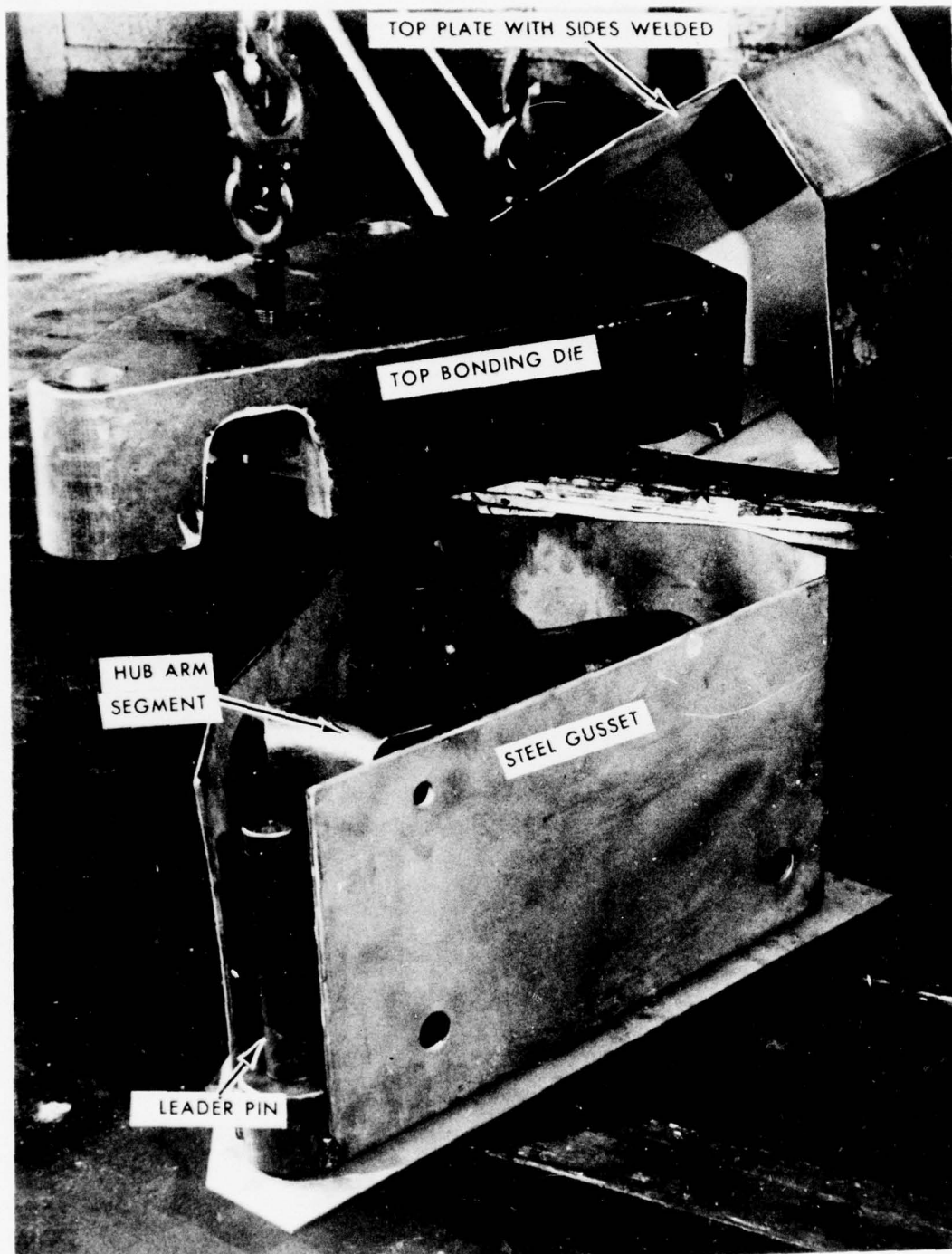


FIGURE 44. BONDING DIE, GUSSET PLATE, AND HUB SEGMENT ASSEMBLY FOR THIRD HUB ARM.

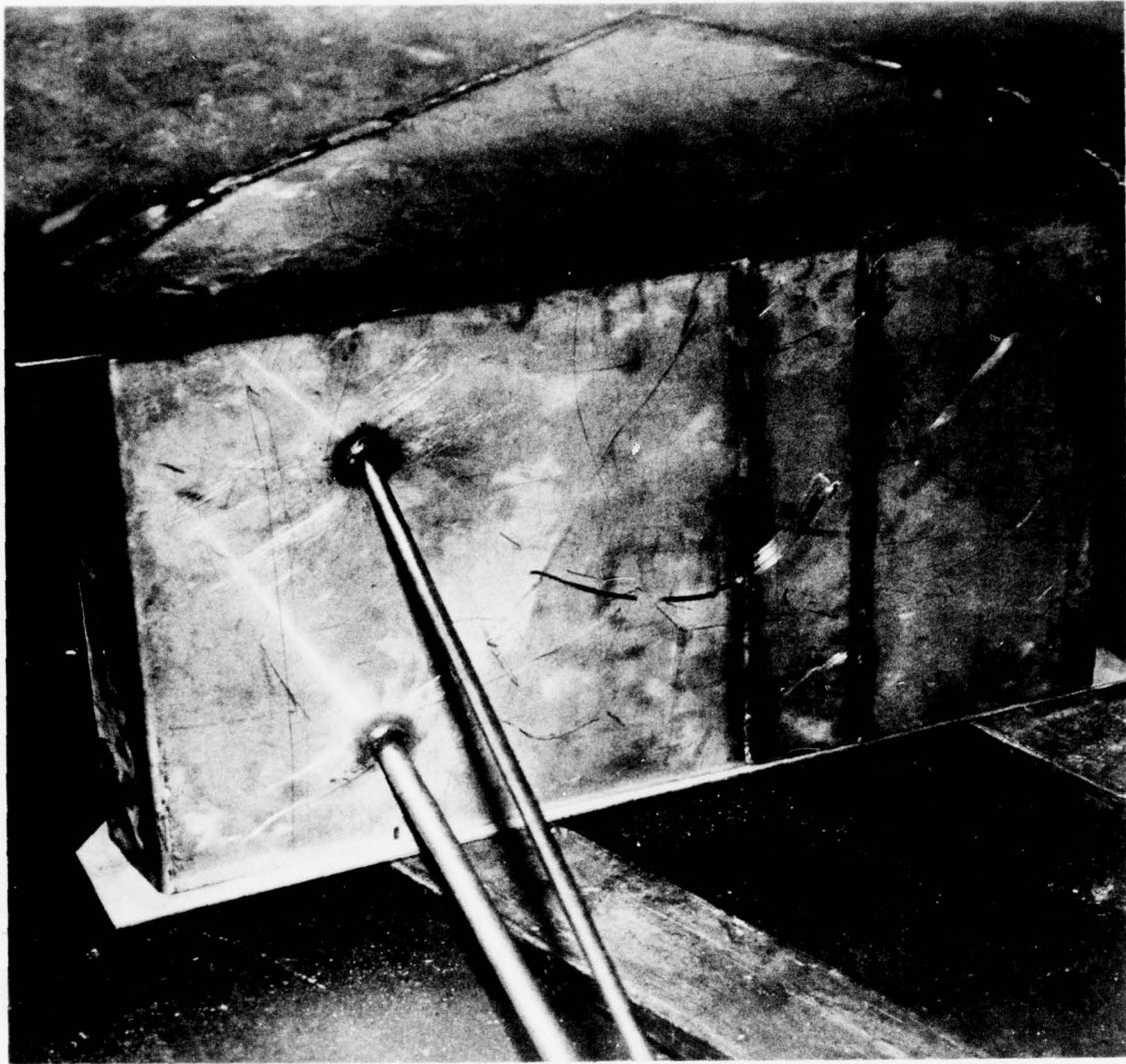


FIGURE 45. RETORT AFTER ASSEMBLY.

The retort unit was placed into the gas-fired, Surface Combustion furnace near the forging press. A temporary front to the furnace was built from light-weight firebrick. The retort unit was attached to the instrumentation and heating was initiated. A schematic diagram of the retort unit in the furnace is illustrated in Figure 46. No significant loss of vacuum occurred during the time between leak testing and installation in the furnace. The time interval from chemical cleaning of the component arms and initial heating of the retort unit in the furnace was only seven hours, minimizing contamination susceptibility.

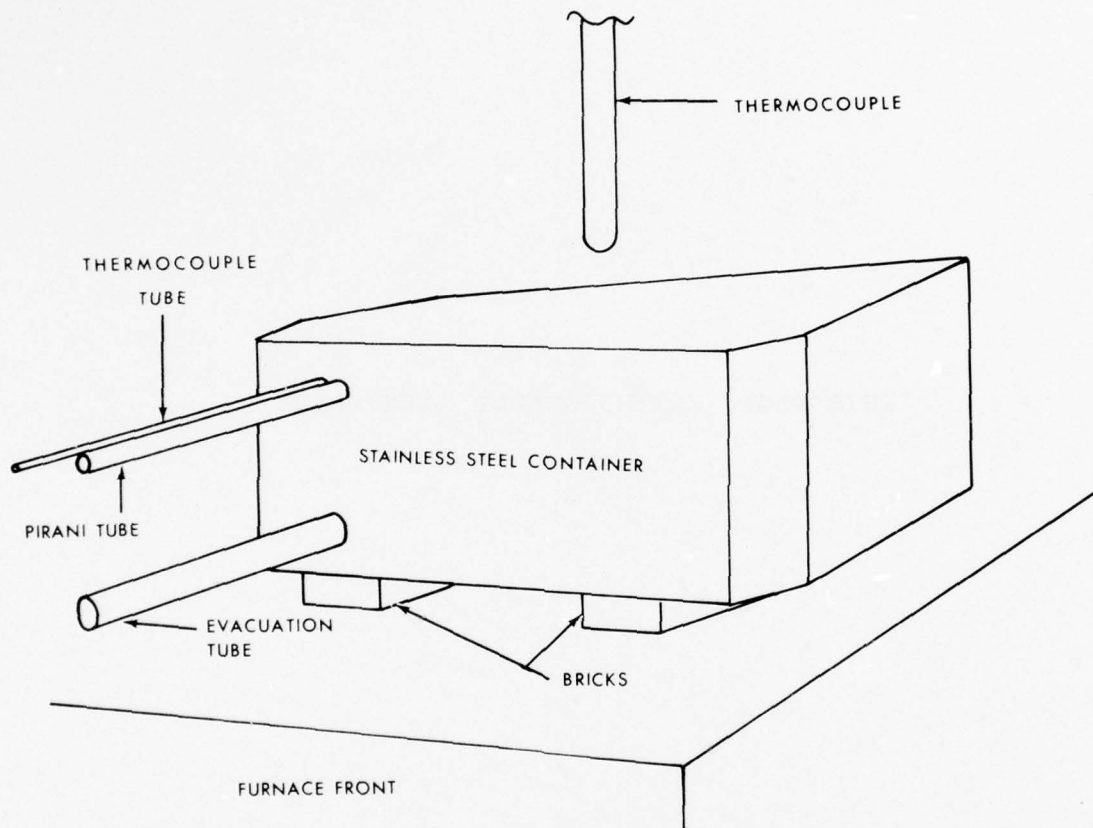


FIGURE 46. DIAGRAM OF RETORT IN FURNACE.

The temperature was gradually increased from room temperature to the alpha-beta temperature of 1750°F. The rate of temperature increase was relatively slow because it was necessary to continually evacuate the retort unit through the 3/4-inch diameter tube during the heating cycle to prevent contamination. The total time of the heating-outgassing operation was forty-eight hours. A plot of the temperature and vacuum is presented in Figure 47. After the hub arm was at 1750°F, for two hours the Ion gage and thermocouple were

THIS PAGE INTENTIONALLY LEFT BLANK

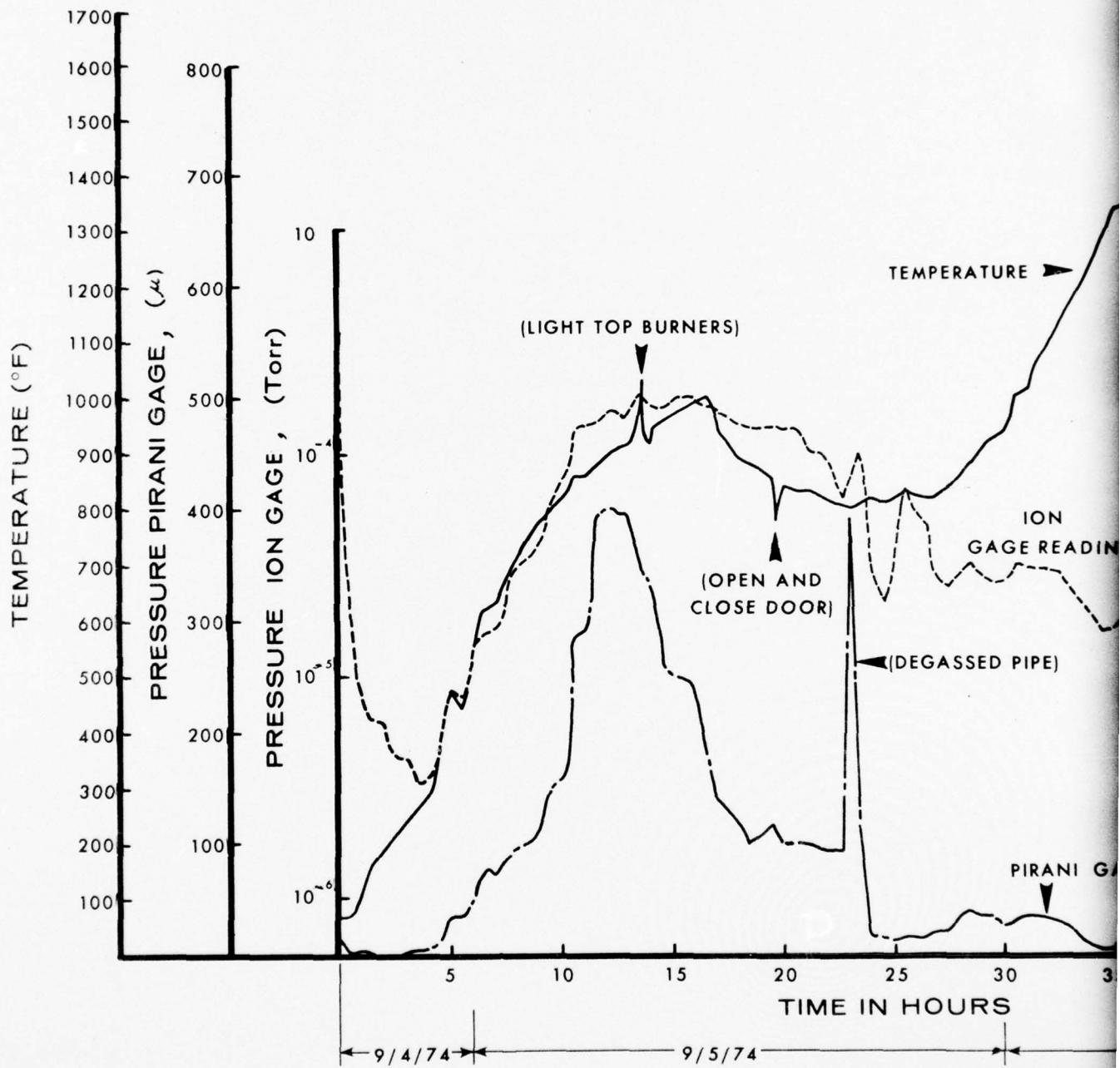
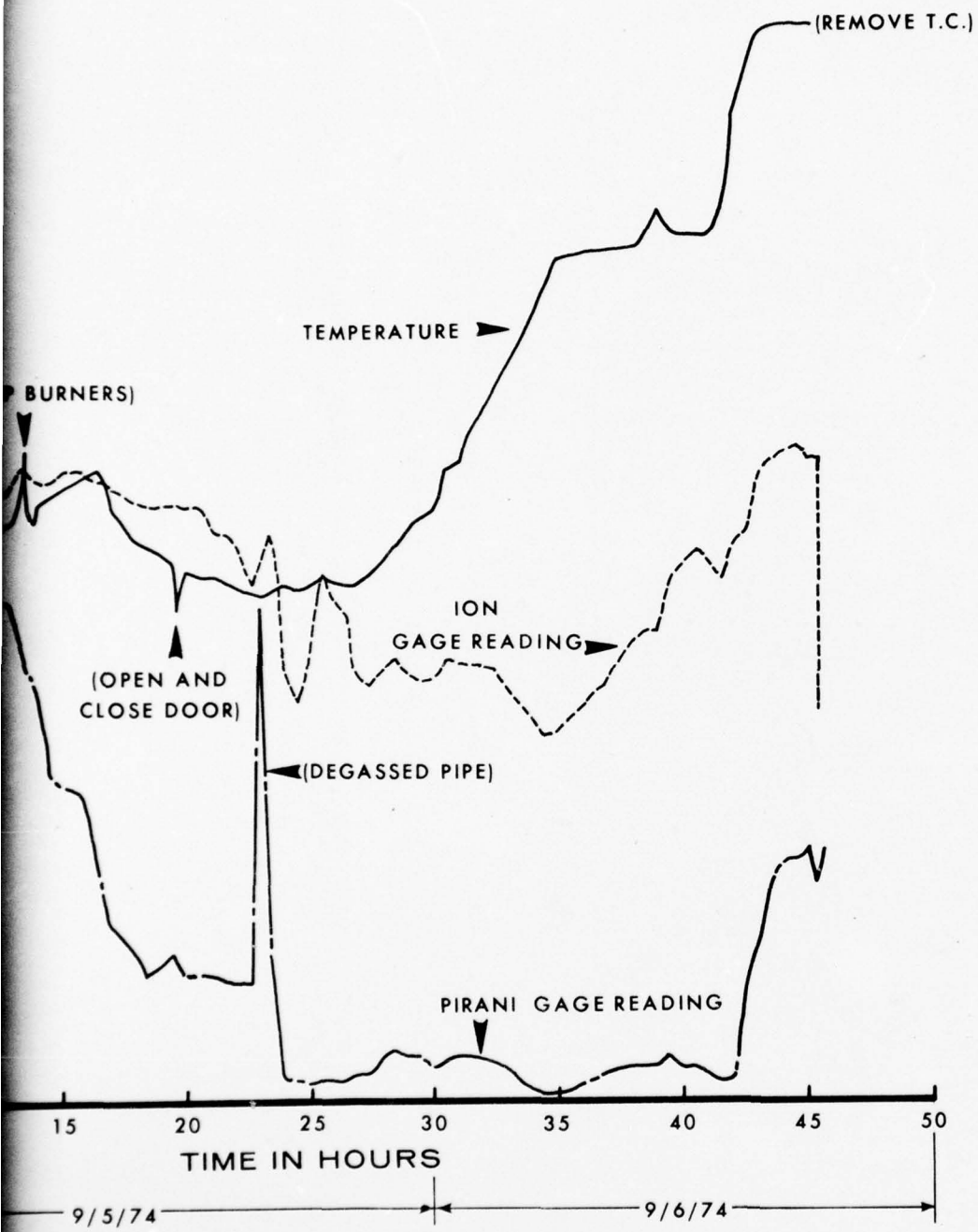


FIGURE 47. PLOT OF HEATING-OUTGASSING IN VACUUM OF THIRD ARM SEGMENT, TEMPERATURE AND PRESSURE VERSUS TIME.



THIRD ARM SEGMENT,

disconnected. The 3/4-inch diameter evacuation tube and 1/4-inch diameter thermocouple tube were sealed by crimping. The Pirani gage monitored the vacuum level during the remainder of the effort. The retort unit was removed from the furnace as quickly as possible in order to minimize diffusion of any contaminants through the 1/8-inch thick walls of the stainless steel retort. Immediately upon removing the retort unit from the furnace, it was placed between the heads of the forging press and pressure applied for bonding. The forging press was located within thirty feet of the furnace and the time required for removal from the furnace to insertion into the forging press was less than sixty seconds. Forge-bond pressure was applied to the retort unit and held for approximately two minutes with 200-250 tons of pressure. A one-inch forge-bond stroke was accomplished at an average closing rate of 0.3 inches per minute. Figure 48 shows the record trace of force and displacement versus time.

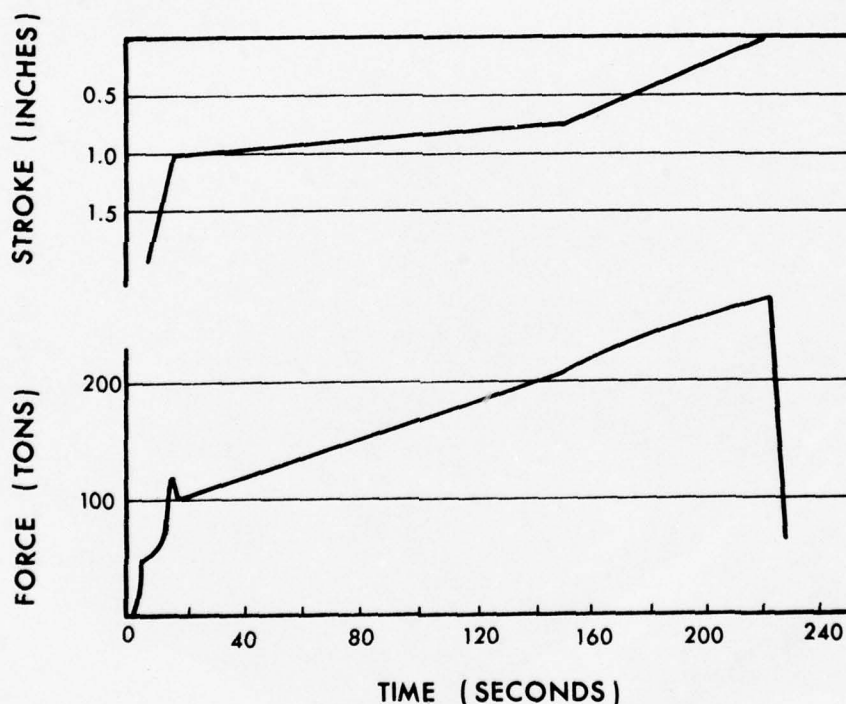


FIGURE 48. FORGE-BOND OPERATION OF THIRD ARM SEGMENT, FORCE, AND DISPLACEMENT VERSUS TIME.

After the forge-bond operation, the Pirani gage was removed from its monitoring position. The gage was noted to be fully operational denoting that the retort unit still maintained an adequate vacuum. The vacuum monitor tube was sealed and both the evacuation and monitoring tubes were bent in order to allow the retort unit to be returned to the furnace for an additional post-bond thermal treatment at 1750°F for two hours. Figure 49 shows the retort unit after the post-bond anneal.

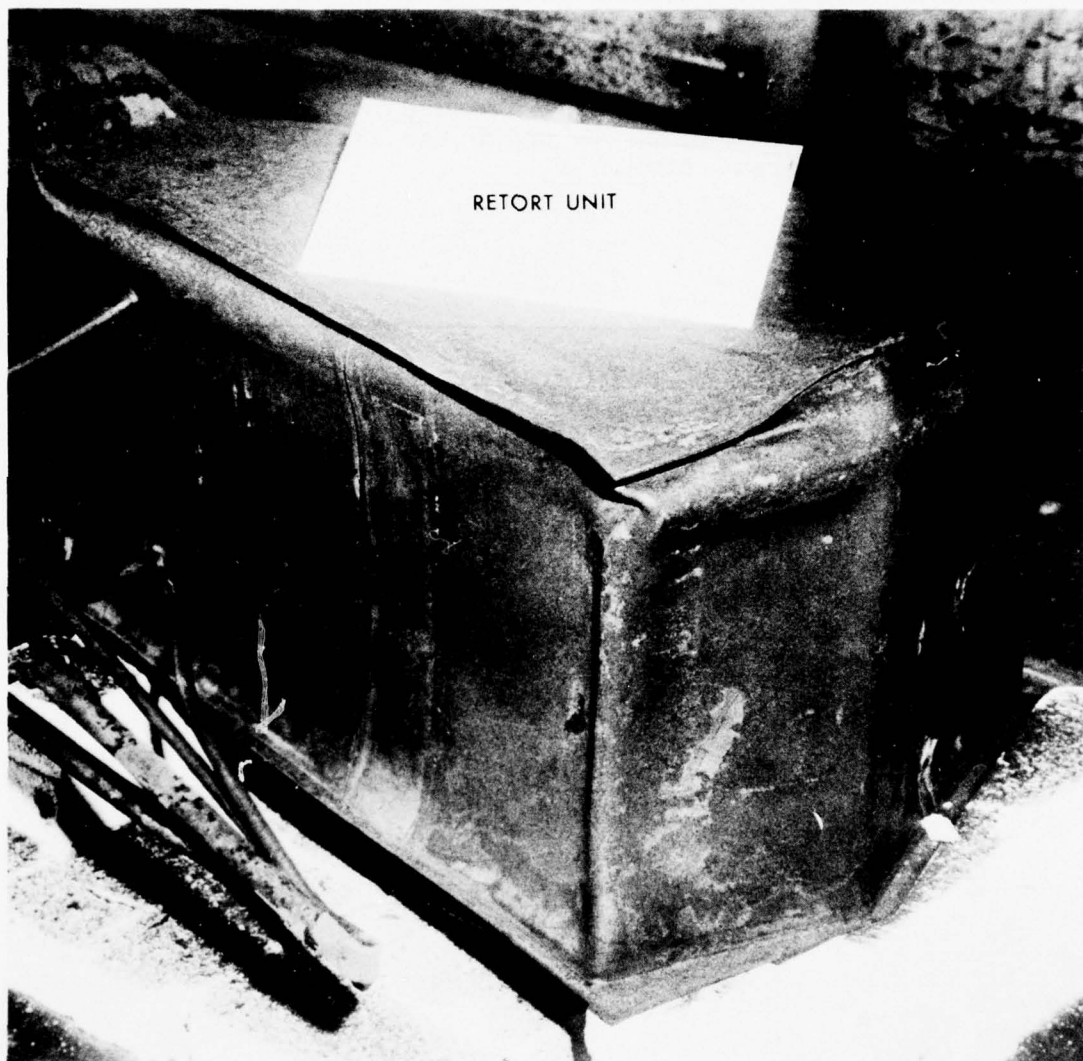


FIGURE 49. RETORT UNIT AFTER POST-BOND ANNEAL, THIRD ARM SEGMENT.

The retort was opened for an early evaluation of the arm segment as shown in Figure 50. Details relating to the investigation of the preliminary sonic indication are presented in Section 5.4.2 on Hub Arm Inspection. The arm segment was then thermally treated at 1900°F for one-hour at temperature, water-quenched, annealed at 1300°F for two-hours and air cooled. These operations completed fabrication of the single hub arm risk reduction segment. Inspection and destructive testing were the next major efforts as discussed in Sections 5.4.3 and 5.5.



FIGURE 50. RETORT, DIE, AND ARM SEGMENT AFTER THE FORGE-BOND AND POST BOND ANNEAL, THIRD ARM SEGMENT.

4th Hub Arm - Detail fabrication of the fourth arm segment was substantially the same as the procedure used on the third arm segment with the following exceptions: Heating-outgassing of the fourth component arm progressed more gradually than the third arm. The time required to raise the temperature from room temperature to 1750°F while maintaining an adequate vacuum was seventy-one hours. A plot of the temperature and vacuum is presented in Figure 51. After the retort unit reached 1750°F the unit was sealed, removed from the furnace, placed in the forging press, and the forge-bond stroke performed. These operations were accomplished in a similar manner as in the previous third arm. Figure 52 shows the traces of force and displacement versus time. The Pirani gage was removed from its

THIS PAGE INTENTIONALLY LEFT BLANK

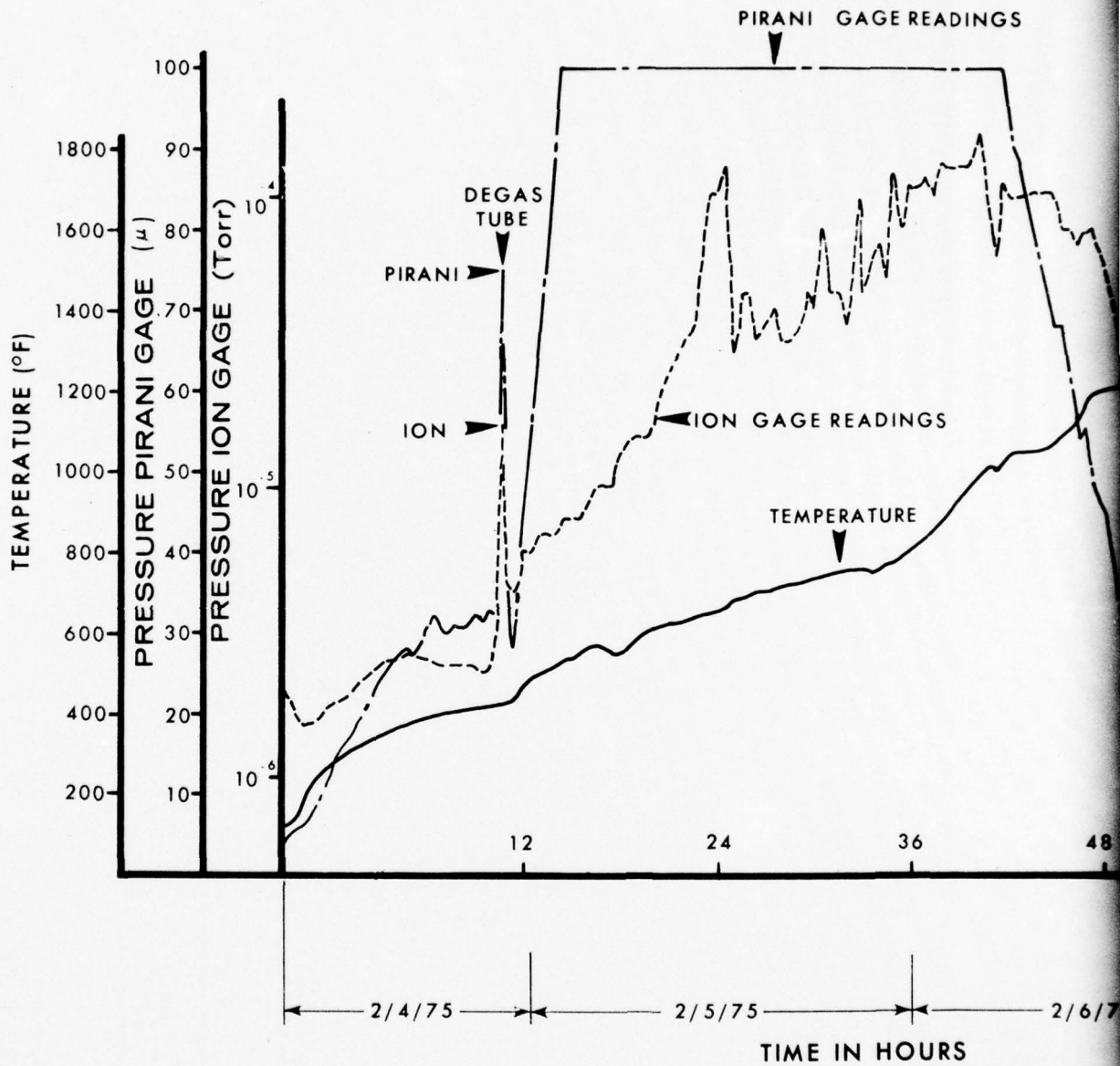
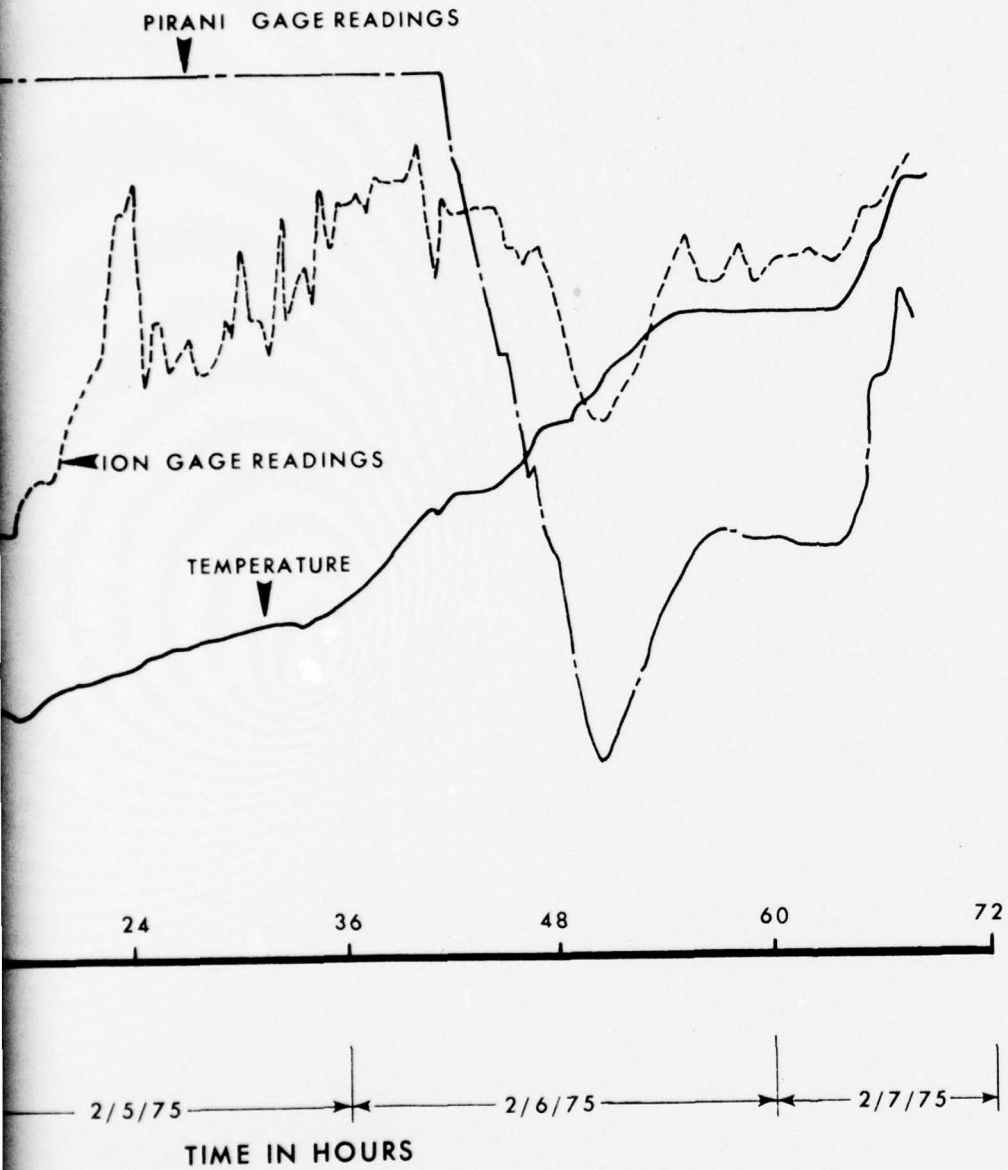


FIGURE 51. PLOT OF HEATING-OUTGASSING IN VACUUM OF FOURTH ARM SEGMENT, TEMPERATURE AND PRESSURE VERSUS TIME.



OF FOURTH ARM SEGMENT,

2

monitoring position and it was again observed to be operational denoting that this retort unit also maintained its vacuum. The vacuum monitoring tubes were bent. The retort unit was returned to the furnace for the additional post-bond thermal treatment at 1750°F for 2 hours. Upon completion of the post-bond diffusion treatment, the retort unit was opened by torch cutting. The sound of the rushing air into the retort confirmed that the retort unit had maintained a vacuum during the post-bond thermal operation. The interior of the retort was observed to be clean, except along the cut areas. The arm segment was bright with no evidence of any contamination.

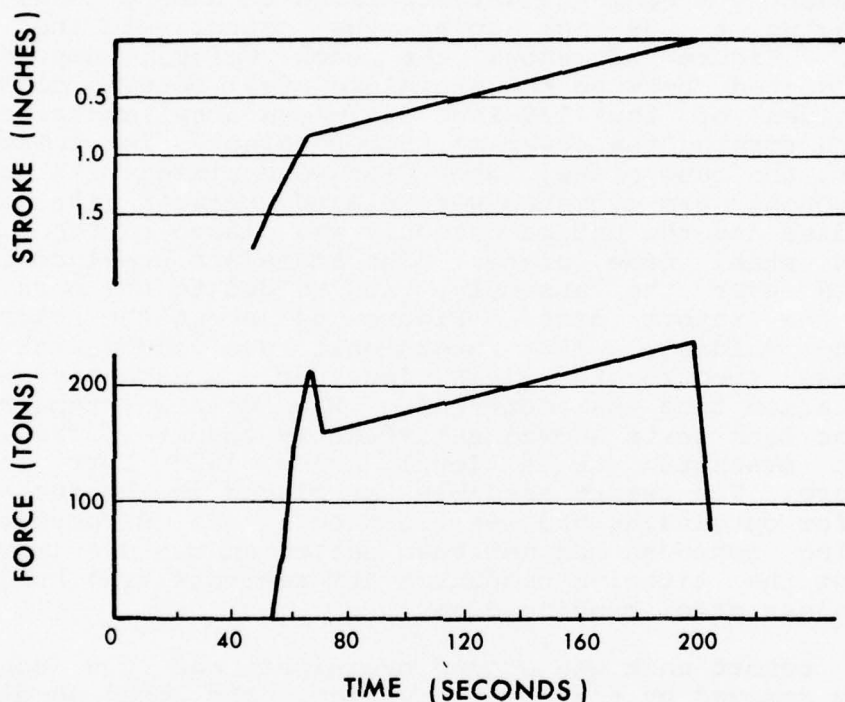


FIGURE 52. FORGE-BOND OPERATION PLOT OF FOURTH ARM SEGMENT, FORCE AND DISPLACEMENT VERSUS TIME.

The arm segment was subsequently beta heat treated at 1900°F followed by a water-quench, aged at 1300°F and finally air cooled. The arm was then nondestructively inspected as detailed in Section 5.4 and shipped to AMMRC (U. S. Army) for additional evaluation.

5.3.2 Fabrication Procedure; 1st and 2nd Hub Arm Segment First Two Unsuccessful Attempts

The purpose of this section is to document the events and procedures used during the first two attempts to diffusion-bond the single hub arm risk reduction segments (1st and 2nd Arms).

1st Nonbonded Hub Arm - The component arms were cleaned by immersion in a standard HF-HNO₃ solution. The surfaces to be bonded were polished and lightly etched by swabbing with HF-HNO₃, rinsed with water, and dried with alcohol. Positive alignment for the 1st hub arm was obtained by tack welding the ends of the arms while flooding the faying surfaces with argon. The component arm segments were observed to have a longitudinal bow, leaving a .09-inch gap at the center of the faying surfaces. Figure 53 shows the tack welded component arm segments seated between the stainless steel bonding dies. The top and sides of the 1/8-inch stainless steel container were TIG welded forming the cover of the container. The interior of the cover, the base plate, and dies were rinsed with acetone. The component arm segments were placed between the set of bonding dies and the entire assembly was placed on the 1/8-inch stainless steel base plate. The stainless steel cover was positioned over the assembly, and welded to the base plate forming the retort unit. Figure 54 shows the retort unit before the welding. The retort unit was vacuum leak tested with a mass spectrometer leak detector. A defective weld at the evacuation tube was detected. The weld was repaired and subsequent leak tests showed satisfactory results. The retort unit was evacuated to a level below 10⁻⁴ Torr at room temperature. The retort assembly was placed in the furnace and heating for outgassing had started when it was discovered that the parting compound had not been coated on the die impression to prevent the titanium component arm segments from bonding to the stainless steel bonding dies.

The retort unit was cooled overnight and the container cover was removed by abrasively cutting. The bonding dies and component arm segments were disassembled. The component arm segments were separated by removing the tack welds by grinding. A new stainless steel cover was prepared. The bonding dies and stainless steel cover were cleaned and washed with acetone. The impressions of the bonding dies were coated with Mg(OH)₂. The component arm segments were re-etched by immersion in HF-HNO₃. The surfaces to be bonded were etched by swabbing, washed with water, and dried with alcohol. The component arm segments were again tack welded; placed between the bonding dies, positioned on the stainless steel plate, and the cover welded to the plate. A leak test showed the retort unit to be vacuum tight.

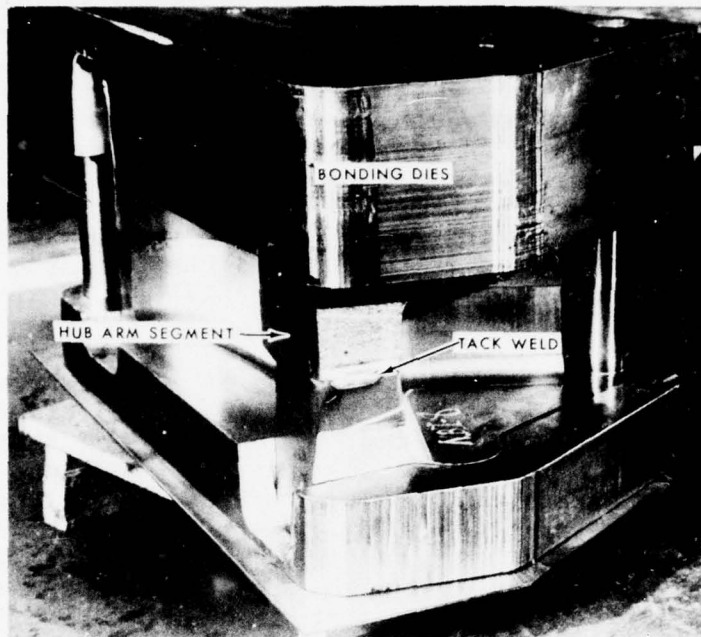


FIGURE 53. FIRST ARM SEGMENT TACK WELDED AND SEATED BETWEEN BONDING DIES.

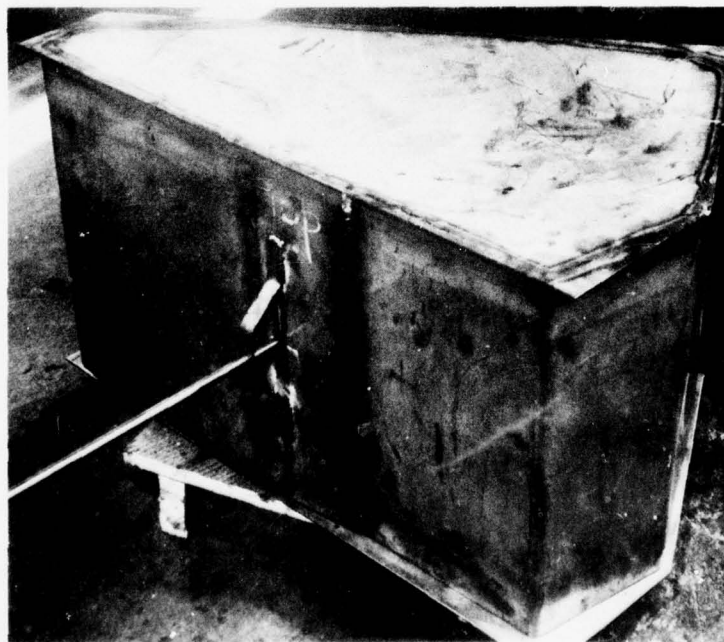


FIGURE 54. FIRST ARM SEGMENT RETORT UNIT BEFORE SEALING WITH FINAL WELD.

The sealing and outgassing of the first arm segment was similar to the procedure used on the pancake assemblies. Evacuation and outgassing of the first arm segment was conducted for twelve hours reaching a maximum temperature of 900°F at the outside of the container and maximum vacuum of 5×10^{-2} Torr. The retort unit was reheated and outgassed a second time. After approximately twenty-four hours of additional heating, the temperature reached 1300°F, the assembly was then cooled to 300°F at which time the vacuum reading was 5×10^{-5} Torr. The retort unit was loaded into the furnace at 1000°F and the furnace controls were set at 1750°F. The furnace temperature recorded 1750°F one hour later.

After twenty-five hours of heating at temperature, 1750°F, the retort unit was removed from the furnace and transferred to the forging press for bonding. It was noted that the side walls of the retort had collapsed into the opening between the bonding dies. Forge-bonding was accomplished with a press head velocity of one-inch per minute. The first thirty seconds of the bonding stroke was required to crush the retort. The actual bonding stroke was one-inch. The pressure was applied during a time interval of about sixty seconds. Initial bonding load was 210 tons, producing an interface of approximately 7,000 psi. A recorded trace of force and displacement versus time for forge-bonding is illustrated in Figure 55.

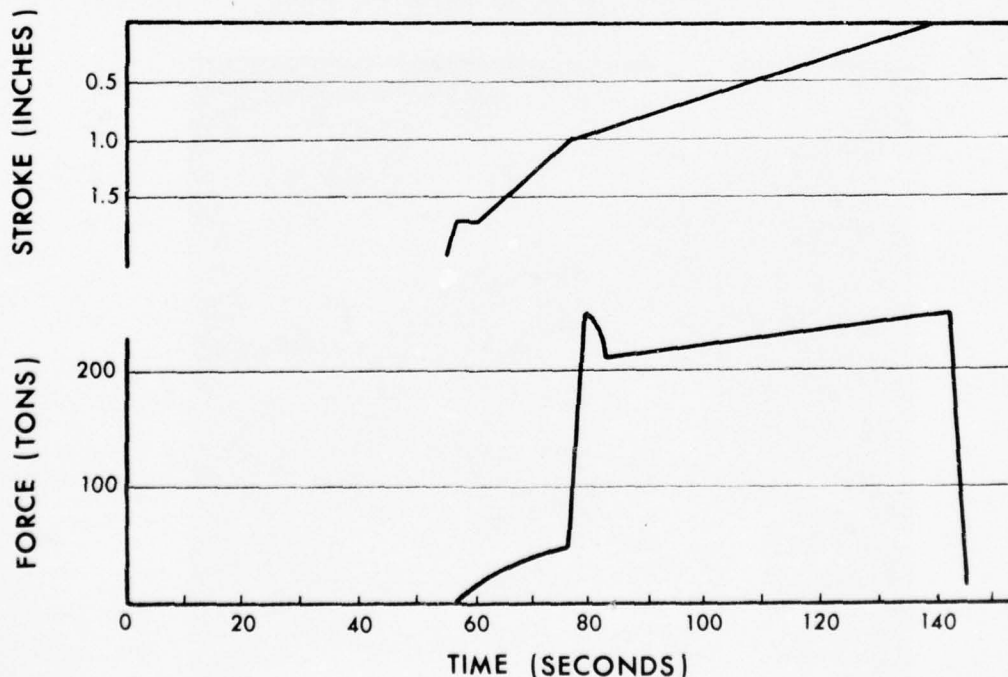


FIGURE 55. FORGE-BOND OPERATION OF FIRST HUB ARM SEGMENT, FORCE AND DISPLACEMENT VERSUS TIME.

AD-A034 829

UNITED TECHNOLOGIES CORP STRATFORD CONN SIKORSKY AIR--ETC F/G 13/8
FORGE-DIFFUSION BOND TITANIUM ROTOR HUB EVALUATION.(U)

JUL 75 M J BONASSAR, J J LUCAS

DAAG46-73-C-0126

UNCLASSIFIED

SER-50938

AMMRC-CTR-75-14

NL

2 of 2
ADA034829



END

DATE
FILMED
2 - 77

During the forge-bond cycle, the sidewalls of the retort were deformed. This deformation caused the evacuation tube support bracket and the evacuation tube itself to bend severely. It was not certain that this condition initiated leaking at the tube weld causing loss of vacuum. However, when the retort unit was removed from the quench operation, the tube weld joint was defective.

Upon completion of the forge-bond operation the retort unit was reloaded into the furnace and the temperature was raised from 1750°F to 1900°F. It is estimated that the temperature of the arm segment was in the vicinity of 1650°F. After two hours, the retort unit was water quenched. Figure 56 shows the deformed retort unit after the forge-bond and water quench operation. The first arm segment was removed from the container and annealed at 1300°F for two hours at temperature. Figure 57 shows the first forge-bond arm segment after bonding. Figure 58 illustrates how the deformation occurs in a section through a typical arm segment.

2nd Nonbonded Hub Arm - After analyzing the results of the first attempt to bond an arm segment and the processing techniques employed, several modifications were established as criteria for the fabrication of the second arm segment. These changes included: Elimination of tack welds. The arm segments will be held in place by the bonding dies; Vapor blasting of the stainless steel retort will be accomplished to remove surface contamination; The retort will be cleaned with acetone at the time of assembly. A positive pressure of argon will be maintained in the retort unit at the time of welding the retort closed to prevent contamination; Increasing the wall thickness and diameter of the evacuation tube for better evacuation rate and eliminating the need for the support bracket; The evacuation tube pad location will be relocated to a more advantageous position to prevent cracking during the bonding cycle; Heat-outgassing rate will be controlled so that an adequate vacuum is maintained at all time; Outgassing will continue up to the forge-bond temperature of 1750°F and the forge-bond operation is to be conducted without any intervening cooling; Adequate heating of the arm segments at the forge-bond temperature, 1750°F will be accomplished with a minimum soaking time to reduce the probability of contamination with increased time; Time between cleaning the surfaces to be bonded and the forge-bond operation shall be no greater than 96 hours and a 24 hour interval should be considered as a goal; After bonding, holding the retort unit at a temperature of 1750°F for two hours and air cool; The retort will be removed prior to beta heat treatment; The parting agent shall be a proven inert material which will not provide a source of contamination; The press cross head velocity will be reduced to approximately 0.5 inches per minute and the pressure-bond time will be doubled.

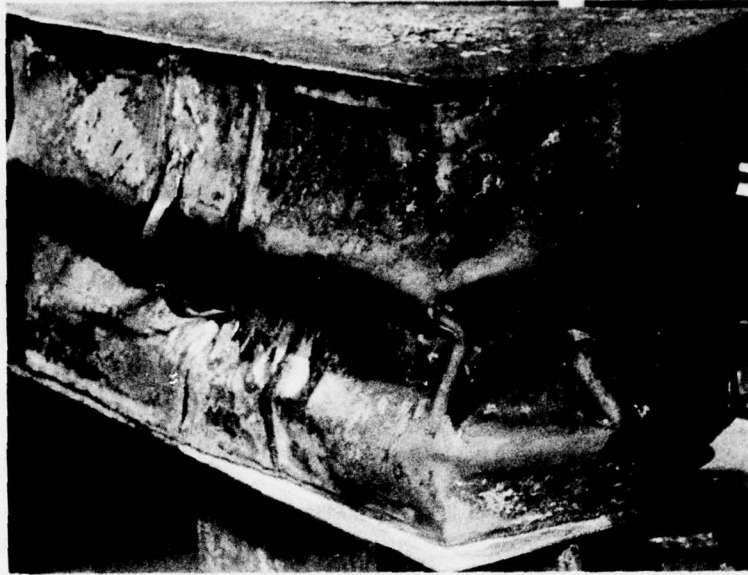


FIGURE 56. RETORT UNIT AFTER FORGE-BOND AND THERMAL TREATMENT, FIRST HUB ARM SEGMENT.

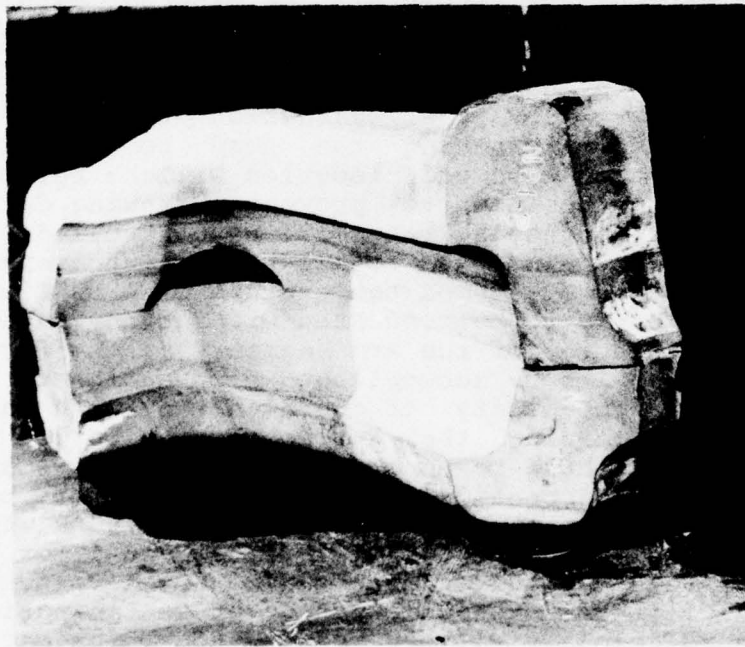


FIGURE 57. FIRST HUB ARM SEGMENT AFTER BONDING.

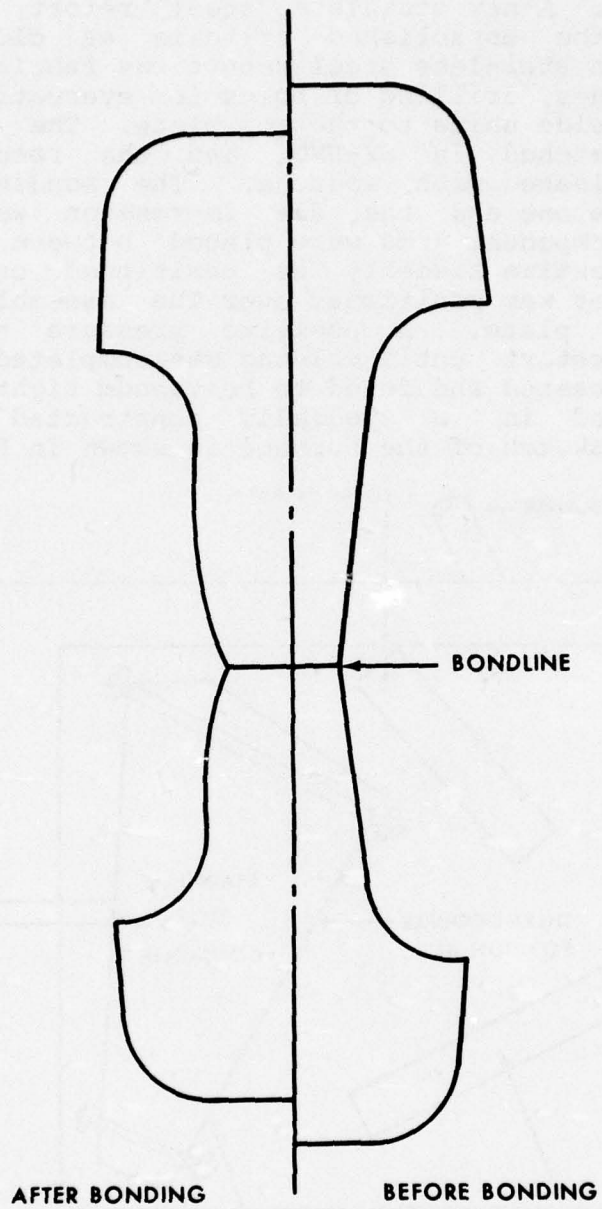


FIGURE 58. SKETCH OF CROSS SECTION THROUGH HUB ARM, BEFORE AND AFTER FORGE-BONDING.

The component arms for the second attempt and the bonding dies were cleaned in the same general manner as described for the first arm. A new stainless steel retort was prepared incorporating the established criteria as closely as was practical. The stainless steel retort was fabricated by seam welding of sides, drilling of holes for evacuation tube, and welding of the side units to the top plate. The component arm segments were etched in HF-HNO_3 and the retort was vapor blasted and cleaned with acetone. The bonding dies were cleaned with acetone and the die impression was coated with Mg(OH)_2 . The component arms were placed between the bonding dies and the entire assembly was positioned on the bottom plate. The cover was positioned over the assembly and welded to the bottom plate. A positive pressure of argon was maintained in retort until welding was completed. The retort unit was leak tested and found to be vacuum tight. The retort unit was placed in a specially constructed furnace for outgassing. A sketch of the furnace is shown in Figure 59.

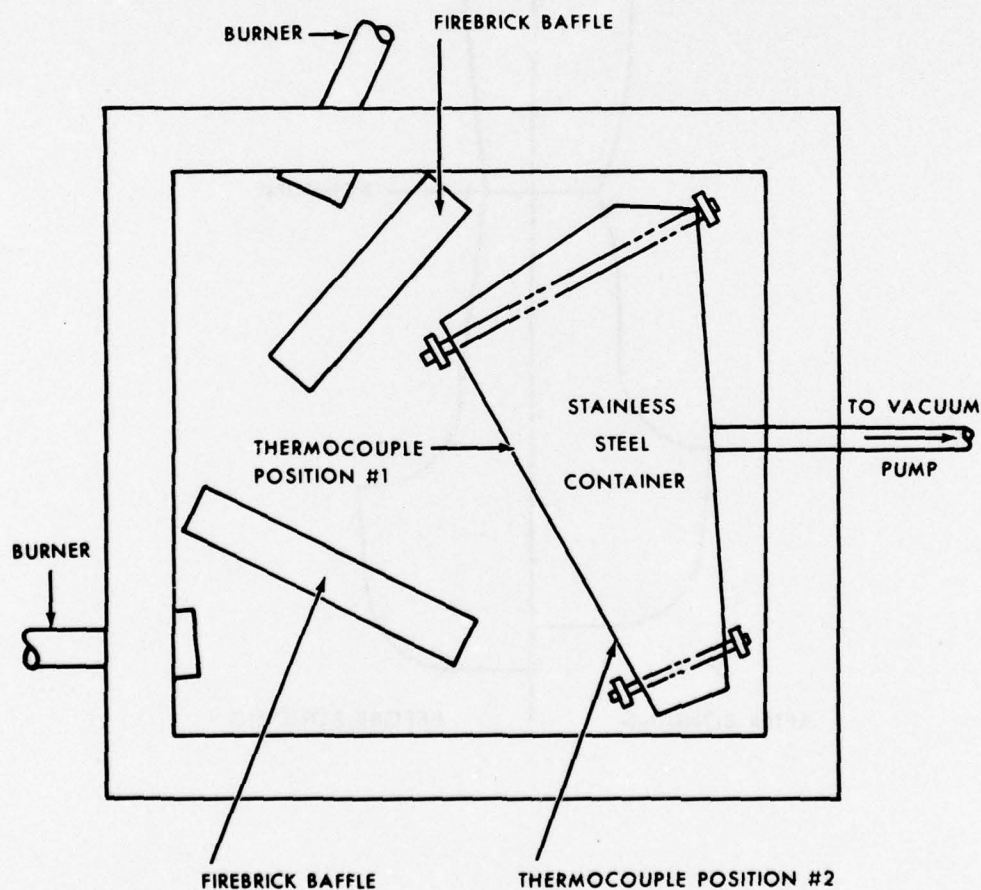


FIGURE 59. SKETCH OF OUTGASSING FURNACE, SECOND HUB ARM SEGMENT.

After 5 1/2 hours of heating-outgassing a power loss occurred, shutting off the vacuum pump. The vacuum pump valve was shut within two minutes after power loss sealing the system. The power returned after approximately two hours and the heating-outgassing continued. A graphical record of the furnace temperature and vacuum is shown in Figure 60.

After thirty hours of heating-outgassing, the evacuation tube was sealed and the retort unit was transferred to an adjacent furnace which was maintaining a temperature of 1750°F. The transferring operation took about three minutes. The retort unit remained in the 1750°F furnace for approximately seventeen hours before it was removed and forge-bonded in the 1,500 ton press. The bonding stroke required 114 seconds to complete and produced approximately 0.5 inch per minute pressing speed. The press force was 195 tons which yielded an interface pressure of approximately 5,600 psi. The retort unit was returned to the 1750°F furnace within five minutes after removal for forge-bonding for the post-bond thermal treatment. After two hours at 1750°F the retort unit was air cooled at room temperature. Figure 61 shows the retort unit after the forge-bond stroke and 1750°F post-bond thermal treatment. Figure 62 shows the recorder trace of displacement and force versus time for the second hub arm segment.

The retort was opened and the second arm segment was removed. Visual observation disclosed that the arm segment, the interior of the retort, and the vertical portion of the dies were slightly discolored. Dimensional examination indicate a bond stroke of 0.9 to 1.1 inches had been achieved. Cracks were observed in the retort. The cracks were located in both the base metal and at the welds where the vacuum had collapsed the retort against sharp corners of the dies. Figure 63 is a photomicrograph of the cracking condition in the parent metal. Metallographic examination revealed oxidation and probably nitride formation in and near the cracking.

After the retort had been removed, the arm segment was beta heat treated at 1900°F for one hour at temperature, water quenched, annealed at 1300°F for two hours and air cooled.

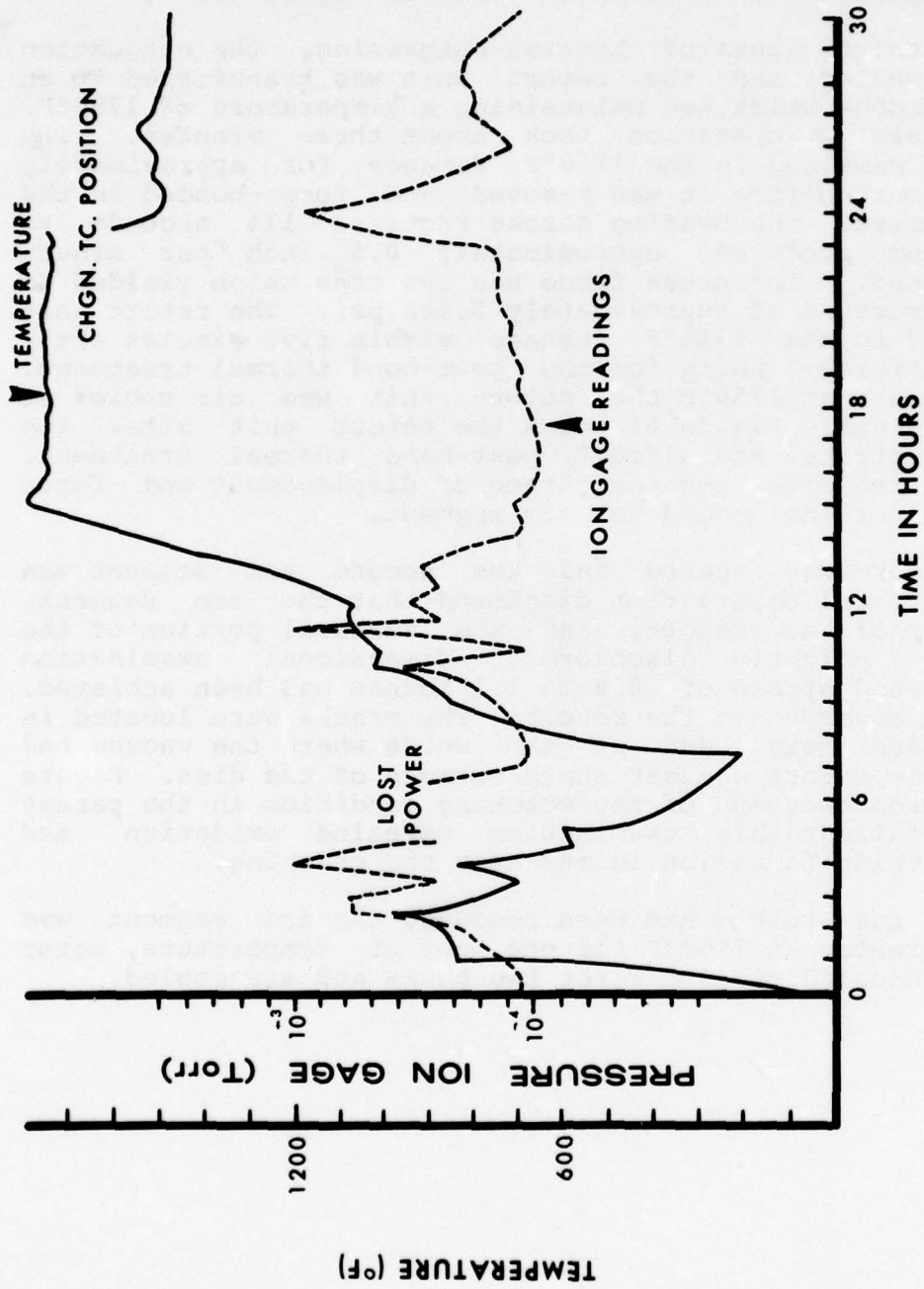


FIGURE 60. PLOT OF HEATING-OUTGASSING IN VACUUM OF SECOND ARM SEGMENT, TEMPERATURE AND PRESSURE VERSUS TIME.

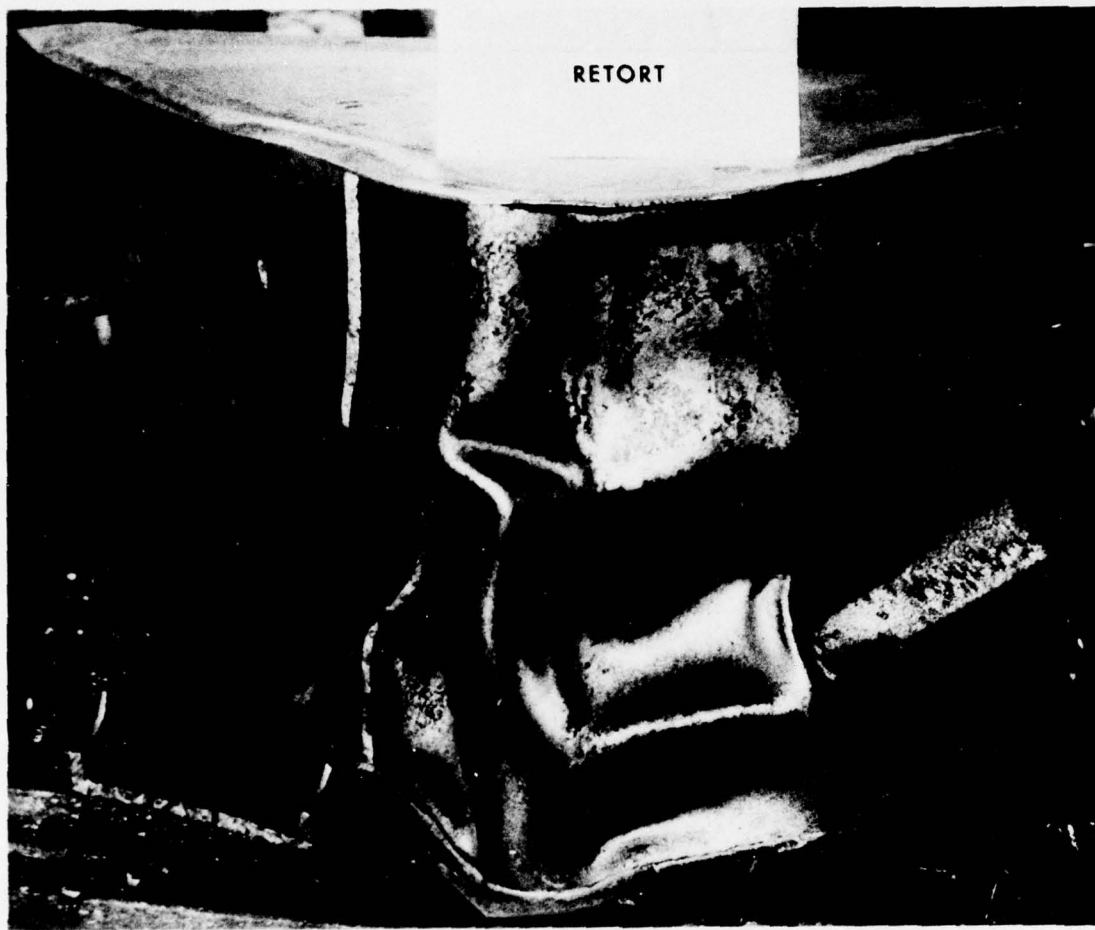


FIGURE 61. RETORT UNIT AFTER FORGE-BOND AND POST-BOND ANNEAL,
SECOND HUB ARM SEGMENT.

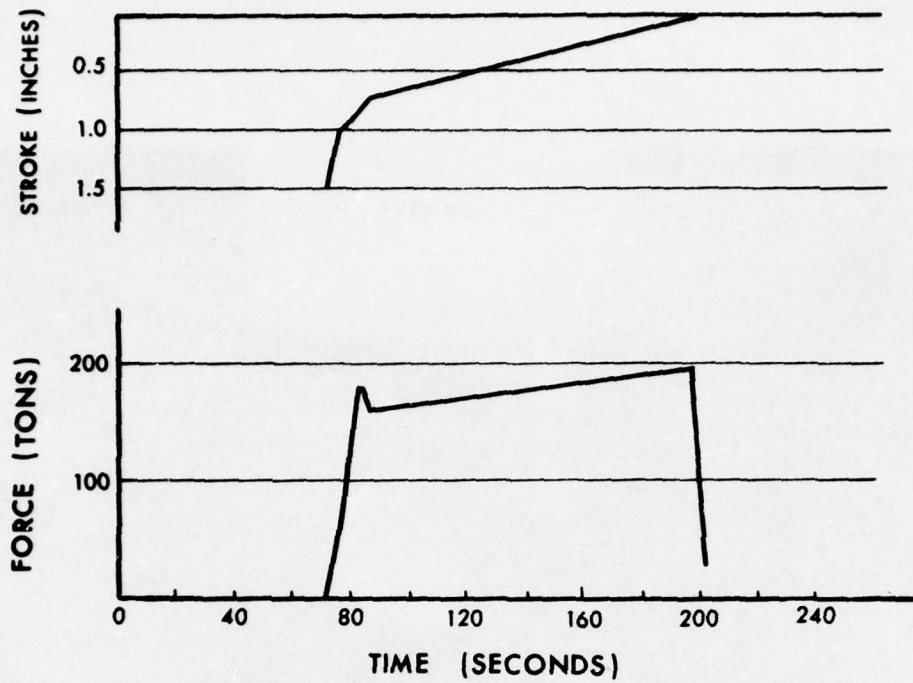


FIGURE 62. FORGE-BOND OPERATION OF SECOND HUB ARM SEGMENT, FORCE AND DISPLACEMENT VERSUS TIME.

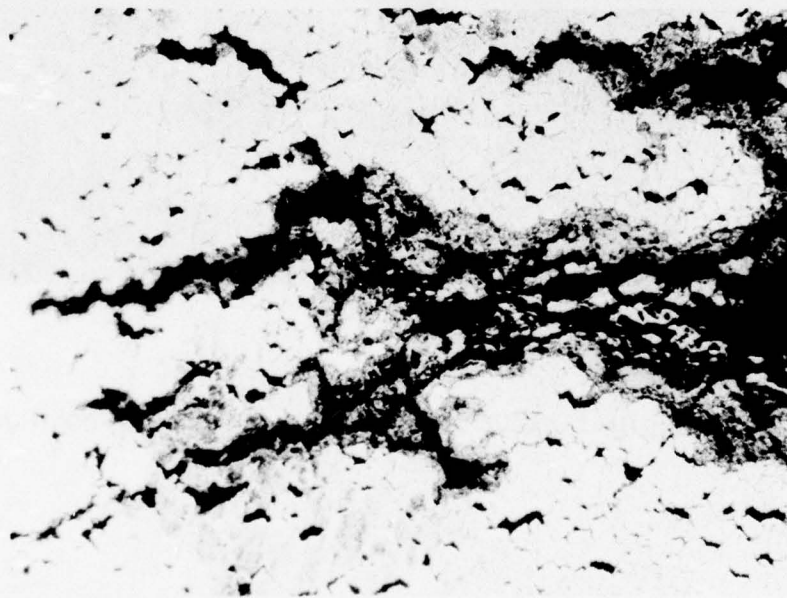


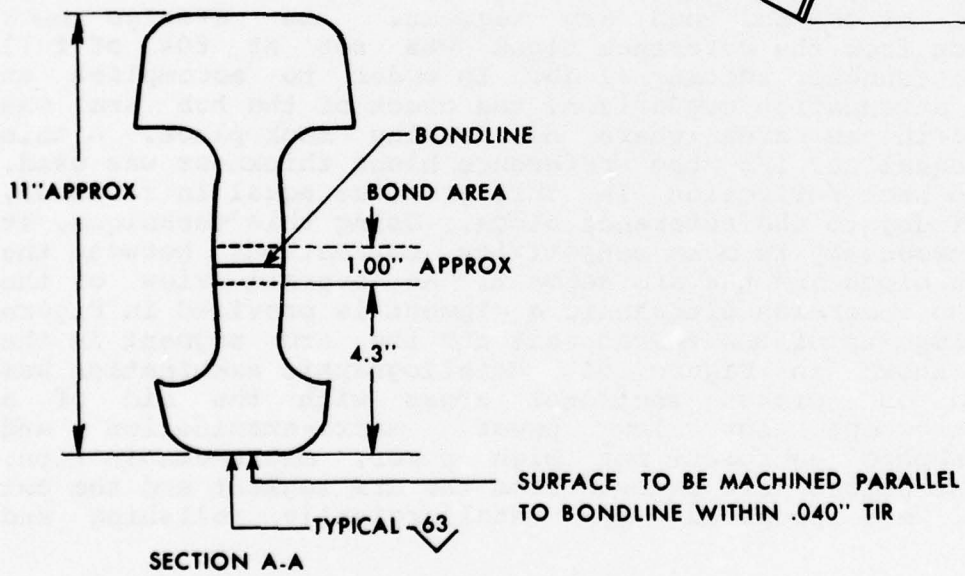
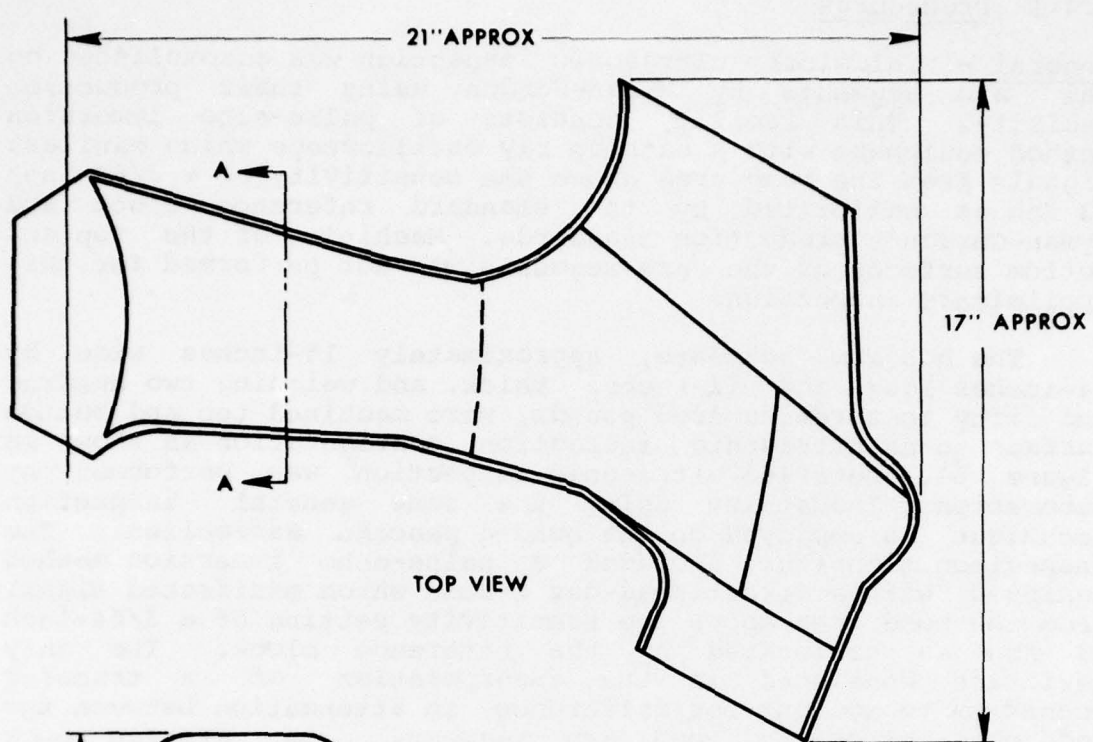
FIGURE 63. CRACKING CONDITION OBSERVED IN PARENT MATERIAL OF RETORT UNIT, SECOND HUB ARM SEGMENT. 100X

5.4 Hub Arm Segment Inspection

5.4.1 Procedures

General - Preliminary ultrasonic inspection was accomplished on the arm segments by Wyman-Gordon using their production facility. This facility consists of pulse-echo immersion method equipment with a cathode ray oscilloscope which manifest signals from the bond area above the sensitivity of a 3/64-inch #3 fbh as calibrated by the standard reference block and Wyman-Gordon's production standards. Machining of the top and bottom surfaces of the arm segments was not performed for this preliminary inspection.

The hub arm segments, approximately 15-inches wide by 24-inches long and 11-inches thick, and weighing two hundred and fifty to three hundred pounds, were machined top and bottom surface to an ultrasonic inspection configuration as shown in Figure 64. Detailed ultrasonic inspection was performed by Automation Industries using the same general inspection technique as employed on the bonded pancake assemblies. The inspection technique included a pulse-echo immersion method equipped with a direct read-out C-scan which manifested signal from the bond area above the sensitivity setting of a 3/64-inch #3 fbh as calibrated by the reference block. The only deviation consisted in the incorporation of a transfer mechanism to account for difference in attenuation between the reference block and hub arm segment. An average back reflection from the reference block was set at 80% of full screen, attenuator setting 41 db. In order to accomplish an accurate attenuation comparison, the check of the hub arm was performed in an area where no bonding took place. A thin section equal to 1/3 the reference block thickness was used. The third back reflection in this area was equal in response, 80% at 41 db, to the reference block. Using this technique, it was not necessary to make sensitivity corrections between the reference block and the arm segment. An overall view of the pulse-echo immersion ultrasonic equipment is provided in Figure 65. A close-up of the search unit and the arm segment in the tank is shown in Figure 66. Metallographic examination was conducted on cross sectional areas with the aid of a stereomicroscope for low power, macro-examination and metallographic equipment for high power, micro-examination. Transverse slices were removed from the arm segment and the cut surfaces were prepared by metallurgically polishing and etching.



HUB ARM SEGMENT Ti 6Al-4V

FIGURE 64. FORGE-DIFFUSION BOND HUB ARM SEGMENT, ULTRASONIC INSPECTION CONFIGURATION.

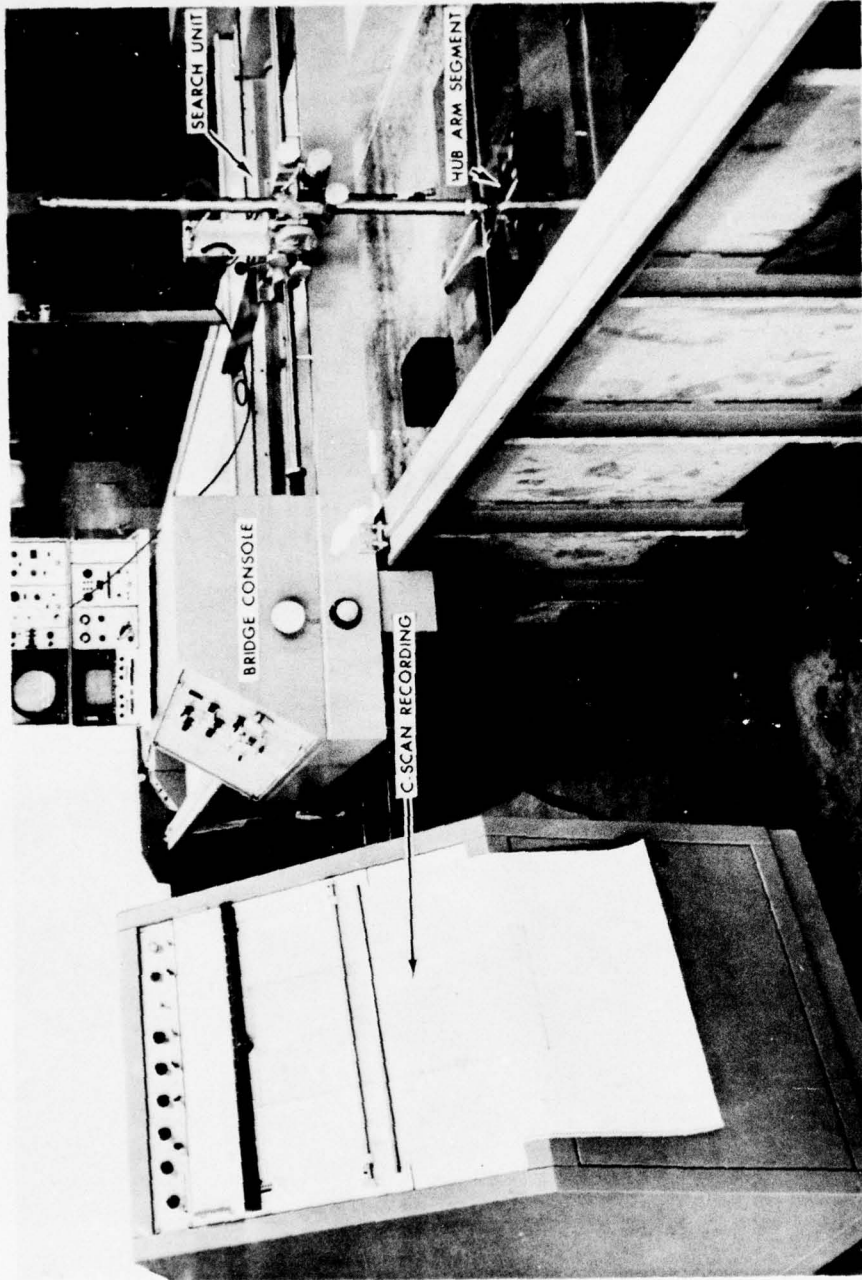


FIGURE 65. PULSE-ECHO IMMERSION ULTRASONIC EQUIPMENT USED IN INSPECTION OF HUB ARM SEGMENTS.

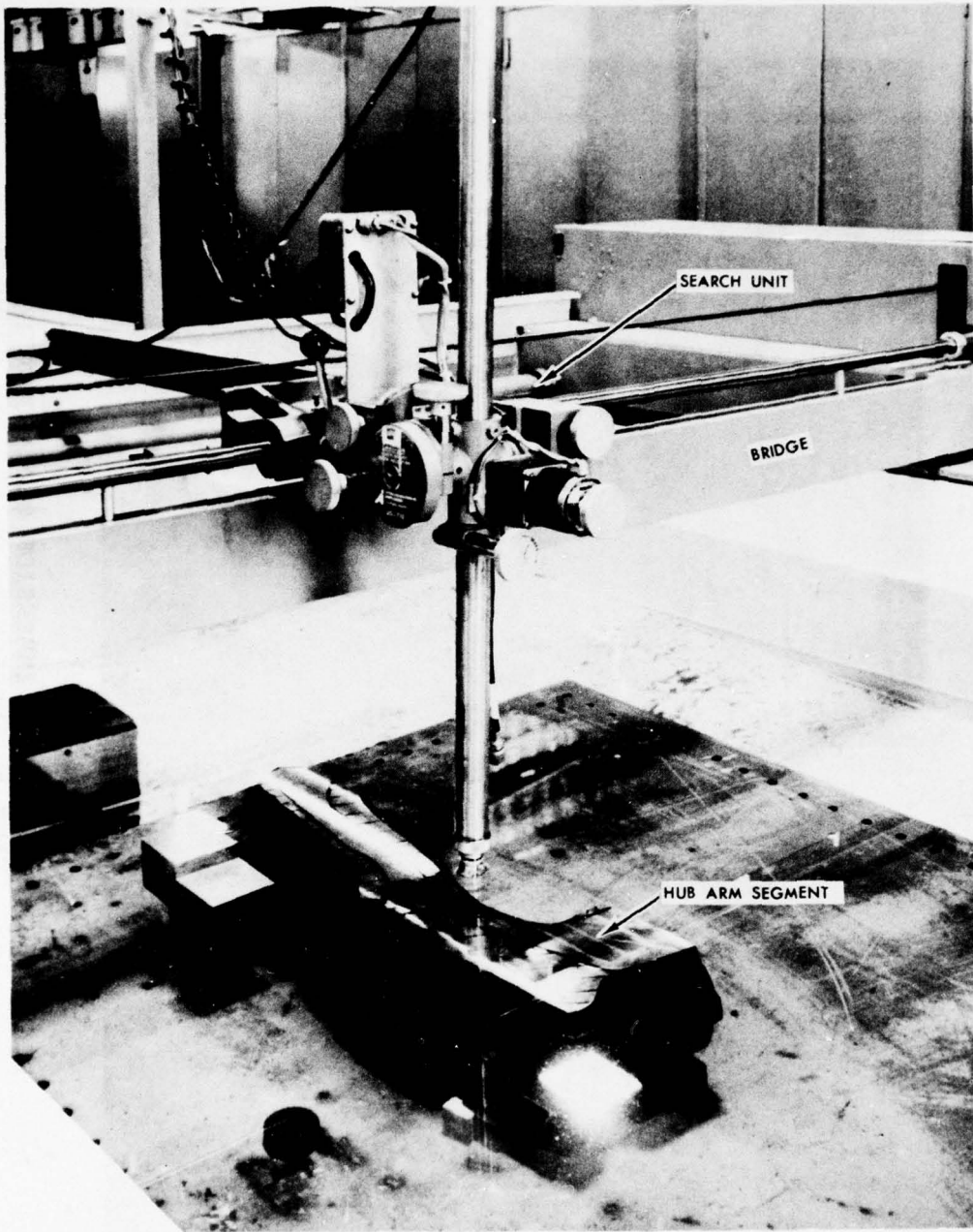


FIGURE 66. CLOSE-UP OF SONIC SEARCH UNIT AND ARM SEGMENT IN TANK.

5.4.2 Inspection Results; 3rd and 4th Hub Arm Segment
First Two Satisfactory Diffusion Bonded Arms

3rd Hub Arm - After the forge-bond and post-bond thermal treatment at 1750°F, the retort was opened by cutting and the third arm segment was removed from the bonding dies. Generally, the arm segment was bright, manifesting a noncontaminated surface. Only one area on the arm segment disclosed a minute area of possible contamination. Figure 67 shows the arm segment as it was removed from the retort.



FIGURE 67. THIRD HUB ARM SEGMENT AS REMOVED FROM REPORT.

Preliminary ultrasonic inspection at Wyman-Gordon prior to the finish beta heat treatment indicated that about half of the mating surface was not bonded. The preliminary ultrasonic inspection was accomplished without surface machining. Flat parallel surfaces are normally required for consistent sonic response. Figure 68 is a sketch of the arm segment and illustrates a suspected area of nonbonding as indicated by this technique.

AFTER FORGE BOND AND #1 ANNEAL AT 1750 F

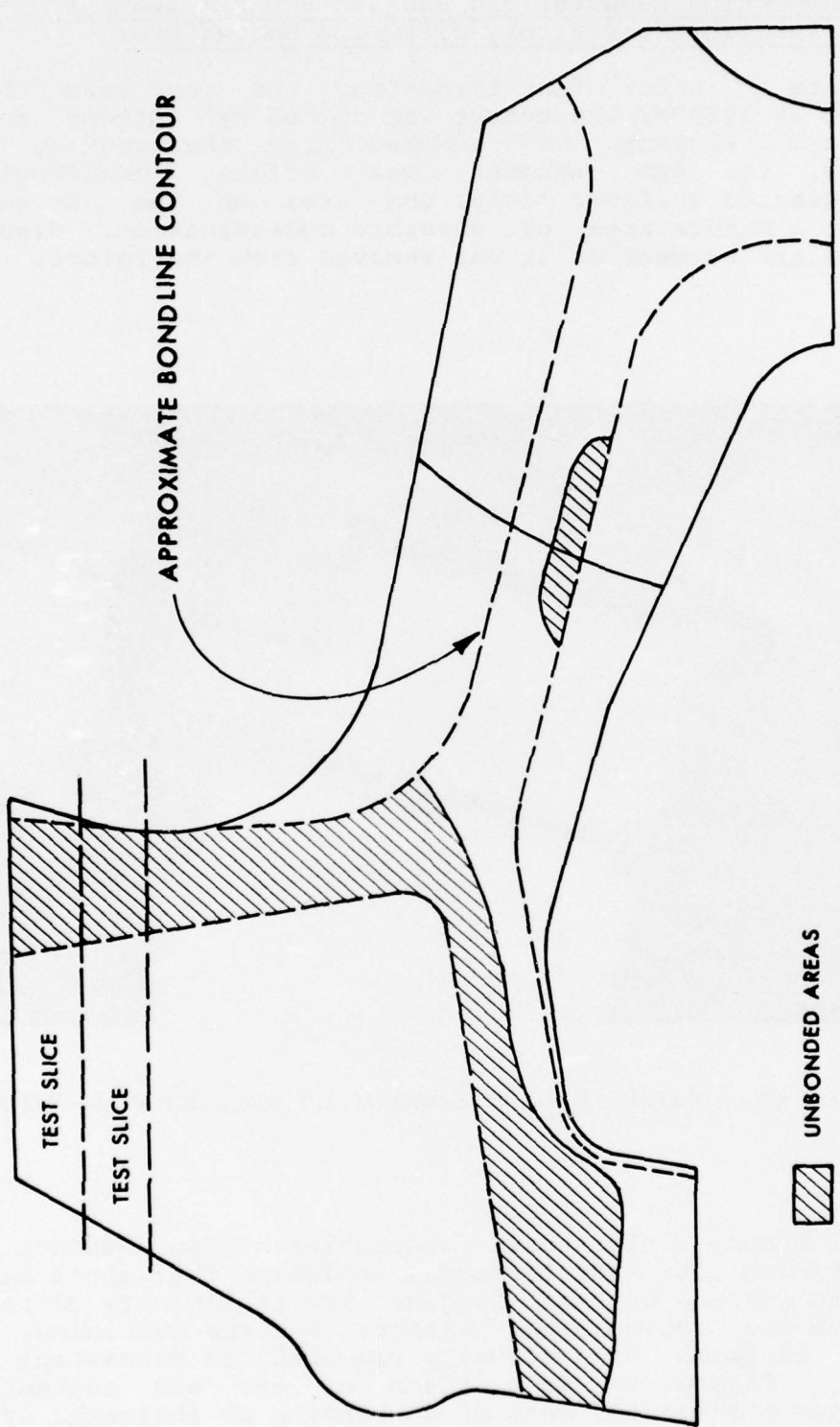


FIGURE 68. SKETCH OF THIRD ARM SEGMENT ILLUSTRATING PRELIMINARY ULTRASONIC INSPECTION INDICATIONS BEFORE FINAL BETA HEAT TREAT.

Transverse slices were cut from an area exhibiting some indications of nonbonding. Contrary to the ultrasonic indications, macrostructure examination disclosed an apparent good diffusion bond. The forging flow lines were evident in the alpha-beta macrostructure and tended to bring out the bondline location. Figure 69 depicts the macrostructure across the bondline. Micro-examination of the same area revealed no evidence of cracking, lack of bond, contamination or other discontinuities at the joint interface. In order to examine the bondline in more detail, a segment of the macrospecimen was processed in accordance with the final beta heat treatment. The heat treatment consisted of 1900°F for one-hour, water-quench, anneal at 1300°F for two hours and air cool. Metallurgical examination again disclosed no gross lack of bond in the beta structure which appeared to be homogeneous as shown in Figure 70 with no indication of the bondline location.

Two coupons approximately 3/8-inches thick were cut from the heat treated macrospecimen, and fractured by bending. One coupon was tested by bending across the bond joint material and the other was tested by bending in the parent material. Comparison of the fracture interfaces revealed the same general type failure with similar ductility characteristics further indicating the existence of a good bonded joint. Figures 71 and 72 show the location of separation and fracture interfaces of both the bond joint and parent material coupon. Fracture loads were not measured for this qualitative assessment.

Because the arm now appeared to be fully bonded it was heat treated in accordance with the remaining thermal treatment, i.e., 1900°F for one hour, water-quench, anneal at 1300°F for two hours and air cooled. The completely heat treated segment was resubmitted for preliminary sonic evaluation by Wyman-Gordon which indicated essentially the same results as previously obtained.

Since the microscopic examination and the ultrasonic results did not correlate, it was theorized that the sonic indications may have been associated with the arm configuration rather than lack of bond. The shape of the arm segment might have caused reflections and diversion of the sonic beam resulting in sonic indication. In order to substantiate this theory, two additional slices, "A" and "B" were taken from the third arm segment. Section "A" was from an area that preliminary sonic inspection had characterized as bonded and Section "B" was taken from an area characterized as nonbonded. The slices were machined into an inspectable sonic configuration, a rectangular shape cube, before conducting a detailed ultrasonic inspection which included C-scans. When the test slices were machined free of the mismatch condition and the inspection surfaces were machined parallel to the faying surface, both slices "A" and "B", test blocks exhibited

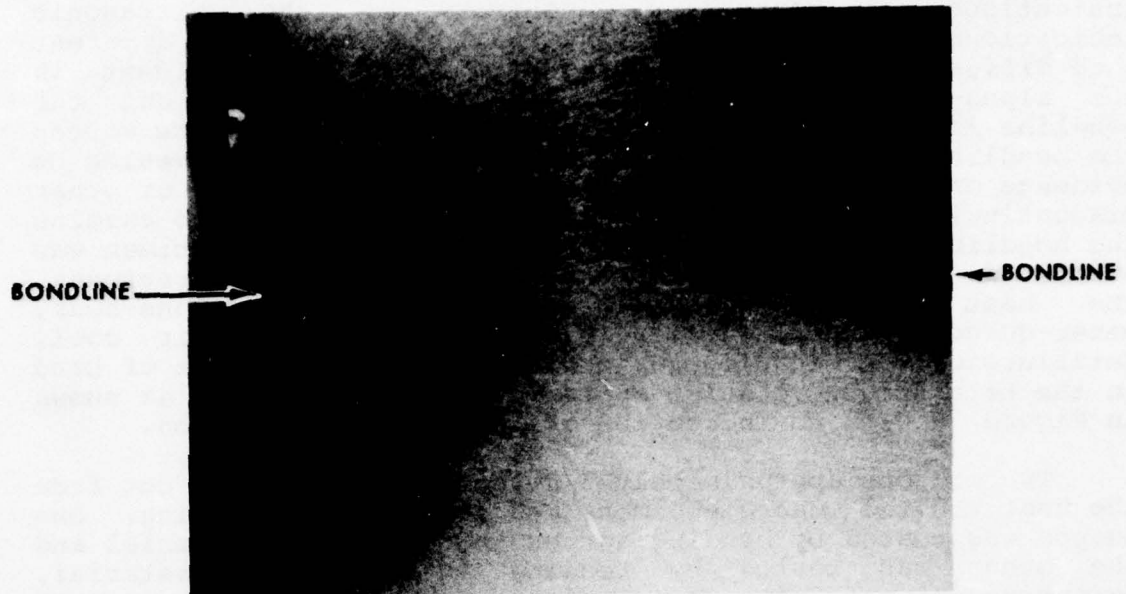


FIGURE 69. MACROSTRUCTURE ACROSS BONDLINE OF THIRD HUB ARM SEGMENT, BEFORE FINAL BETA HEAT TREAT DISCLOSES NO GROSS LACK OF BOND. 1.2X



FIGURE 70. MICROSTRUCTURE ACROSS BONDLINE OF THIRD HUB ARM SEGMENT, AFTER FINAL BETA HEAT TREAT AGAIN DISCLOSED NO GROSS LACK OF BOND. 50X

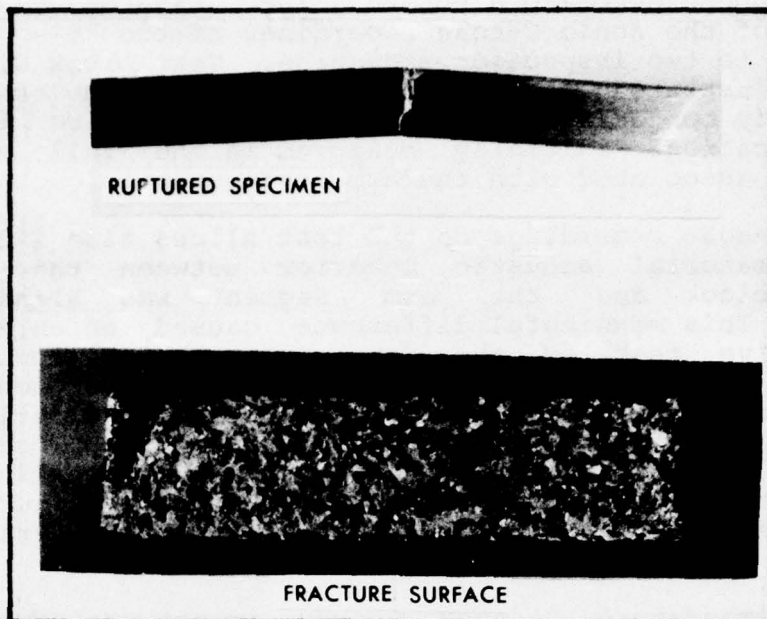


FIGURE 71. BEND SPECIMEN ACROSS BONDLINE, THIRD HUB ARM SEGMENT.

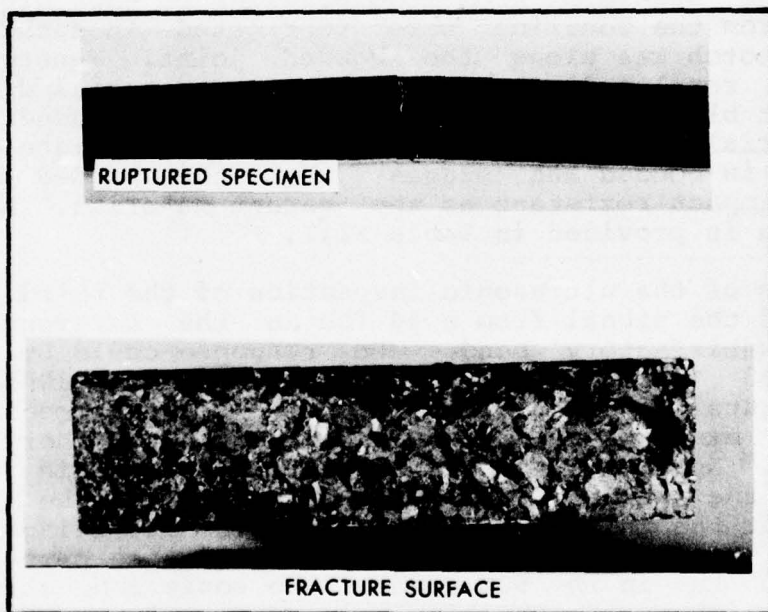


FIGURE 72. BEND SPECIMEN FROM PARENT MATERIAL, THIRD HUB ARM SEGMENT.

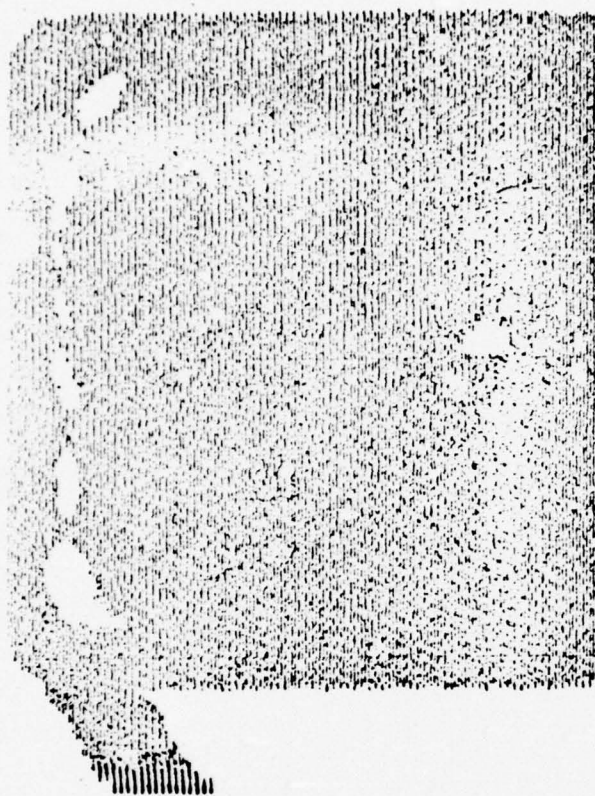
a sonic response denoting a bonded joint. Figures 73 and 74 are copies of the sonic C-scan recordings of the two machined test blocks to two inspection standards. Test block dimensions are also illustrated in these figures. These results indicate an adequately bonded arm and substantially confirm that the sonic indications initially observed in the full size arm segment are associated with the arm configuration.

The C-scan recordings on the test slices also illustrated that the material acoustic behavior between the standard reference block and the arm segment was significantly different. This meaningful difference caused an unrealistic, ultrasensitive test of the arm segment. Discontinuities relating to the alignment of the half-forging component at the mating surface and edge effect were magnified indicating gross nonbond area along the edge of the arm segment. These sonic indications of gross nonbond areas were in reality minute anomalies or mismatch associated with the arm configuration at the bond joint and sensitivity level employed during sonic inspection.

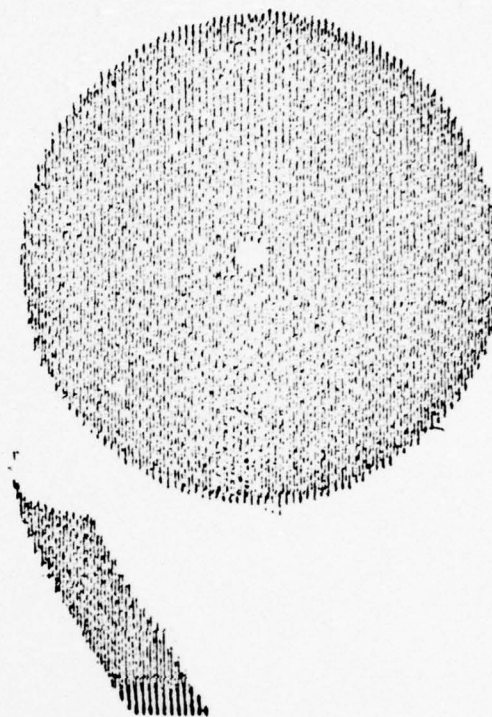
Room temperature V-notch Charpy impact resistance tests were conducted as an additional quantitative measure of the integrity of bonded titanium components. A total of four Charpy impact specimens were taken from both the "A" and "B" test blocks. One specimen from the parent material of each block and one specimen from the bondline of each block. The specimens from the bondline were fabricated in such a manner that the V-notch was along the bonded joint. V-notch Charpy impact test results disclosed little or no material difference between test blocks, "A" and "B" or between bonded joint or parent material. These results further substantiate that the arm segment is bonded and suggest that the bonded joint is equally as impact resistant as the parent material. A summary of test data is provided in Table XIII.

Results of the ultrasonic inspection of the third hub arm using 80% of the signal from a #4 fbh in the reference block revealed a satisfactory bond. No response could be obtained from the #3 fbh in the reference block even at 100% of the signal. Figure 75 is a copy of the C-scan recording and illustrates minimum abnormalities along the periphery of the arm segment. No sonic indications were detected in the area away from the edge. C-scan recordings confirm the previous position that the third arm was bonded. The recordings map-out the general bond area and have approximated the percentage of bond area to be in the 90% range. The sonic indications were along the periphery of the faying surface and were related to minute nonbonded areas or mismatch associated with the arm configuration at the bond joint.

SECTION A



SIKORSKY BLOCK
#3 HOLE $-3^{3/8}$ " M.T.
CRYSTAL #LH6635-5MHZ, $3/4$ " FLAT
GAIN=3.6 AT $\times 1$ 2" AMP
ALARM LEVEL=25%
BR=1

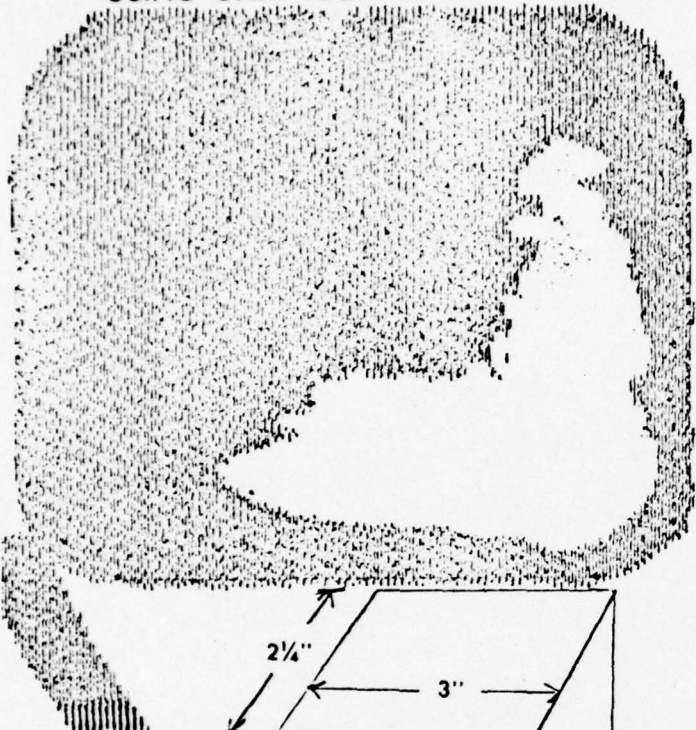


W-G STD #3, $2^{1/4}$ 3" MT
CRYSTAL #LH6635-5MHZ: $3/4$ " FLAT
GAIN=0.4 AT $\times 1$ 2" AMP
ALARM LEVEL=25%
BR=4 +

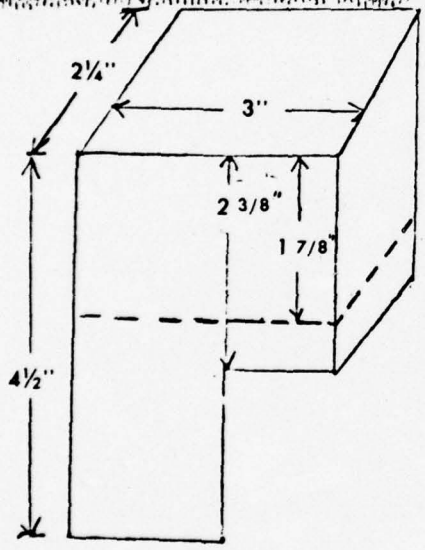
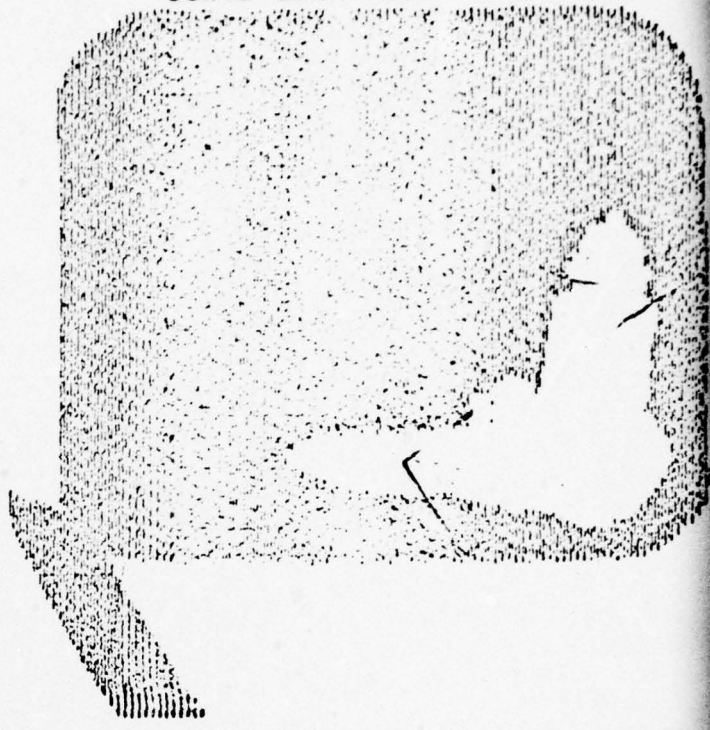
FIGURE 73. C-SCAN RECORDINGS OF MACHINED TEST BLOCK "A"
FROM THIRD HUB ARM SEGMENT WITH NO PRELIMINARY
SONIC INDICATION.

SECTION A

USING GAIN FROM SIKORSKY BLOCK

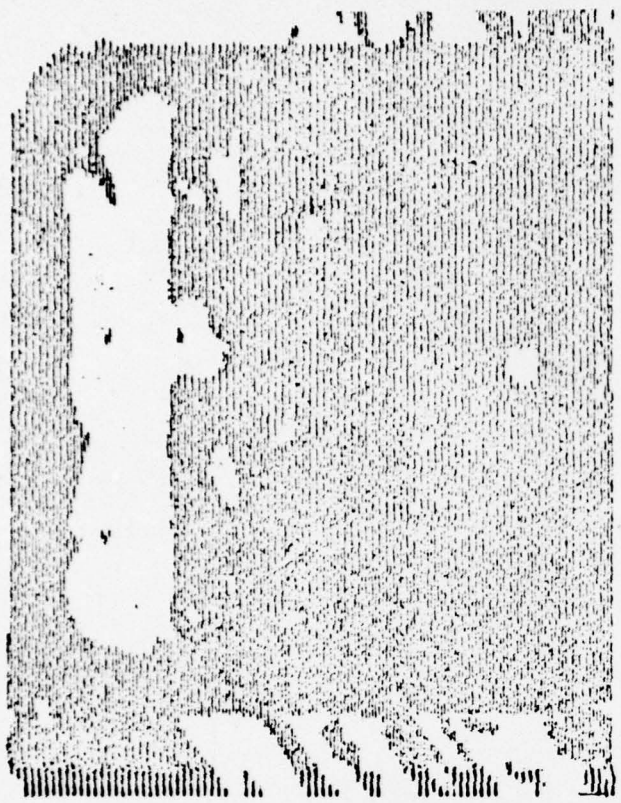


USING GAIN FROM W.G. BLOCK

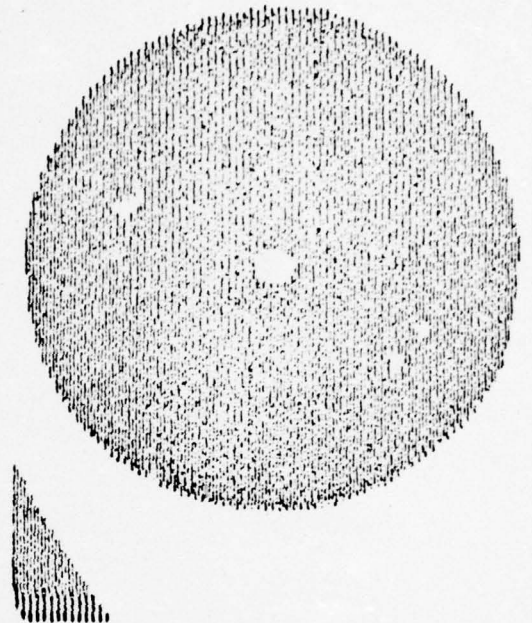


1/4" FLAT

J



SIKORSKY BLOCK
 #3 HOLE -3 3/8" M.T.
 CRYSTAL #LH6635-5MHZ 3/4" FLAT
 GAIN=3.6 AT x 1 2" AMP
 ALARM LEVEL =25% BR=1

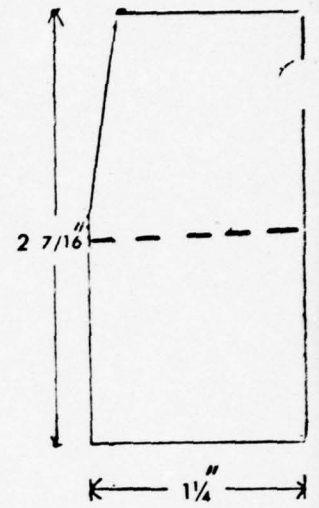
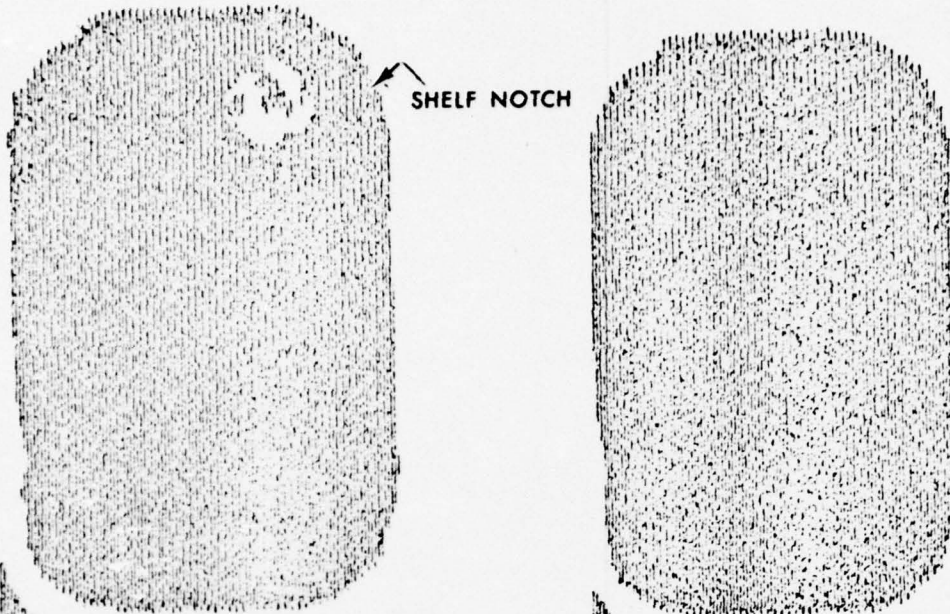


W-G STD
 #3 2 1/4 3" MT
 CRYSTAL #LH 6635-5MHZ 3/4" FLAT
 GAIN=0.4 AT x1 2" AMP
 ALARM LEVEL =25% BR=4+

FIGURE 74. C-SCAN RECORDINGS OF MACHINED TEST BLOCK "B" FROM THIRD HUB ARM SEGMENT WITH PRELIMINARY SONIC INDICATION.

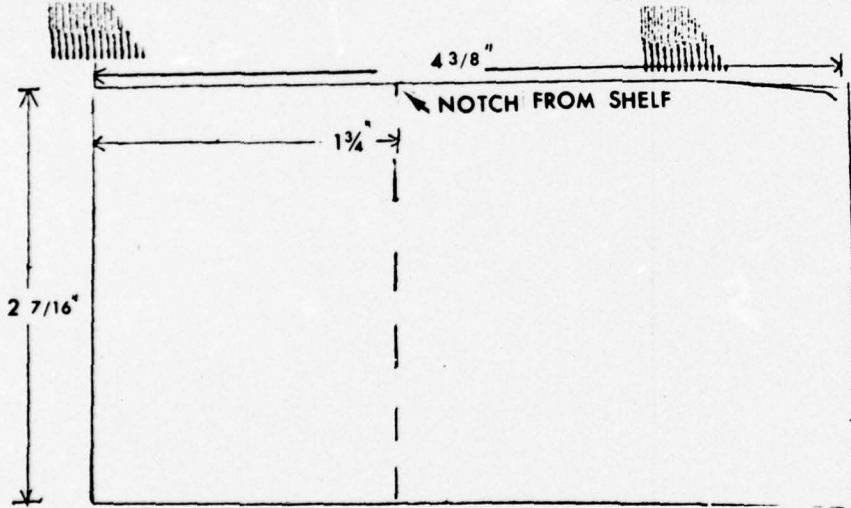
SECTION B

PLANE VIEW



USING GAIN FROM SIKORSKY BLOCK

USING GAIN FROM W-G BLOCK



Z 3/4" FLAT
MP
R=4+

2

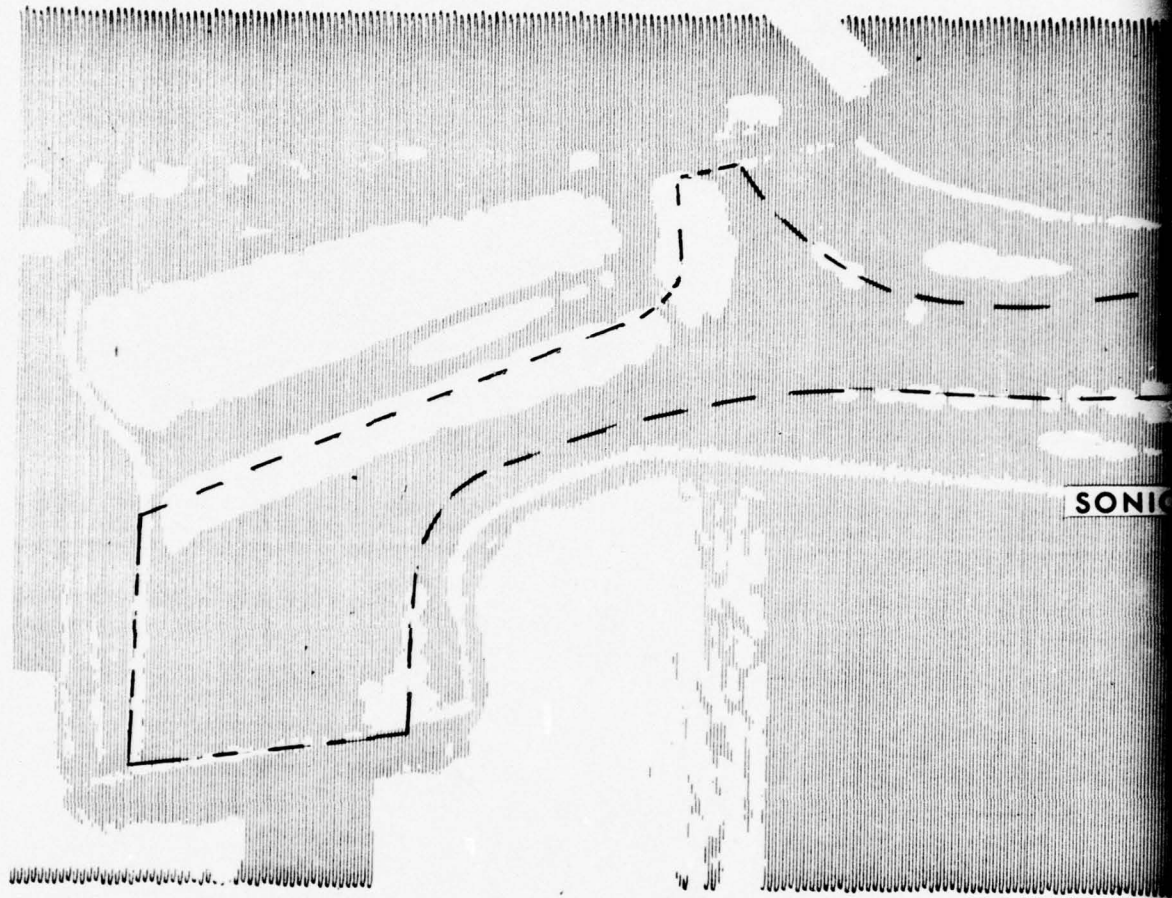


FIGURE 75. C-SCAN RECORDING OF THIRD HUB ARM SEGMENT,
ALARM LEVEL 80% OF #4 fbh IN REFERENCE BLOCK.



APPROXIMATE BONDLINE CONTOUR

SONIC INDICATION

ARM SEGMENT,
REFERENCE BLOCK.

2

TABLE XIII		
ROOM TEMPERATURE "V"-NOTCH IMPACT RESISTANCE TEST		
THIRD HUB ARM SEGMENT		
TEST BLOCK DESIGNATION*	"V"-NOTCH LOCATION	IMPACT RESISTANCE (Foot-Pounds)
A	Bond Joint	10.5
A	Parent Material	9.5
B	Bond Joint	9.0
B	Parent Material	11.0

*Test Block A Was Initially Characterized As "Bonded" By Sonic; B Nonbonded.

4th Hub Arm - Following completion of the fabrication process, the fourth arm segment was machined top and bottom surfaces to an ultrasonic inspection configuration. The technique used in inspection of the fourth arm was the same as employed for the third arm. Results of this inspection disclosed a satisfactory joint with no evidence of gross lack of bond. C-scan recordings portrayed a similar read-out, as obtained previously from the third arm. Figure 76 is a copy of a C-scan recording of the fourth arm segment depicting the familiar anomalies along the periphery.

THIS PAGE INTENTIONALLY LEFT BLANK



FIGURE 76. C-SCAN RECORDING OF FOURTH HUB ARM SEGMENT,
80% OF #4 fbh IN REFERENCE BLOCK.

APPROXIMATE BONDLINE CONTOUR

SONIC INDICATION

SEGMENT,

2

5.4.3 Inspection Results; 1st and 2nd Hub Arm Segments First Two Unsuccessful Attempts

The purpose of this section is to document the events, procedures, and results of the inspection of the first two attempts to diffusion bond the single hub arm risk reduction segment.

1st Hub Arm - Upon completion of the forge-bond, post-bond, and finish heat treatment, the first arm segment was given a preliminary ultrasonic inspection. Results of this inspection revealed several areas exhibiting evidence of nonbonding. These indications were lenticular bands approximately 1/4-inches wide by 3 to 5 1/2-inches in length, located longitudinally in the center region of the bond area.

The arm segment was machined to the ultrasonic inspection configuration for detail inspection with permanent C-scan recordings. Sonic inspection with C-scan recordings substantially confirmed the areas of nonbonding indicated previously by the preliminary ultrasonic inspection. The C-scan recordings manifested sonic indications for approximately 40% of the bond joint as shown in C-scan recording, Figure 77. Metallographic examination of a cross section through the most extensive area of sonic indication, Section AA, Figure 77, revealed a one-inch nonbond area extending from the outside edge. Figure 78 is a photomicrograph of a cross section of a typical area manifesting nonbonding and illustrates the lack of bond at the periphery. Evidence of contamination extending onto the interface can be observed on the outside surface of the arm as shown in Figure 79. Examination of subsurface areas, inboard-away from the periphery, revealed regions of nonbonding associated with an enveloping layer of contamination as shown in photomicrograph, Figure 80.

2nd Hub Arm - Subsequent to the final beta heat treatment, the second arm segment was subjected to a preliminary ultrasonic inspection. Results of this inspection disclosed that the arm segment exhibited several areas of sonic indications on apparent nonbond areas. Two slices were cut from the locations designated bonded and nonbonded. Metallographic examination of the slices confirm the sonic results as shown in Figures 81 and 82. Both the bonded and nonbonded areas revealed contamination along the bondline. This contamination was more extensive in the nonbonded areas. Figure 83 portrays the extent of alpha contamination along the bondline of a typical bonded area.

5.5 Hub Arm Segment (#3) Mechanical Property Testing of First "Good" Arm

5.5.1 Procedure

General - The first "good" arm, the third arm segment, was used as the risk reduction component to evaluate and compare the mechanical properties of the parent material and the forge-bond joint material. Mechanical property tests consisting of tensile, fracture toughness, in-line shear, and fatigue initiation were conducted on the parent material and at the forge-bond material bondline. Nine fatigue initiation specimens and three each: tensile, fracture toughness, and in-line shear specimens were fabricated and tested from the parent material and bondline. Figure 84 illustrates the types of specimen tested and the general location of the specimen within the arm segment. Bondline test specimens were fabricated in a manner to insure testing along the forge-bond joint. Tensile, fracture toughness, in-line shear, and fatigue initiation testing were performed in a similar manner as described previously in 3.3.1 Procedure, Pancake Testing.

5.5.2 Results

General - Analysis of the mechanical properties of the parent material and the forge-bond joint revealed no significant differences. The results indicated a high quality diffusion bonded joint had been obtained. A summary of the test results is provided in Figure 85. Visual evaluation of the tested specimens, parent material and bondline revealed that all the specimens failed in the test region and are considered valid tests. The bondline specimens separated within the test section as designed. Fracture examination of the tensile, fracture toughness, in-line shear, and fatigue initiation specimens for the parent material and bondline specimens revealed the mode and mechanism of failure to be typical as related to the particular type of tests conducted. No evidence of any abnormalities were detected on the fracture surface of the bondline specimens that could have caused or contributed to premature failures. Microstructure examination of cross sectional areas of bondline specimens revealed no evidence of failure initiation due to an anomaly at the bondline. No significant differences were observed between the parent material and bondline specimens. Metallographic examination of cross sectional segments of bondline specimens and macroslices disclosed no evidence of voids, contamination, or lack of bond. In most instances, metallographic examination could not distinguish the bond joint from the parent material, as illustrated in Figure 86.

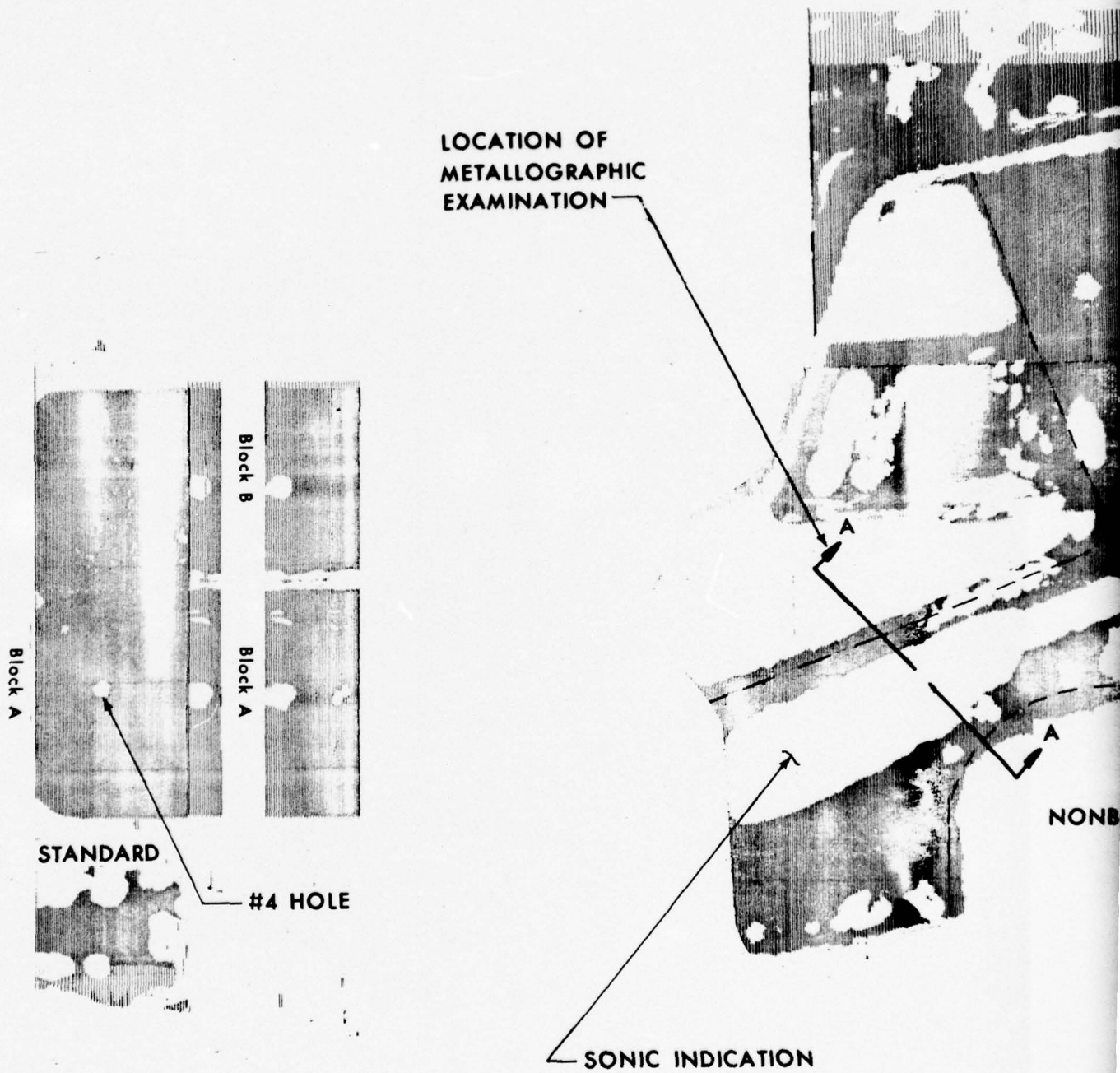
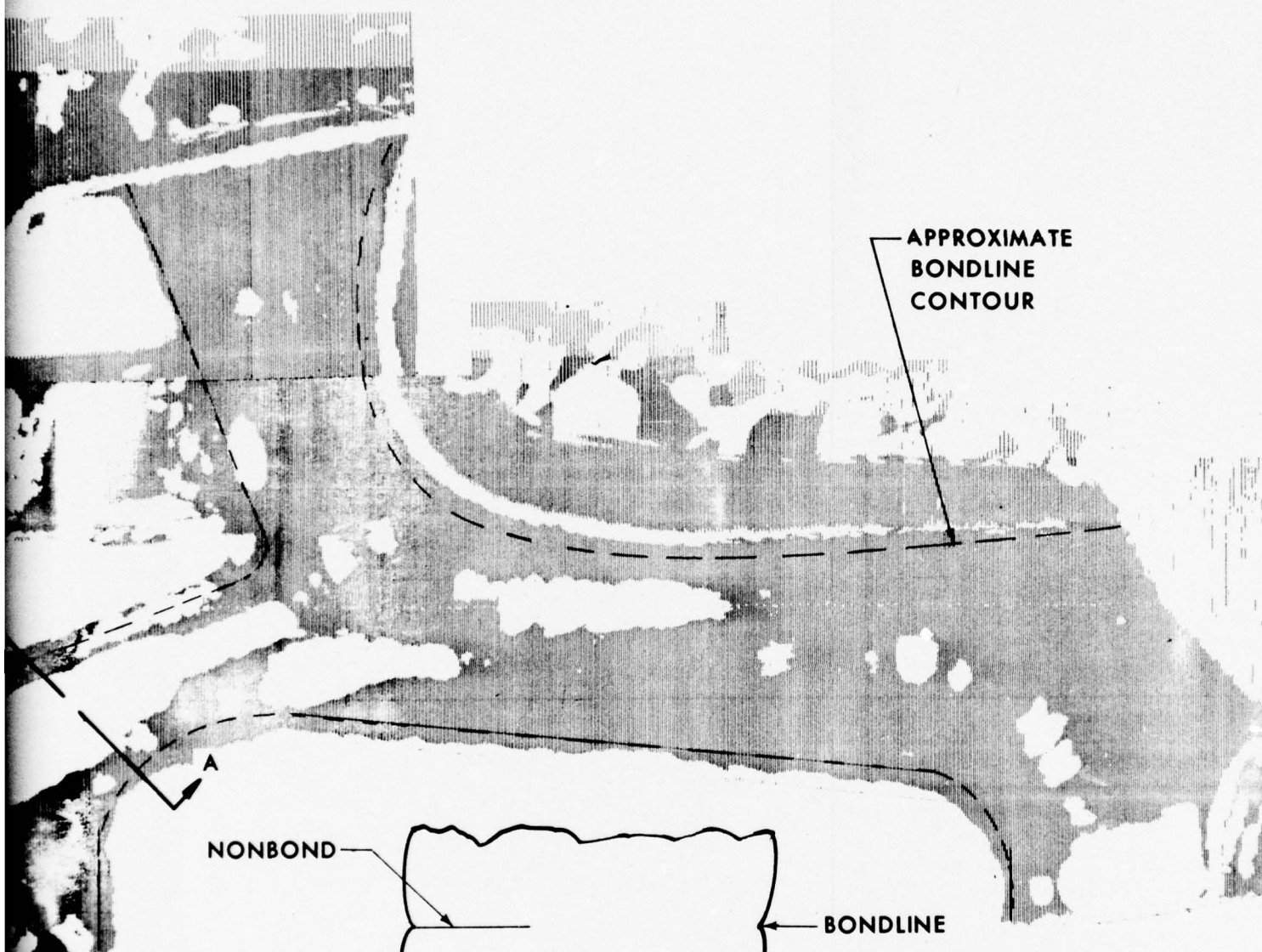


FIGURE 77. C-SCAN RECORDING OF FIRT'S HUB ARM SEGMENT, ALARM LEVEL 80% OF #4 fbh IN REFERENCE BLOCK.



NONBOND

APPROXIMATE
BONDLINE
CONTOUR

BONDLINE

CROSS SECTION THROUGH SONIC INDICATION
SECTION A-A

2

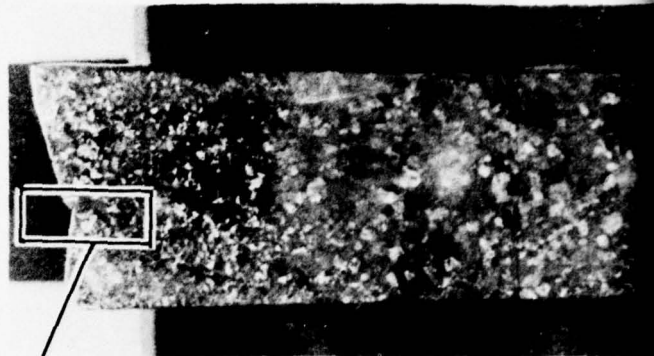


FIGURE 78. CROSS SECTION OF FIRST
TYPICAL AREA OF SONIC II
GROSS NONBONDED CONDITIO

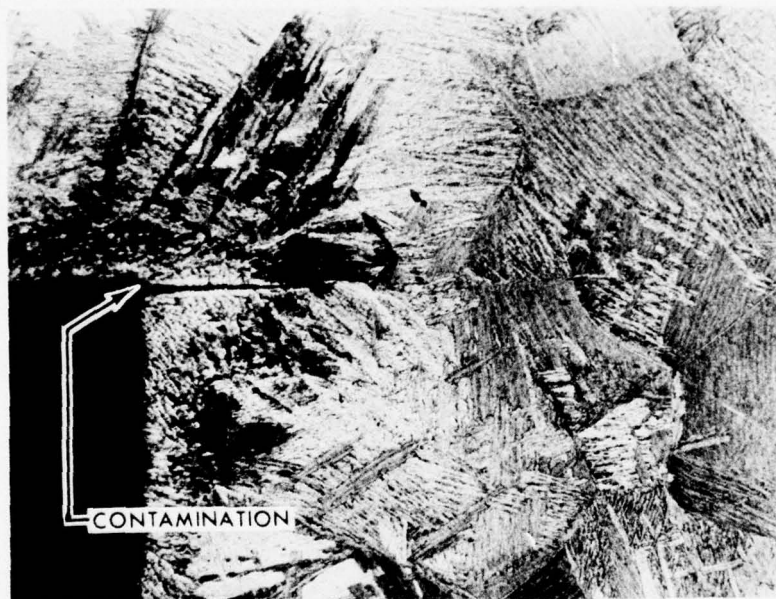
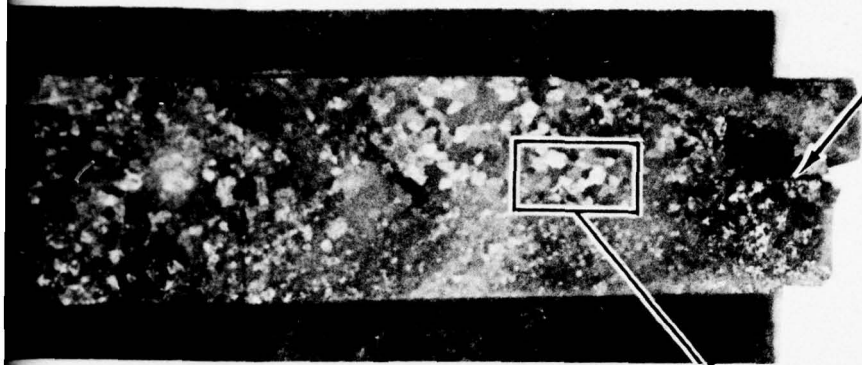


FIGURE 79. CONTAMINATION ON OUTSIDE SURFACE EXTENDS ONTO
FAYING SURFACE, FIRST ARM SEGMENT. 50X

NONBOND AREA



CROSS SECTION OF FIRST ARM SEGMENT THROUGH
TYPICAL AREA OF SONIC INDICATION ILLUSTRATES
CROSS NONBONDED CONDITION. 1X



EXTENDS ONTO
• 50X

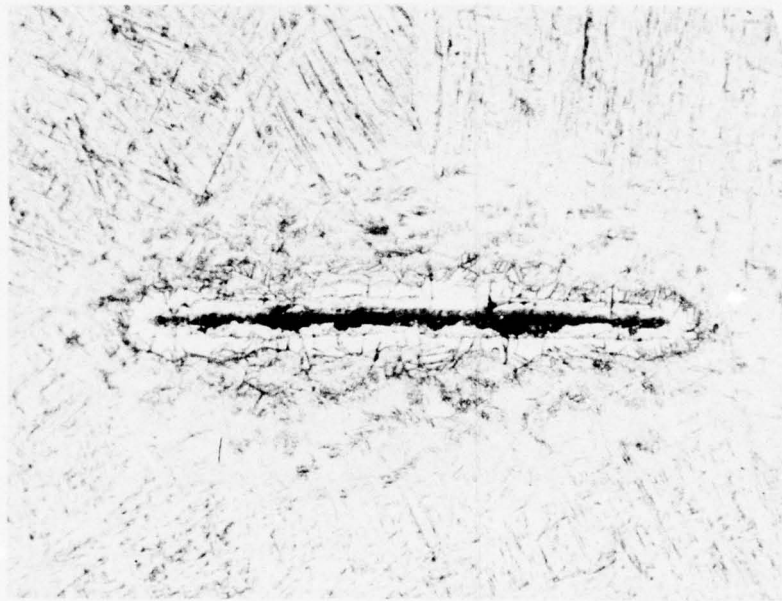


FIGURE 80. SUBSURFACE REGIONS OF NONBONDING ENVELOPED
IN A LAYER OF CONTAMINATION, FIRST ARM SEGMENT.
200X

2

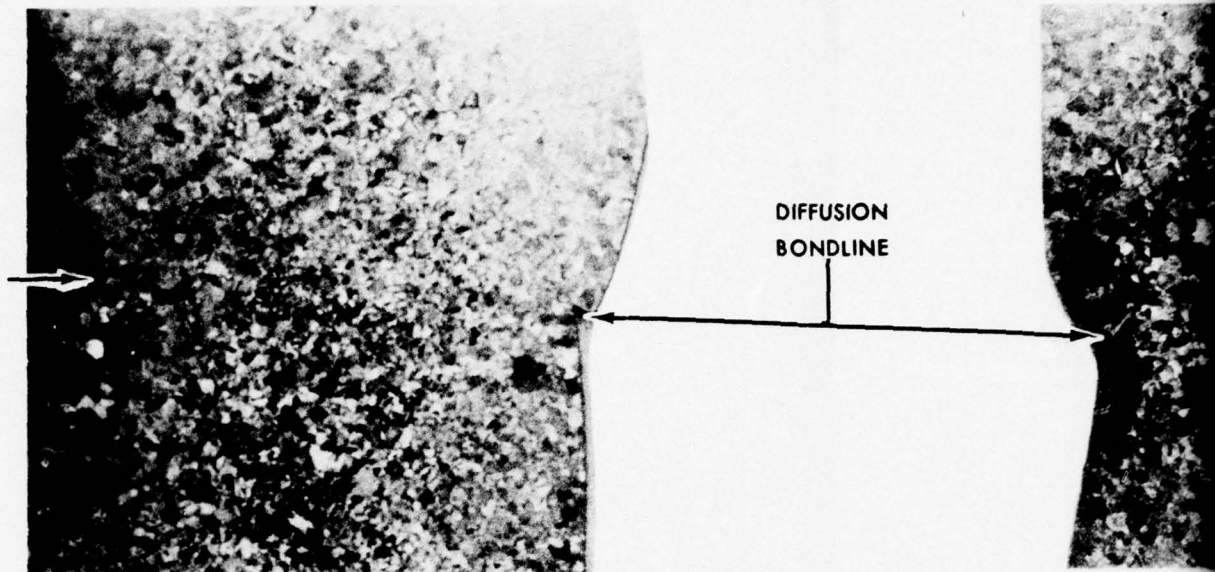


FIGURE 81. MACROSTRUCTURE ACROSS BONDLINE OF SECOND ARM SEGMENT FROM AN AREA OF SOUND BOND INDICATION DISCLOSE NO GROSS LACK OF BOND. 2X

FIGURE 82. MACROSTRUCTURE ACROSS BONDLINE OF SECOND ARM SEGMENT FROM AN AREA OF SOUND BOND INDICATION DISCLOSE NO GROSS LACK OF BOND. 2X

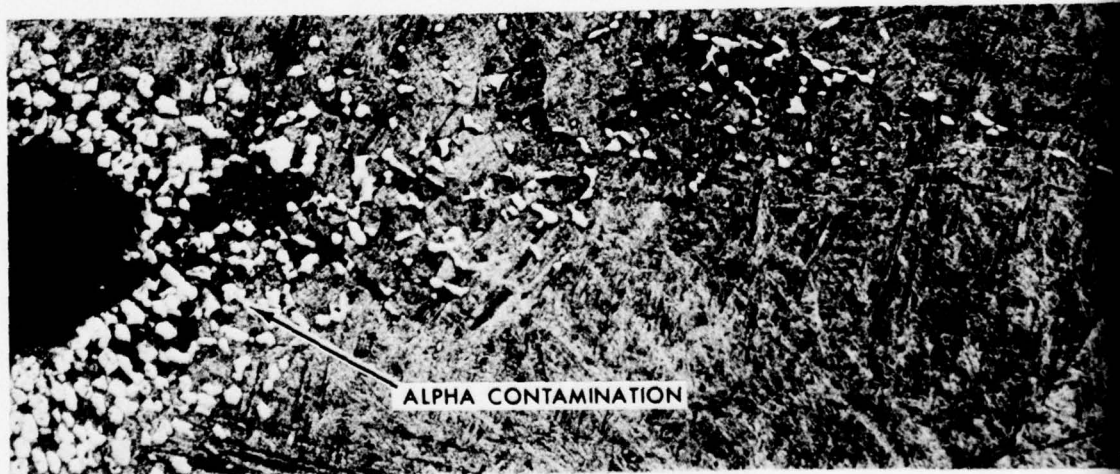
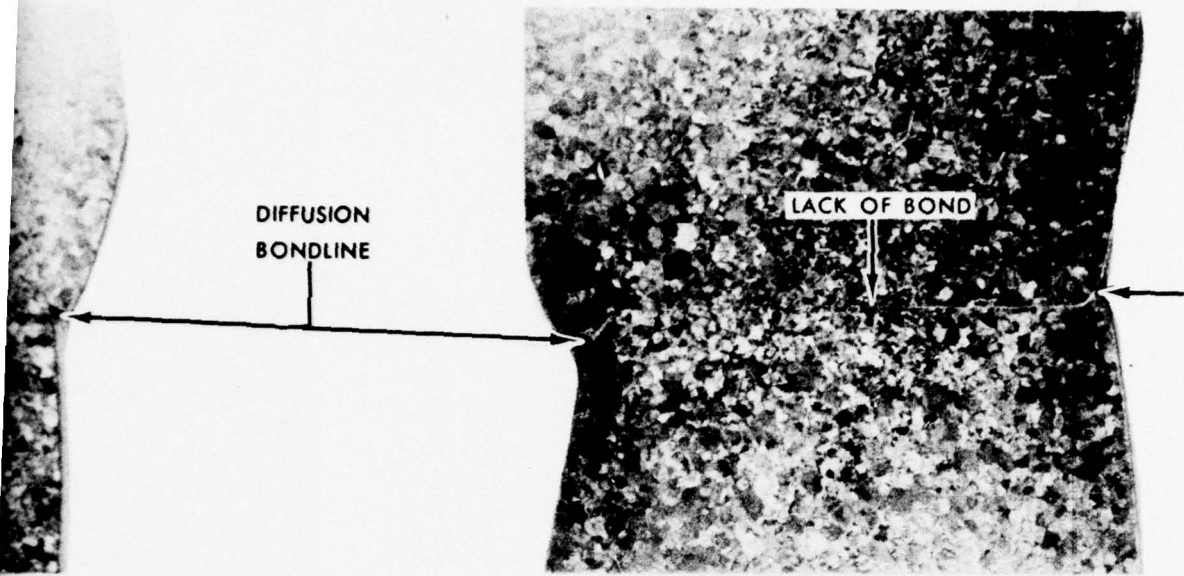
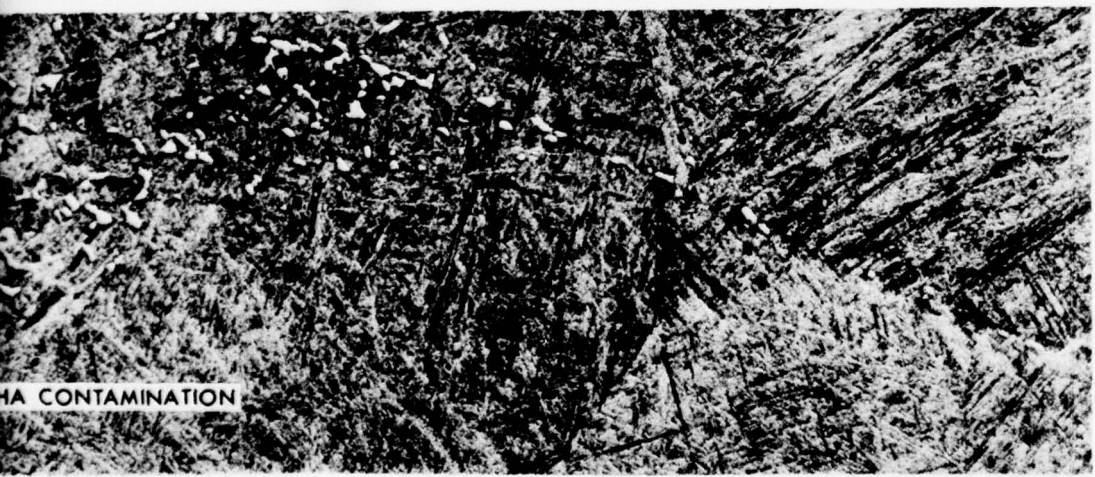


FIGURE 83. MICROSTRUCTURE ACROSS BONDLINE OF SECOND ARM SEGMENT FROM AN AREA OF SOUND BOND INDICATION DISCLOSE NO GROSS LACK OF BOND. 2X
ALPHA CONTAMINATION ALONG BONDLINE.



LINE OF SECOND ARM
AND BOND INDICATION
BOND. 2X

FIGURE 82. MACROSTRUCTURE ACROSS BONDLINE OF SECOND ARM
SEGMENT FROM AN AREA OF SONIC INDICATION
DISCLOSES GROSS LACK OF BOND. 2X



MICROSTRUCTURE ACROSS BONDLINE OF SECOND ARM
SEGMENT FROM AN AREA OF SOUND BOND DEPICTING
ALPHA CONTAMINATION ALONG BONDLINE. 100X

2

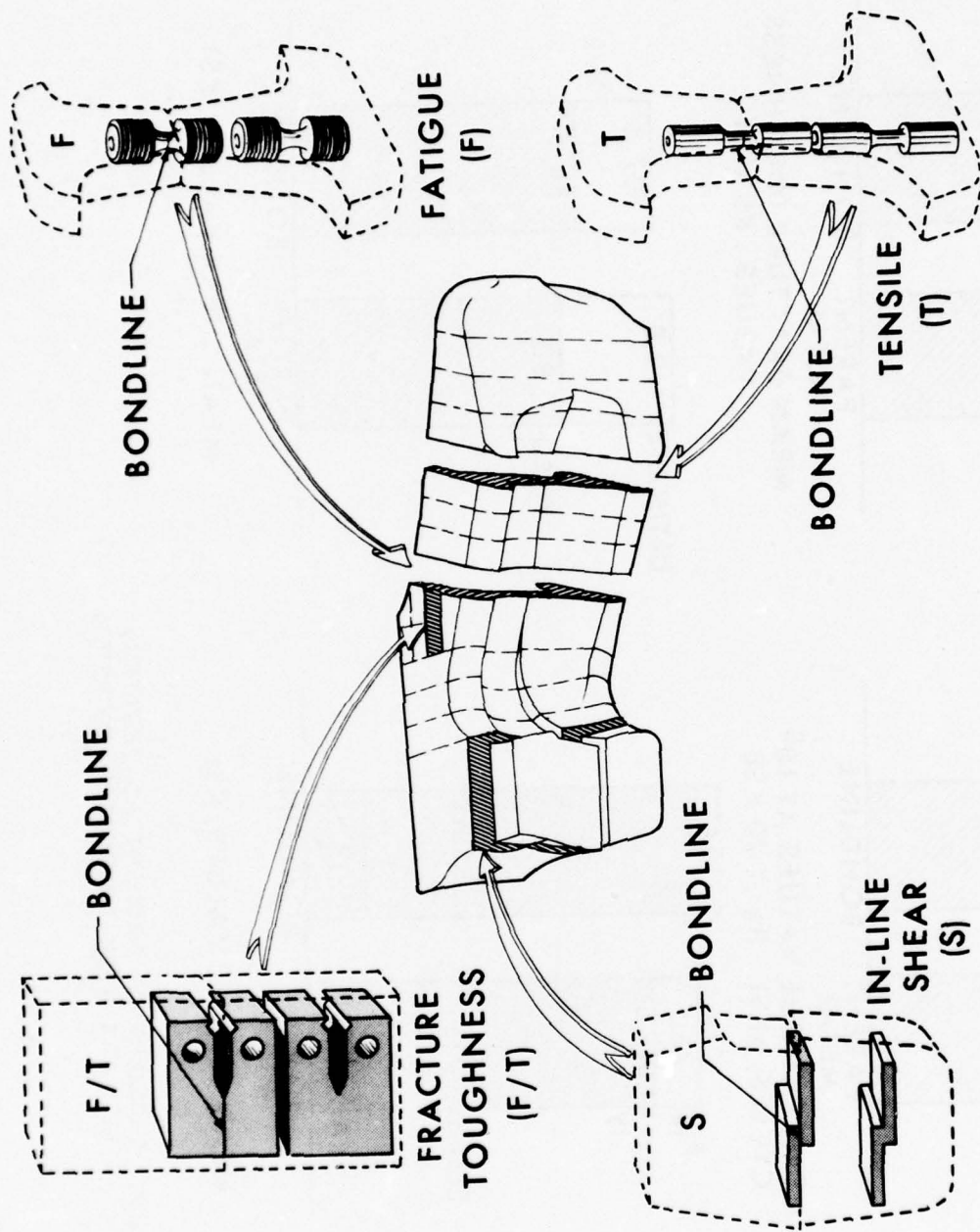


FIGURE 84. SKETCH OF THIRD HUB ARM SEGMENT ILLUSTRATING TYPE AND LOCATION OF TEST SPECIMENS.

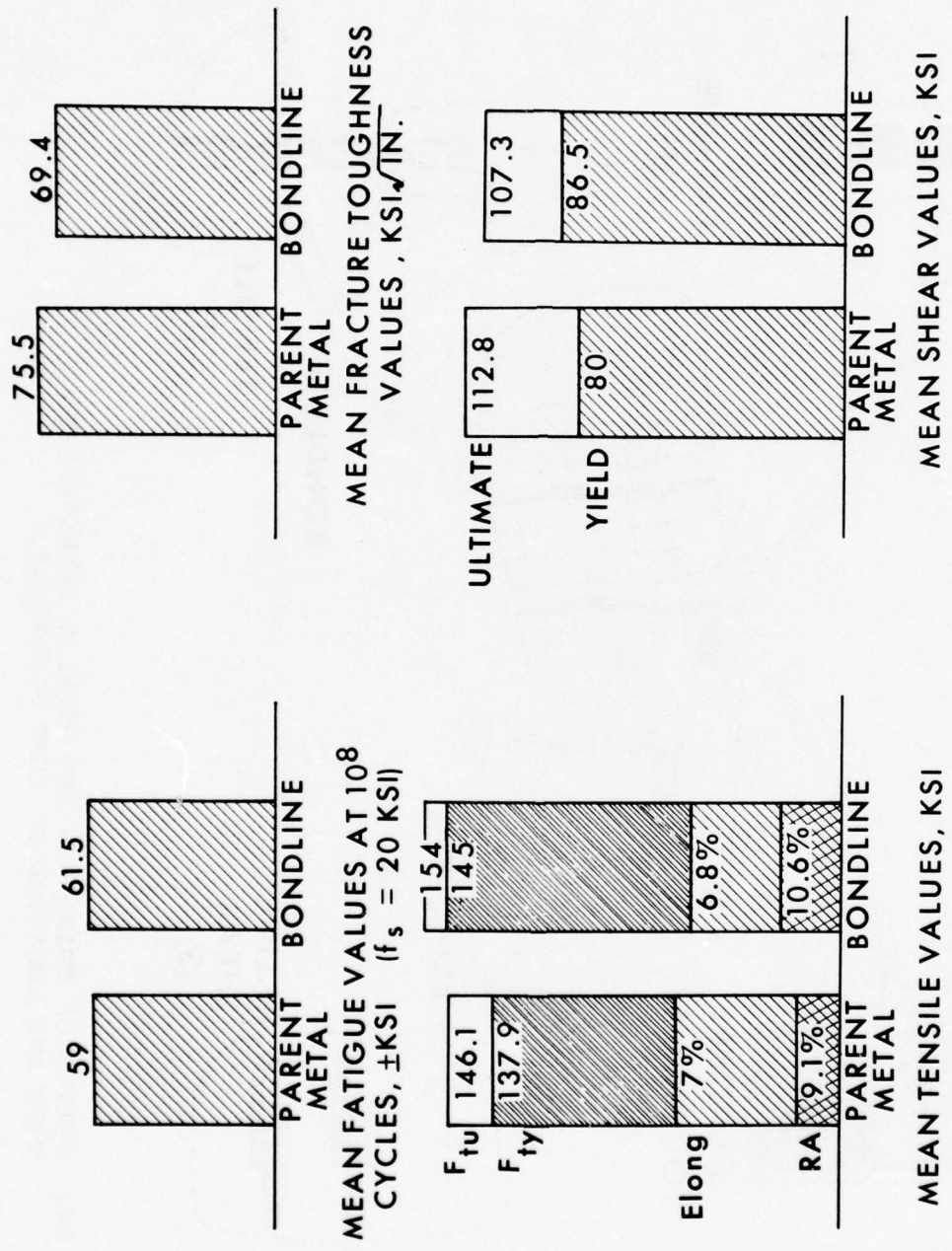


FIGURE 85. SUMMARY OF MECHANICAL TESTING, HUB ARM RISK REDUCTION SEGMENT.



FIGURE 86. TYPICAL CROSS SECTION OF BONDLINE, NO EVIDENCE OF ANY ANOMALIES, BOND JOINT IS NOT DISTINGUISHABLE FROM PARENT MATERIAL. 50X

Tensile - Comparison of the tensile test data, Table XIV showed that the tensile values were generally the same for both parent material and bondline specimens. Both the parent material and bondline failed tensile specimens exhibited typical ductile breaks with cup-cone interfaces as shown in Figure 87. No evidence of bondline separation was observed. No significant differences were observed between the parent material and bondline fracture interfaces.

TABLE XIV					
TENSILE TEST RESULTS					
HUB ARM SEGMENT					
SPECIMEN TYPE	SPECIMEN NUMBER	YIELD STRENGTH F_{ty} (KSI)	TENSILE STRENGTH F_{tu} (KSI)	ELONGATION (%)	REDUCTION OF AREA (%)
Bondline	T-1	148.0	158.1	6.0	9.0
	T-2	146.1	156.3	6.0	9.5
	T-3	148.0	155.5	8.0	15.5
	T-4	<u>138.1</u>	<u>146.0</u>	<u>7.0</u>	<u>8.5</u>
	AVERAGE	145.0	154.0	6.8	10.6
Parent Material	T-1	142.7	145.3	7.0	9.0
	T-2	135.6	146.0	6.0	9.5
	T-3	136.6	147.0	8.0	9.0
	T-4	<u>136.6</u>	<u>146.0</u>	<u>7.0</u>	<u>9.0</u>
	AVERAGE	137.9	146.1	7.0	9.1

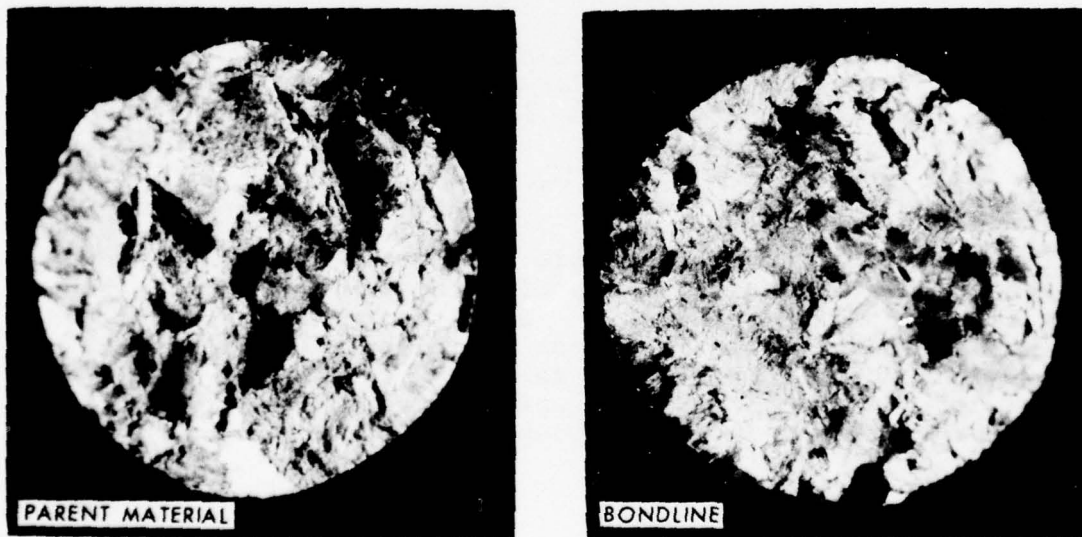


FIGURE 87. TENSILE FRACTURE, TYPICAL DUCTILE BREAK, HUB ARM SEGMENT. 10X

Fracture Toughness - Fracture toughness results are presented in Table XV. Review of the data disclosed no significant differences and all the test values are valid, meeting all criteria for determination of valid K_{IC} measurements described in ASTM-E399-72 (Reference (7)). The specimens displayed fracture surfaces with normal flat brittle fatigue precracking followed by overload, plane strain cracking for both the parent material and bondline specimens. Crack propagation was transgranular in nature exhibiting a fine grain fracture interface for both the precrack and plane strain crack region of both type specimens as shown in Figure 88. No evidence of voids, contamination, or lack of bond was observed on the fracture interface of the bondline specimens that could have generated a premature failure.

TABLE XV
PLANE-STRAIN FRACTURE-TOUGHNESS TEST DATA
HUB ARM SEGMENT

SPECIMEN TYPE	NUMBER	YIELD STRENGTH AVE. F_{ty} (KSI)	K_{IC} (KSI \sqrt{in})
Bondline ↓	FT-1	145	82.1
	FT-2	145	64.1
	FT-3	145	64.8
	<u>FT-4</u>	<u>145</u>	<u>66.5</u>
	AVERAGE	---	69.4
Parent Material ↓	FT-1	137.9	74.4
	FT-2	137.9	72.2
	FT-3	137.9	67.1
	<u>FT-4</u>	<u>137.9</u>	<u>78.5</u>
	AVERAGE	---	73.1



FIGURE 88. FRACTURE TOUGHNESS TYPICAL FRACTURE INTERFACE, HUB ARM SEGMENT. 1.5X

Shear - In-line shear test results are provided in Table XVI. Comparison of the test data disclosed no significant difference between parent material and bondline specimens. Specimens from the parent material and bondline manifested standard overload fractures. The fracture interfaces of these specimens were very similar. No outstanding deviations or differences were observed on the fracture interfaces between the parent material and bondline specimens as shown in Figure 89.

TABLE XVI			
IN-LINE SHEAR TEST RESULTS			
HUB ARM SEGMENT			
SPECIMEN TYPE	SPECIMEN NUMBER	SHEAR STRENGTH ULTIMATE F_{su} (KSI)	SHEAR STRENGTH YIELD F_{sy} (KSI)
Bondline	S-1	104.5	83.4
	<u>S-2</u>	<u>110.0</u>	<u>89.5</u>
	AVERAGE	107.3	86.5
Parent Materials	S-1	125.0	82.5
	S-2	110.0	70.4
	S-3	108.0	87.8
	<u>S-4</u>	<u>108.0</u>	<u>71.2</u>
	AVERAGE	112.8	80.0

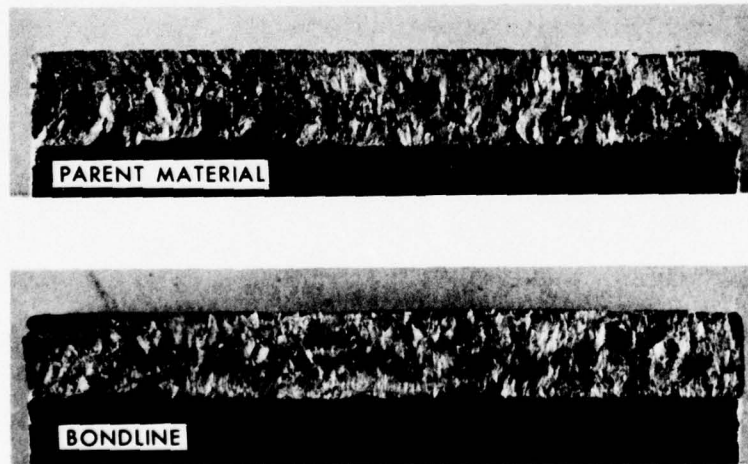


FIGURE 89. IN-LINE SHEAR FRACTURE, TYPICAL
STATIC OVERLOAD FRACTURE SURFACE,
HUB ARM SEGMENT. 4X

Fatigue - Results of the fatigue test data are summarized in Table XVII. This data is also presented on a mean S/N curve, Figure 90. Statistical analysis of the mean fatigue strength at 10^8 cycles for the parent material and bondline specimens plus the results obtained from Condition 1 of the pancake forging initially evaluated revealed no significant differences. The parent material and bondline specimens exhibited origins on the O.D. Cracking propagated in cyclic loading before complete separation of the specimens due to overload. The relationship of cyclic propagation and overload was contingent on the load level of testing. As expected, specimens tested at the higher load level manifested a smaller cyclic region and larger static overload zone. The fracture interfaces of both type specimens were similar with no evidence of abnormalities at the origin site that could have initiated cracking as shown in Figure 91. The fracture interface of the one, slightly lower bondline specimen revealed no discrepancies that could account for the slightly lower test point.

TABLE XVII
FATIGUE TEST RESULTS
HUB ARM SEGMENT

TYPE	SPECIMEN NUMBER	VIBRATORY STRESS ($f_s = 20$ KSI)	CYCLES X1000
Bondline ↓	14-F-20	80	45
	7-F-14	80	181**
	17-F-23	80	100
	9-F-15	80	5,130
	5-F-12	70	1,900
	6-F-13	70	10,000→
	17-F-24	70	7,800
	4-F-10	60	10,000→
	10-F-16	60	10,000→
	11-F-19	60	84
	7-F-14	50	10,000→
Parent Material ↓	2-F-3	80	24
	10-F-18	80	45
	2-F-4	80	93
	3-F-7	80	18**
	3-F-6	70	2,400
	4-F-11	70	1,600
	1-F-2	70	1,400
	4-F-8	60	10,000→
	1-F-1	60	10,000→
	4-F-9	60	5,100→
	3-F-7	50	10,000→

→ Runout 10×10^6 Cycles Min.

**Specimen Previously Tested At ± 50 KSI Vibratory Level

Specimen Number Prefix Indicates Macroslice From Which Specimen Was Fabricated.

THIS PAGE INTENTIONALLY LEFT BLANK

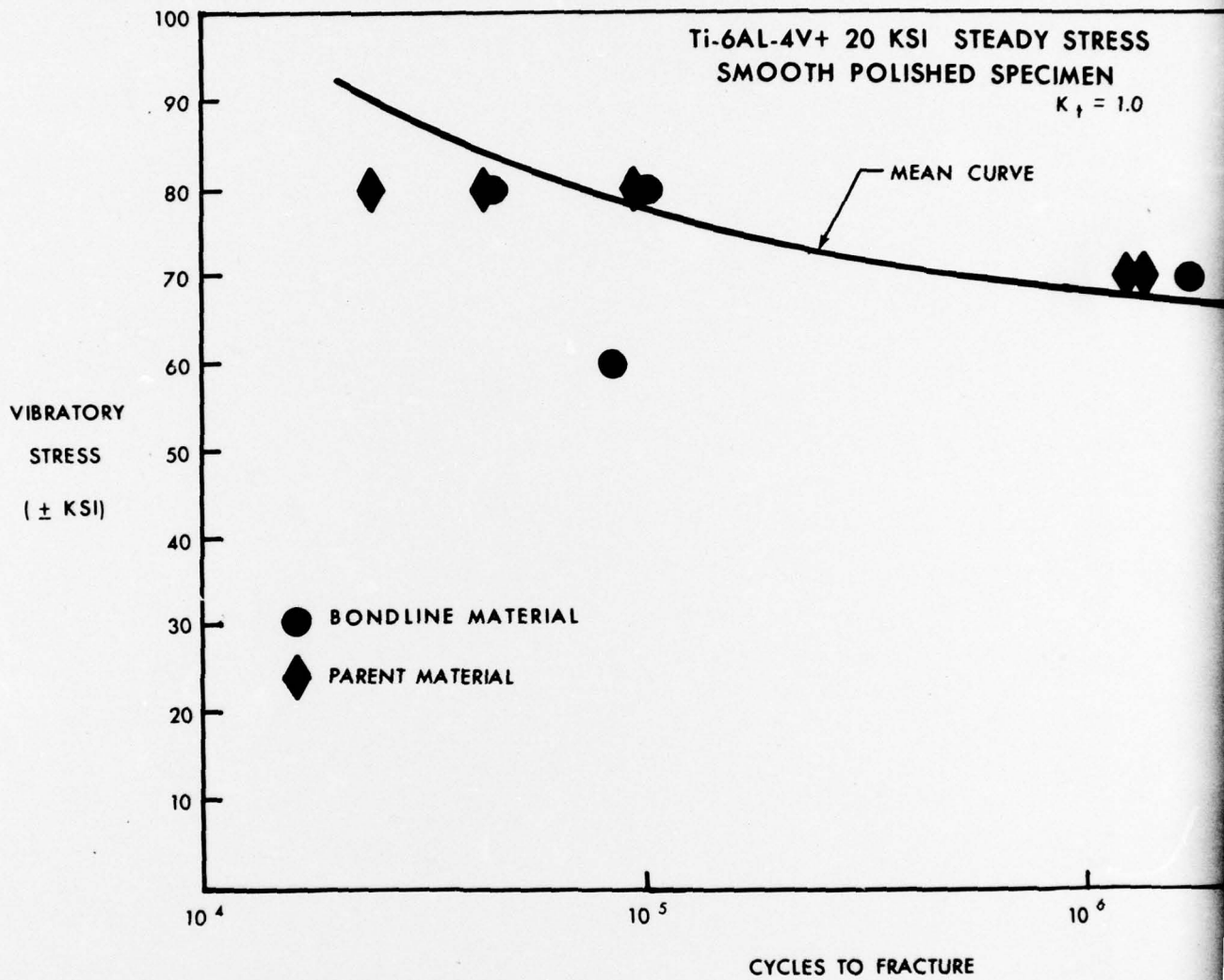
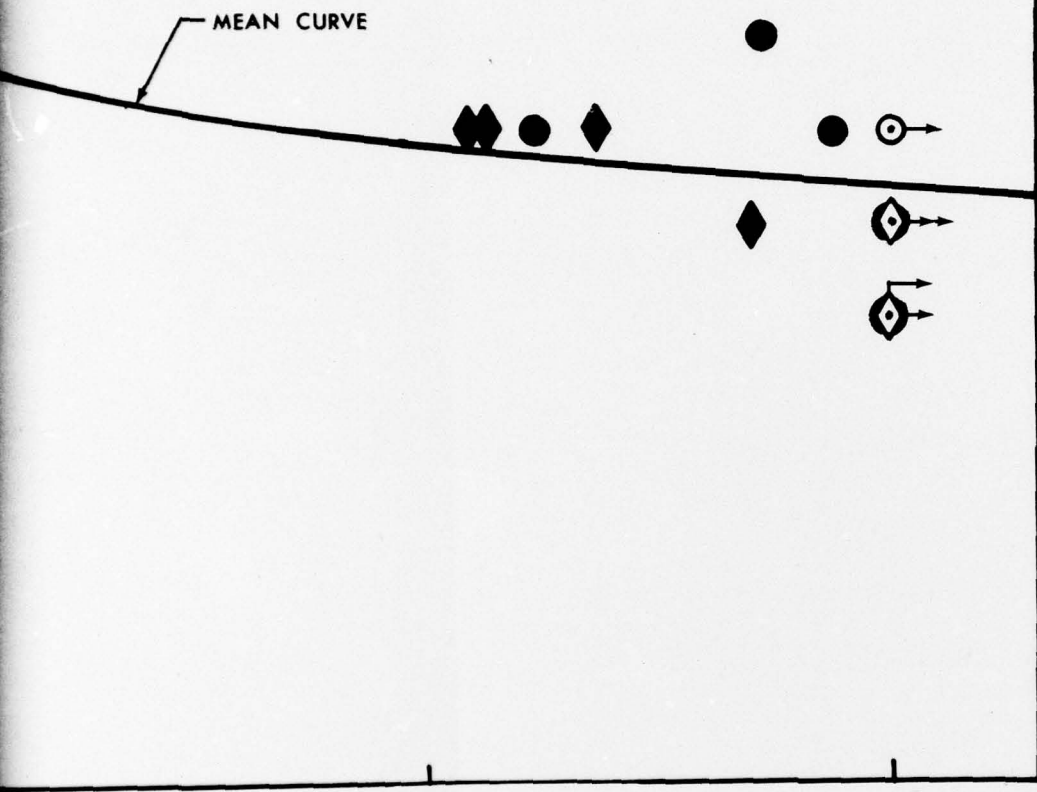


FIGURE 90. MEAN S/N CURVE FOR HUB ARM SEGMENT, BONDLINE MATERIAL AND PARENT MATERIAL.

Ti-6AL-4V+ 20 KSI STEADY STRESS
SMOOTH POLISHED SPECIMEN
 $K_t = 1.0$



10⁶ 10⁷

CYCLES TO FRACTURE

NT,
ERIAL.

2

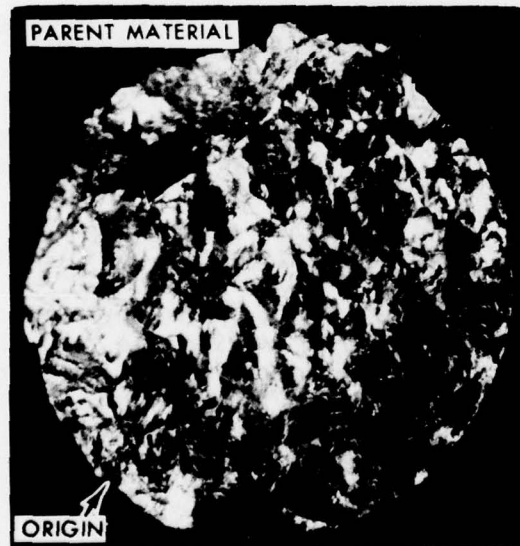


FIGURE 91. FATIGUE FRACTURE, TYPICAL FRACTURE SURFACE WITH ORIGIN ON O.D., HUB ARM SEGMENT. 11X

6.0 COST PROJECTION

Although technically feasible, the current manufacturing method was found not to be cost effective in its present approach for the full-size H-53 Elastomeric Main Rotor Hub.

A study of the cost projection for 100 and 1,000 forge-diffusion bonded full-size Elastomeric Hubs compared to the conventional forging of the Elastomeric Hubs revealed that scaling-up the hardware and equipment necessary to accommodate a full-size H-53 Elastomeric Main Rotor Hub would not be cost effective.

New tooling including two sets of forging dies and one set of bonding dies, necessary for fabrication of the forge-diffusion bond half-forging would require an initial expenditure of \$175,000 to \$200,000. This would include a one time, nonrecurring material and equipment cost. Recurring material cost, such as, the canning material are reflected in the individual hub price. Cost of the completed full-size forge-diffusion bonded hub would range from \$50,000 to \$55,000 per hub for twelve or more. No decrease in unit price can be quoted at this time for 1,000 units. Machining cost for the diffusion-bonded forging is estimated to be approximately \$5,000, making the cost of a fully machined forge-bonded hub \$55,000 to \$60,000.

Present cost of the Elastomeric Hub Forging is \$30,000. Machining cost for this forging is approximately \$10,000 for a total cost of \$40,000.

Therefore, cost of a Forge-Diffusion Bonded Elastomeric Hub is projected to be \$15,000 to \$20,000 in excess of the present conventional Elastomeric Hub.

The prime reason for the high cost in the fabrication of a full-size H-53 Elastomeric Forge-Diffusion Bonded Hub is its massiveness. Scaling-up from a 1/6 arm segment to a full-size hub becomes extremely expensive because of the problems and time incurred in fabricating, cleaning, canning, evacuating, and heating a hub of this size. An intermediate size component would be cost effective and is the next logical plateau in the establishment of forge-diffusion bond technology as a low cost method of manufacture.

7.0 CONCLUSIONS

The objective of this program was the establishment of the manufacturing methods and technologies necessary to fabricate large titanium components at low overall cost, by means of the forge-diffusion bond process. The process optimization phase of this program established optimum processing conditions that would produce high quality parts with parent material mechanical properties. Two single arms of the H-53 Elastomeric Rotor Hub were satisfactorily fabricated using these procedures. The hub arms were determined to be of high quality with parent material mechanical properties. Subsequent investigation revealed that scaling-up the hardware and equipment necessary to accommodate a full-size H-53 Elastomeric Main Rotor Hub is technically feasible but would not be cost effective. However, other similar, smaller components would be more readily adaptable.

8.0 RECOMMENDATIONS

It is recommended that consideration be given to fabrication of an intermediate size hub, e.g., UTTAS Main Rotor Hub.

REFERENCES

1. Dutton, W. J., Development of H-53 Elastomeric Rotor Head, Sikorsky Aircraft, Paper Presented at the 29th Annual National Forum of the American Helicopter Society, Washington, D. C., May, 1973.
2. Lucas, J. J., Fatigue Strength Improvements in Ti-6Al-4V Forgings, Sikorsky Aircraft, Journal of the American Helicopter Society, July, 1972. Presented at National A.H.S. Meeting, May, 1971, Washington, D. C.
3. Lucas, J. J., Improvements in the Fatigue Strength of Ti-6Al-4V Forgings, Sikorsky Aircraft, Titanium Science and Technology, Vol. 3, pp 2081 - 2096. Presented at 2nd International Conference on Titanium, Cambridge, Mass., May, 1972.
4. Sikorsky Standard No. SS8445, Titanium Alloy 6Al-4V Forging, Dynamic, Rev. 4, December 16, 1971.
5. ASTM-E8-68, "Tension Testing of Metallic Material."
6. Federal Test Method Metals; Test Methods STD 151a.
7. ASTM-E-399-72, "Standard Method of Test for Plane-Strain Fracture Toughness of Metallic Materials."
8. ASTM-E-466-72T, "Recommended Practice for Constant Amplitude Axial Fatigue Tests of Metallic Materials."

LIST OF SYMBOLS

f_v	Vibratory Stress
f_s	Steady Stress
KSI	Thousand Pounds Per Square Inch
psi	Pounds Per Square Inch
F_{tu}	Ultimate Tensile Strength
F_{ty}	Yield Strength (.2% Strain Offset)
Elong.	Elongation (% Strain in Two Inches)
X	Optical Magnification
$^{\circ}F$	Degree Fahrenheit
TIG	Tungsten Inert Gas
cc/sec	Cubic Centimeters Per Second
HF-HNO ₃	Hydroflouric-nitric Acid
Mg(OH) ₂	Magnesium Hydroxide
db	Decibel
σ	Shear Stress
K_{IC}	Plane-Strain Fracture Toughness
K_Q	Plane-Strain Fracture Toughness Not Valid
S/N	Stress Versus Cycles
%	Percent
NA	Neutral Axis
fbh	Flat Bottom Hole
GAG	Ground-Air-Ground
β -STOA	Beta Solution Treated and Overaged
KTS	Knots
AA	Arithmetical Average
OD	Outer Diameter
R_{Cal}	Calibration Resistor as Physical Calibration Transfer Standard
TIR	Total Indicator Reading
K_t	Stress Concentration Factor
Torr	Pressure of a Millimeter of Mercury
μ	Micron of Mercury

US ARMY AVIATION SYSTEMS COMMAND
DISTRIBUTION LIST

No. of Copies	To
4	Commander, U. S. Army Materiel Command, 5001 Eisenhower Avenue, Alexandria, Virginia 22333 ATTN: AMCRD-EA
6	Commander, USAAVSCOM, P. O. Box 209, St. Louis, Missouri 63166 ATTN: AMSAV-ERE
1	AMSAV-LE
1	AMSAV-ZDR
1	Director, U. S. Army Air Mobility R&D Lab, Ames Research Center (Mail Stop 207-5), Moffett Field, California 94035 ATTN: SAVDL-AS
1	Director, Ames Directorate, U. S. Army Air Mobility R&D Lab, (Mail Stop 215-1), Ames Research Center, Moffett Field, California 94035 ATTN: SAVDL-AM
1	Director, Lewis Directorate, U. S. Army Air Mobility R&D Lab, Lewis Research Center (Mail Stop 500-317), 2100 Brook Park Road, Cleveland, Ohio 44135 ATTN: SAVDL-LE
1	Director, Eustis Directorate, U. S. Army Air Mobility R&D Lab, Fort Eustis, Virginia 23604 ATTN: SAVDL-EU-TAS
1	Director, Langley Directorate, U. S. Army Air Mobility R&D Lab, Langley Research Center (Mail Stop 124), Hampton, Virginia 23365 ATTN: SAVDL-L
1	Commander, U. S. Army Aeronautical Depot Maintenance Center, Corpus Christi, Texas 78419 ATTN: SAVAE-EFT
1	Commander, U. S. Army Electronics Command, 225 South 18th Street, Philadelphia, Pennsylvania 19103 ATTN: AMSEL-PP/P-IM
1	Commander, U. S. Army Missile Command, Redstone Arsenal, Alabama 35809 ATTN: AMSMI-IIE
1	Commander, U. S. Army Troop Support Command, 4300 Goodfellow Boulevard, St. Louis, Missouri 63120 ATTN: AMSTS-PLC

No. of Copies	To
1	Commander, U. S. Army Armament Command, Rock Island Arsenal, Rock Island, Illinois 61201 ATTN: AMSAR-PPR-IW
1	Commander, U. S. Army Tank-Automotive Command, Warren, Michigan 48090 ATTN: AMSTA-RCM.1
1	Commander, Frankford Arsenal, Bridge & Tacony Streets, Philadelphia, Pennsylvania 19137 ATTN: SARFA-T1000
1	Commander, Rock Island Arsenal, Rock Island, Illinois 61201 ATTN: SWERI-PPE-5311
1	Commander, Watervliet Arsenal, Watervliet, New York 12189 ATTN: SWEVW-PP-WP
1	Director, U. S. Army Materials & Mechanics Research Center, Watertown, Massachusetts 02172 ATTN: AMXMR-M
3	Director, Production Equipment Agency, Rock Island Arsenal, Rock Island, Illinois 61201 ATTN: AMXPE-MT
1	Director, Harry Diamond Labs, Connecticut Avenue & Van Ness Streets, N. W. Washington, DC 20436 ATTN: AMXDO-PP
1	OIC: U. S. Naval Materiel Industrial Resources Office, Philadelphia, Pennsylvania 19112 ATTN: Code 227
2	Commander, AF Material Lab, Manufacturing Technology Division, Wright Patterson AFB, Ohio 45433 ATTN: AFML-MAT-P
12	Commander, Defense Documentation Center, Cameron Station, Alexandria, Virginia 22314
1	Commander, U. S. Army Foreign Science and Technology Center, 220 Seventh Street, N. E., Charlottesville, Virginia 22901
2	Director, Army Materials and Mechanics Research Center, Watertown, Massachusetts 02172 ATTN: AMXMR-PL
1	AMXMR-PR
1	AMXMR-CT
1	AMXMR-XC
1	AMXMR-AP
1	AMXMR-M
1	AMXMR-PT, Farrow
1	Author

AD
UNCLASSIFIED
UNLIMITED DISTRIBUTION

AD
UNCLASSIFIED
UNLIMITED DISTRIBUTION

Key Words
Titanium Motor Hub
Diffusion Bonding
Heat Treatment
Mechanical Properties

Key Words
Titanium Motor Hub
Diffusion Bonding
Heat Treatment
Mechanical Properties

The purpose of this program was to establish the manufacturing methods and technology necessary to fabricate large T1-6Al-4V components at low overall cost by means of the forge-diffusion bond process. The technical approach to achieve this concept consisted of three phases: the determination of an optimum process condition by evaluation of small test specimens cut from simply pancake forgings which had been fabricated with different processing conditions; the utilization of the optimum process condition in the fabrication and evaluation of a risk reduction component which was a single arm of the H-53 Helicopter Elastomeric Main Rotor Hub; and finally, the manufacture of the full-size main rotor hub. The first two phases of this concept have been successfully completed in this program. The forge-diffusion bond material of the risk reduction component was found to exhibit properties equivalent to parent material values. The process was shown not to be cost effective for the full-size H-53 Elastomeric rotor hub. Although technically feasible, fabrication of the full-size hub will not be demonstrated.

The purpose of this program was to establish the manufacturing methods and technology necessary to fabricate large T1-6Al-4V components at low overall cost by means of the forge-diffusion bond process. The technical approach to achieve this concept consisted of three phases: the determination of an optimum process condition by evaluation of small test specimens cut from simply pancake forgings which had been fabricated with different processing conditions; the utilization of the optimum process condition in the fabrication and evaluation of a risk reduction component which was a single arm of the H-53 Helicopter Elastomeric Main Rotor Hub; and finally, the manufacture of the full-size main rotor hub. The first two phases of this concept have been successfully completed in this program. The forge-diffusion bond material of the risk reduction component was found to exhibit properties equivalent to parent material values. The process was shown not to be cost effective for the full-size H-53 Elastomeric rotor hub. Although technically feasible, fabrication of the full-size hub will not be demonstrated.

AD
UNCLASSIFIED
UNLIMITED DISTRIBUTION

AD
UNCLASSIFIED
UNLIMITED DISTRIBUTION

Key Words
Titanium Motor Hub
Diffusion Bonding
Heat Treatment
Mechanical Properties

Key Words
Titanium Motor Hub
Diffusion Bonding
Heat Treatment
Mechanical Properties

The purpose of this program was to establish the manufacturing methods and technology necessary to fabricate large T1-6Al-4V components at low overall cost by means of the forge-diffusion bond process. The technical approach to achieve this concept consisted of three phases: the determination of an optimum process condition by evaluation of small test specimens cut from simply pancake forgings which had been fabricated with different processing conditions; the utilization of the optimum process condition in the fabrication and evaluation of a risk reduction component which was a single arm of the H-53 Helicopter Elastomeric Main Rotor Hub; and finally, the manufacture of the full-size main rotor hub. The first two phases of this concept have been successfully completed in this program. The forge-diffusion bond material of the risk reduction component was found to exhibit properties equivalent to parent material values. The process was shown not to be cost effective for the full-size H-53 Elastomeric rotor hub. Although technically feasible, fabrication of the full-size hub will not be demonstrated.

The purpose of this program was to establish the manufacturing methods and technology necessary to fabricate large T1-6Al-4V components at low overall cost by means of the forge-diffusion bond process. The technical approach to achieve this concept consisted of three phases: the determination of an optimum process condition by evaluation of small test specimens cut from simply pancake forgings which had been fabricated with different processing conditions; the utilization of the optimum process condition in the fabrication and evaluation of a risk reduction component which was a single arm of the H-53 Helicopter Elastomeric Main Rotor Hub; and finally, the manufacture of the full-size main rotor hub. The first two phases of this concept have been successfully completed in this program. The forge-diffusion bond material of the risk reduction component was found to exhibit properties equivalent to parent material values. The process was shown not to be cost effective for the full-size H-53 Elastomeric rotor hub. Although technically feasible, fabrication of the full-size hub will not be demonstrated.

AD
Army Materials and Mechanics Research Center
Watertown, Massachusetts 02172
TITANIUM ROTOR HUB EVALUATION
Marion J. Bonassar and John J. Lucas
Sikorsky Aircraft Division
United Technologies Corporation
Stratford, Connecticut 06602

Key Words
Titanium Rotor Hub
Diffusion Bonding
Heat Treatment
Mechanical Properties

Technical Report AMMRC CTR 75-14, June 1975,
111us - Tables, Contract DAAG46-73-C-0126,
D/A Project: 172804, AMCRC Code: 3197.06.7141
Final Report, March 8, 1973 to May 15, 1975

The purpose of this program was to establish the manufacturing methods and technology necessary to fabricate large Ti-6Al-4V components at low overall cost by means of the forge-diffusion bond process. The technical approach to achieve this concept consisted of three phases: the determination of an optimum process condition by evaluation of small test specimens cut from simply pancake forgings which had been fabricated with different processing conditions; the utilization of the optimum process condition in the fabrication and evaluation of a risk reduction component which was a single arm of the H-53 Helicopter Elastomeric Main Rotor Hub; and finally, the manufacture of the full-size main rotor hub. The first two phases of this concept have been successfully completed in this program. The forge-diffusion bond material of the risk reduction component was found to exhibit properties equivalent to parent material values. The process was shown not to be cost effective for the full-size H-53 Elastomeric rotor hub. Although technically feasible, fabrication of the full-size hub will not be demonstrated.

AD
Army Materials and Mechanics Research Center
Watertown, Massachusetts 02172
TITANIUM ROTOR HUB EVALUATION
Marion J. Bonassar and John J. Lucas
Sikorsky Aircraft Division
United Technologies Corporation
Stratford, Connecticut 06602

Key Words
Titanium Rotor Hub
Diffusion Bonding
Heat Treatment
Mechanical Properties

Technical Report AMMRC CTR 75-14, June 1975,
111us - Tables, Contract DAAG46-73-C-0126,
D/A Project: 172804, AMCRC Code: 3197.06.7141
Final Report, March 8, 1973 to May 15, 1975

The purpose of this program was to establish the manufacturing methods and technology necessary to fabricate large Ti-6Al-4V components at low overall cost by means of the forge-diffusion bond process. The technical approach to achieve this concept consisted of three phases: the determination of an optimum process condition by evaluation of small test specimens cut from simply pancake forgings which had been fabricated with different processing conditions; the utilization of the optimum process condition in the fabrication and evaluation of a risk reduction component which was a single arm of the H-53 Helicopter Elastomeric Main Rotor Hub; and finally, the manufacture of the full-size main rotor hub. The first two phases of this concept have been successfully completed in this program. The forge-diffusion bond material of the risk reduction component was found to exhibit properties equivalent to parent material values. The process was shown not to be cost effective for the full-size H-53 Elastomeric rotor hub. Although technically feasible, fabrication of the full-size hub will not be demonstrated.

AD
Army Materials and Mechanics Research Center
Watertown, Massachusetts 02172
FORGE-DIFFUSION BOND
TITANIUM ROTOR HUB EVALUATION
Marion J. Bonassar and John J. Lucas
Sikorsky Aircraft Division
United Technologies Corporation
Stratford, Connecticut 06602

Key Words
Titanium Rotor Hub
Diffusion Bonding
Heat Treatment
Mechanical Properties

Technical Report AMMRC CTR 75-14, June 1975,
111us - Tables, Contract DAAG46-73-C-0126,
D/A Project: 172804, AMCRC Code: 3197.06.7141
Final Report, March 8, 1973 to May 15, 1975

The purpose of this program was to establish the manufacturing methods and technology necessary to fabricate large Ti-6Al-4V components at low overall cost by means of the forge-diffusion bond process. The technical approach to achieve this concept consisted of three phases: the determination of an optimum process condition by evaluation of small test specimens cut from simply pancake forgings which had been fabricated with different processing conditions; the utilization of the optimum process condition in the fabrication and evaluation of a risk reduction component which was a single arm of the H-53 Helicopter Elastomeric Main Rotor Hub; and finally, the manufacture of the full-size main rotor hub. The first two phases of this concept have been successfully completed in this program. The forge-diffusion bond material of the risk reduction component was found to exhibit properties equivalent to parent material values. The process was shown not to be cost effective for the full-size H-53 Elastomeric rotor hub. Although technically feasible, fabrication of the full-size hub will not be demonstrated.

AD
Army Materials and Mechanics Research Center
Watertown, Massachusetts 02172
FORGE-DIFFUSION BOND
TITANIUM ROTOR HUB EVALUATION
Marion J. Bonassar and John J. Lucas
Sikorsky Aircraft Division
United Technologies Corporation
Stratford, Connecticut 06602

Key Words
Titanium Rotor Hub
Diffusion Bonding
Heat Treatment
Mechanical Properties

Technical Report AMMRC CTR 75-14, June 1975,
111us - Tables, Contract DAAG46-73-C-0126,
D/A Project: 172804, AMCRC Code: 3197.06.7141
Final Report, March 8, 1973 to May 15, 1975

The purpose of this program was to establish the manufacturing methods and technology necessary to fabricate large Ti-6Al-4V components at low overall cost by means of the forge-diffusion bond process. The technical approach to achieve this concept consisted of three phases: the determination of an optimum process condition by evaluation of small test specimens cut from simply pancake forgings which had been fabricated with different processing conditions; the utilization of the optimum process condition in the fabrication and evaluation of a risk reduction component which was a single arm of the H-53 Helicopter Elastomeric Main Rotor Hub; and finally, the manufacture of the full-size main rotor hub. The first two phases of this concept have been successfully completed in this program. The forge-diffusion bond material of the risk reduction component was found to exhibit properties equivalent to parent material values. The process was shown not to be cost effective for the full-size H-53 Elastomeric rotor hub. Although technically feasible, fabrication of the full-size hub will not be demonstrated.